Alma Mater Studiorum – Università di Bologna

DOTTORATO DI RICERCA IN

Scienze della terra, della vita e dell'ambiente

Ciclo 29°

Settore Concorsuale di afferenza: 04/A2

Settore Scientifico disciplinare: GEO/02

ISOTOPIC SIGNATURES OF DEEP FLUIDS ON AUTHIGENIC CARBONATES FORMATION

Presentata da: **IRENE VIOLA**

Coordinatore Dottorato **Relatore**

Barbara Mantovani **Rossella Capozzi**

Esame finale anno 2017

Index

Figure Index

Acknowledgements

All the results obtained in this thesis have been reached thanks to all the people that supported me and to all the professors and researchers I worked with.
Above everyone, I would like to thank professor Rossella Capozzi for giving me the possibility to carry out this project, for her constant support, comments, suggestions and for all the things she teaches me every time.
The research activities were conducted in the BiGeA department in Bologna, in particular geochemical and sedimentology labs, in CIRSA labs in Ravenna, in ETHz isotopic labs in Zurich, at CSA Rimini and at the CNR isotopic labs.
Thanks to professor Enrico Dinelli from BiGeA Department for his support on geochemical data from the very start of this PhD.
I would also thank Professor Stefano Bernasconi and Professor Derek Vance for giving me the possibility to work in ETHz in Zurich, for teaching me about isotopes, techniques and for their support during data interpretation.
Thanks also to ISMAR-CNR professor Paolo Montagna for the micro-driller, ISMAR-CNR professor Leonardo Langone for TOC analysis; to IGG-CNR Doc. Mario Mussi for the first isotopic results.
I would also thank all the technicians and researchers that followed and helped me in the different labs: Madalina, Stewart, Alvaro, Jörg, Daniel, Piero and Denis.
Beside all the persons directly involved that worked with me, I would also thank ETHz Professor Crisógono Vasconcelos for his availability, support and suggestions; Ruhr-University Bochum Professor Adrian Immenhauser for the interest demonstrated in my research, for the email exchange and for all his priceless suggestions and comments during the review of this thesis; and ETHz Professor Tomaso Bontognali for all the comments and suggestions on microbial dolomite formation during the review of this thesis.

In the end I want to thank all my friends and family for the support and unconditional faith in me also during the darker sides of this project.

Abstract

The formation of authigenic carbonates linked to hydrocarbon-enriched fluids is a well-known phenomenon documented in modern and ancient marine sedimentary basins worldwide; particularly, but not exclusively, in compressive tectonic regimes at convergent margins. Microbially mediated anaerobic oxidation of methane coupled with sulphate reduction, methanogenesis process and CO_2 reduction increase the pore water alkalinity, favouring the precipitation of authigenic carbonates. Depending on porosity, permeability and migration pathways, different carbonate morphologies were discovered: slabs, crusts, cylindrical and pipe-like conduits, and irregularly shaped bodies. The authigenic carbonates show peculiar mineralogy and geochemistry depending on formation environment, fluids involved and specific formation processes. The relations among fluid sources, fluid migration in the sediment where carbonate cements form and the isotopic signature resulting during carbonate precipitation, are the focus of my PhD. The Northern Apennines, the study area in this thesis, presents a very active spontaneous fluid migration system, from the deep reservoirs to the surface. Furthermore, this system has been deeply characterised in previous works together with the petroleum system. In association, fossils record of natural fluid migration, such as authigenic carbonate occurrences, has been identified in three different locations along the Northern Apennine foothills: Enza River field, Stirone River field and Secchia River field. All the outcrops have been exposed along the riverbanks thanks to fluvial incisions through the Apennine foothills, geologically where Plio-Pleistocene Argille Azzurre marine successions are present. Starting from a morphological description, a total of 73 carbonate subsamples have been characterised from the three outcrops. Each sample has been divided in two or more subsamples in order to have a micro characterisation by petrography, SEM-EDX observation, together with XRD and XRF analyses. The samples are mainly composed by microcristalline dolomite, above 50%; also if in some of them calcite is present. The remaining siliciclastic grains are composed by silicate, feldspars and clay minerals reflecting embedding sediment composition. $\delta^{13}C$, $\delta^{18}O$, $^{87/86}Sr$ have been analysed on selected carbonate subsamples at ETHz in Zurich. Seven samples of saline waters coming from different present-day seepages and drilled wells of the Northern Apennines foothills, close to the authigenic carbonate outcrops, have been selected for this study. Local parameters and geochemical characterisation, coupled with $\delta^{13}C$ on DIC, $\delta^{18}O$, $^{87/86}Sr$ and $\delta^{34}S$ have been analysed to have a characterisation of these waters, which belong to deep reservoirs. Hydrocarbon components present in the fluids were analysed and characterised in previous works: the reservoirs in the subsurface of the foothills contain gas

composed of mixed thermogenic, secondary biogenic methane and CO_2, which are presently seeping in mud volcanoes, located close to the sites where carbonate concretions have been found. The $\delta^{13}C$ in the carbonates strongly varies among different areas and also within the same outcrop. Processes acting on the different carbon sources have been identified in the sampled carbonates: they include AOM of mixed methane (thermogenic and biogenic) from different reservoirs, incorporation of heavy C from CO_2 derived by secondary methanogenesis and oxidation of primary biogenic methane. The variability recorded among the outcrops and the samples within a single site, testifies that authigenic carbonates represent a record of varying biogeochemical cycles during formation. The possibility to find a correlation between the fluid migration system, responsible for the active cold seepages, and the fossil authigenic carbonates, suggests that the generation and migration processes within the reservoirs are long-lasting along the Northern Apennines foothills. Furthermore, by studying the $\delta^{18}O$ and $^{87/86}Sr$ in dolomite cements it was possible to stress that the marine pore water, present in the sediment pile during carbonate precipitation, was not always the main source of oxygen. The mixing models permitted to quantify the mixing factor and the amount of seawater and connate water in the isotopic signature of each subsamples of authigenic carbonates, emphasising the changes in the fluid feeding system.

1. Introduction

The presence of authigenic carbonate formation associated to seepages emissions in different geological setting is a well known and investigated phenomenon in modern and ancient marine environment worldwide (Campbell et al., 2002; Nyman and Nelson, 2011; Hensen et al., 2015) (Fig.1). Natural fluid emissions occur in a wide range of geologic and geodynamic settings, with new seepage sites being discovered all around the world (Campbell et al., 2002; Nyman and Nelson, 2011; Van Landeghem et al., 2015 and references therein; Mazzini et al., 2016 and references therein; Marzec et al., 2016; Roy et al., 2016).

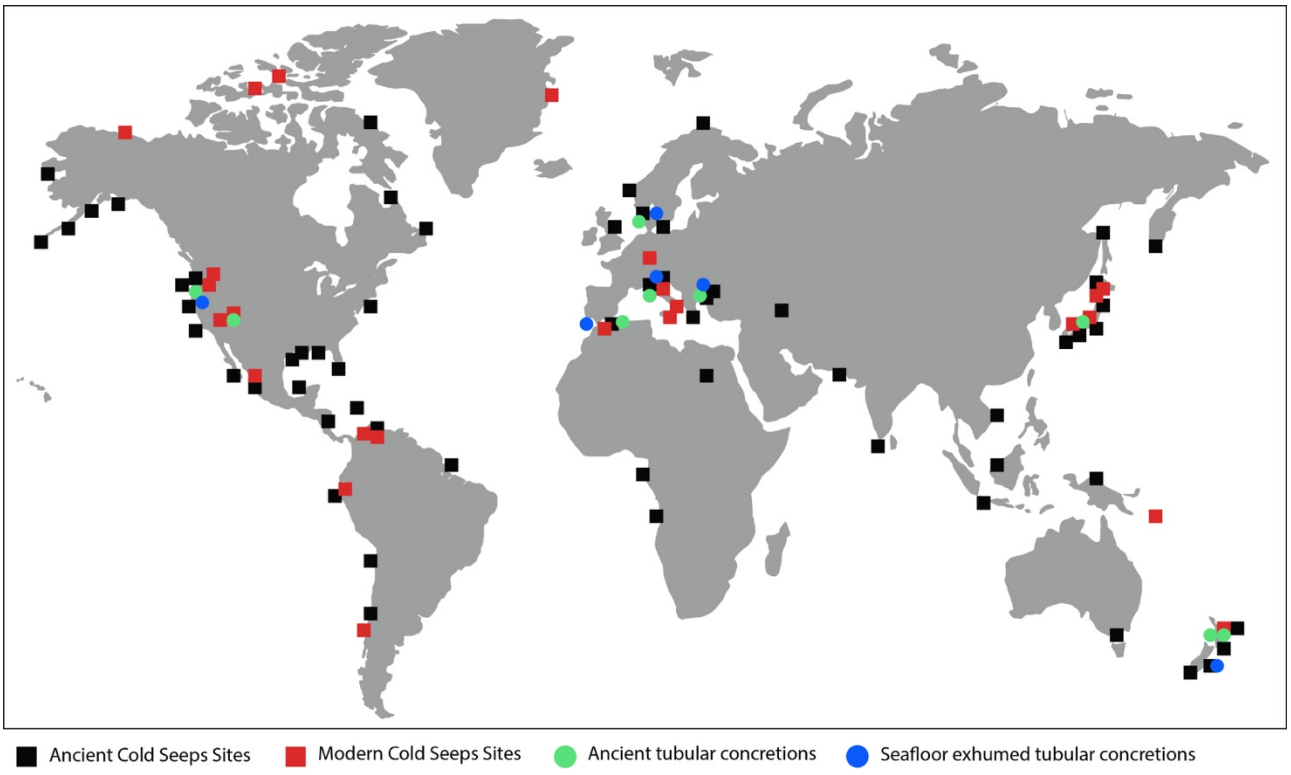

Fig 1: Map showing the global distribution of fossil and modern cold seepages and concretion site. Compiled based on references cited in this thesis.

Several studies have been recently done on the relations between the evolution of local petroleum systems and the development of fluid emissions (Bonini, 2007; Capozzi and Picotti, 2010; Oppo et al., 2013; Unterseh, 2013; Wang et al., 2015; Loyd et al., 2016). During the last years, attention has been addressed to the microbiological communities associated with the cold seeps (Reitner et al., 2005; Foucher et al., 2009; Heller et al., 2011) and to their role in degrading the hydrocarbons present in the fluids (Oppo et al. 2013 and references therein). Microbe consortia can promote different processes: the anaerobic oxidation of methane (AOM), CO_2 reduction during methanogenesis process, sulphate reduction (SR), often resulting in the formation of authigenic

carbonates (AC) (Whiticar, 1999; Boetius et al., 2000; Formolo et al. 2004, Lein, 2004; Tong et al., 2013; Saitoh et a., 2015; Wang et al., 2015; Liang et al., 2016, Loyd et al., 2016). That because in marine cold seeps environments, methane and other hydrocarbons components present in the migrating fluids are oxidised by microbial consortium of sulphate-reducing bacteria and methanotrophic archea (Boetius et al., 2000). It is known, so far, that anaerobic oxidation of methane is the main microbial process driving the precipitation of authigenic carbonate (Peckmann and Thiel 2004, Reitner et al., 2015; Loyd et al., 2016 and references therein). The extension of the phenomenon is normally determined by the environmental conditions, sedimentation rate, venting fluid flux (Luff et al., 2004; Foucher et al., 2009; Pierre et al., 2014). The authigenic carbonates occurrence is reported in different present-day marine settings, such as passive and active continental margins, as well as in the geological record (Fig.1) (Campbell et al., 2002; Magalhães et al., 2012 and references there in; Van Landeghem et al., 2015 and references therein). The carbonate constructions exhibit different morphologies: crusts, mounds, conduits and irregular bodies (Clari et al., 2004; Mazzini et al., 2006; Nyman et al., 2010; Magalhães et al., 2012; Talukder 2012; Wang et al., 2015**)**. The dimension of these bodies is very variable ranging from centimetres to few meters. Exceptionally large structures are also documented, reaching more than 10 m in length and 4 m in diameter (Nyman et al., 2010). Authigenic carbonates provide an historical record through geological eras of seepages activities and fluid migration. The geochemistry, mineralogy and isotopic signatures associated depend on the composition of the fluids and provide information on the fluids sources, their possible mixing, process of formation, paleoenvironment, depth on the sediment with respect to the sulphate-methane transition zone (SMTZ) (Peckmann and Thiel, 2004; Magalhães et al., 2012; Pierre et al., 2014; Reitner et al., 2015; Oppo et al., 2015; Loyd et al., 2016). The area of interest of this thesis are the Northern Apennines, in Italy. In this area, during the last centuries, accurate lists and numerous descriptions of fluid seepages occurring in the Northern Apennines have been compiled (Spallanzani, 1795; Stoppani, 1871; Scicli, 1972; Ferrari and Vianello, 1985). An increased interest was documented during the last years on the natural emissions, such as mud volcanoes, and on their correlation with oil and gas fields occurring in the reservoirs of the Northern Apennines hydrocarbon province (Martinelli and Rabbi, 1998; Martinelli and Judd, 2004; Capozzi et al., 2006; Bonini, 2007; Picotti et al., 2007; Capozzi and Picotti, 2010; Oppo et al; 2013). Because of this concern, many studies have been carried out on the geochemistry of the emitted fluids (Mattavelli et al., 1983a; Minissale et al., 2000; Capozzi and Picotti, 2002, 2010; Oppo et al 2013). This is the first time that is possible to compare still seeping fluids migrating in a well known system with fossil authigenic carbonates originated by them during

Pleistocene. This work wants to find a pack of geochemical analysis that, coupled with morphologies characterisation, geology and stratigraphy settings and embedding sediments characterisation can give precise information on the fluids and processes promoting carbonates precipitation. This integrated geological stratigraphic and geochemical combination of data, in this area is supported by the integration with direct analysis on fluids, but the forward objective is to understand if, in a authigenic carbonates site characterised by the absence of the possibility to reach directly the original fluids, this approach will give the same informations about fluid characteristics and formation processes.

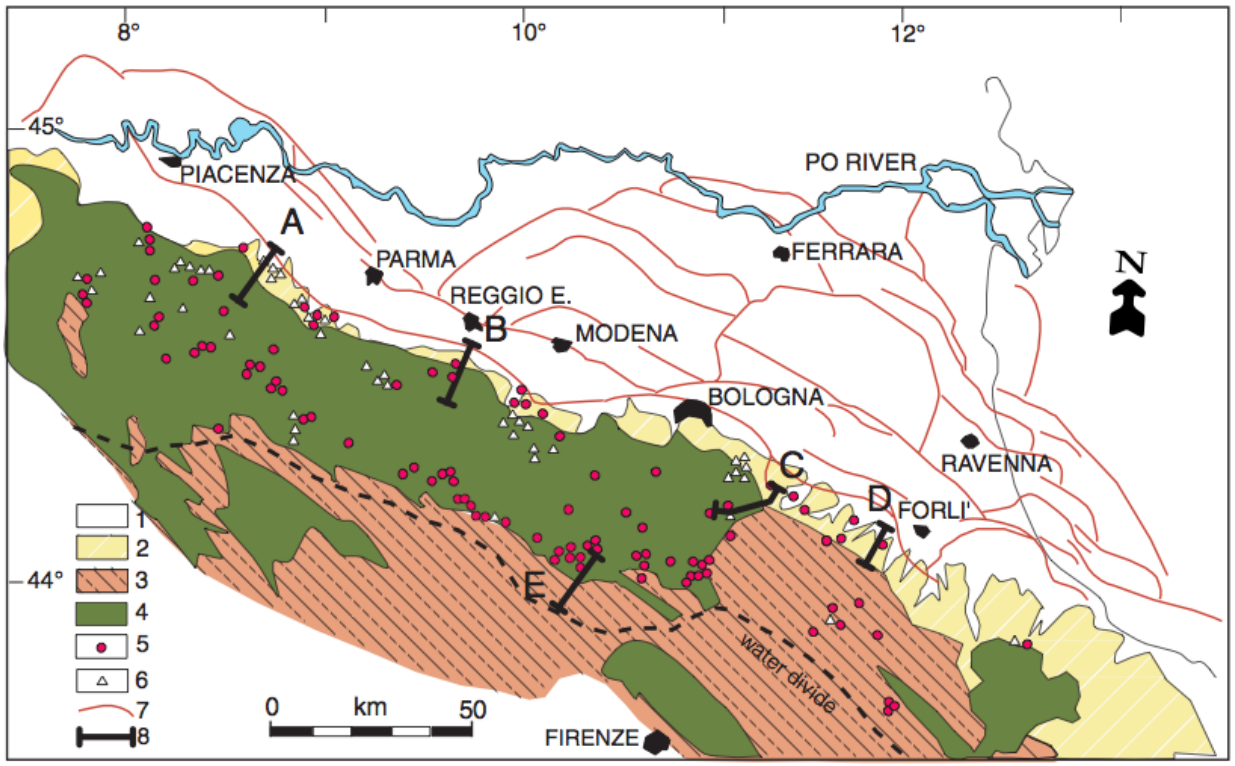

Fig. 2: Geological sketch map and locations of the fluid emissions of the Northern Apennines (after Capozzi and Picotti 2010). Legend: 1. Continental Quaternary; 2. marine to continental Plio-Pleistocene foredeep units at the foothills; 3. Miocene foredeep units; 4. Ligurian – Epiligurian units; 5. spontaneous fluid emissions and 6. oil and gas from surficial drilled wells; 7. thrust front in the subsurface.

In the study area of the Northern Apennines, cold seeps are roughly aligned along two bands striking northwestwards, located close to the main water divide and along the foothills (Fig.2). In this sector of the Northern Apennines the fluids migration is related with the regional tectonic deformations and with the burial, mainly caused by the upper tectonic nappe of the chain (the Ligurian Units) (Oppo et al., 2013 and references therein). In the same area, there are three outcrops where authigenic carbonates occurs: Enza River field, Stirone River field and Secchia River field. In all the outcrops authigenic carbonates and sedimentary succession are exposed along the

riverbanks thanks to fluvial erosion. The hosting sediments belongs in all the outcrops to the Argille Azzure Plio-Pleistocene marine successions deposited before the foothills uplift and emersion, in different conditions from upper slope to shelfal water depth (Gunderson et al., 2014; Oppo et al., 2015; Viola et al., 2015; Cau et al., 2015). Different morphologies and shapes have been found: slabs, globular concretions and chimneys representative of different paths of gas seeping from the reservoir to the seafloor, of porosity and permeability of the sediments (Cau et al., 2015; Viola et al., 2015; Oppo et al., 2015 and Viola et al., submitted). Associated to the carbonate fields has been noticed the presence of spontaneous still active seeping and deep wells connected to the deep Miocene reservoirs (Oppo et al., 2013 and references therein). The aim of this thesis is to identify and understand the different fluid sources that promoted the carbonate precipitation and discern seawater and deep fluids contribution in AC formation using isotope measurements. This is a rare case of study where it is possible to compare still active fluid migration system, from a known petroleum system, to fossil authigenic carbonates. In particular, in this project new geochemical data have been collected on formation waters and on the authigenic carbonates, with the aim to have a better chemical and isotopic characterisation of the waters and identify isotopic signals that could be recorded in the carbonate formation as indicative of fluid sources. Geochemical, mineralogical and isotopic analysis on sediments, carbonates and waters has been carried out during this three years PhD project. In particular, to determine how fluids, deriving from reservoirs at different depth with different type of methane and different geochemical and isotopic signatures, can influence the formation process, mineral composition, chemical composition, shape and isotopic signature of carbonate bodies in the three outcrops. Furthermore, to the challenge is to understand if the different fluid sources can be assessed ad to quantify the mixing between different fluid sources. Focusing of these objectives, the work has followed different steps:

- Geochemical, mineralogical and isotopic characterisation of the carbonates recovered in the three study outcrops.

In particular X-Ray Diffraction and X-Ray Fluorescence has been performed to have a geochemical characterisation. Petrographic observations on thin sections and Scanning Electronic Microscope observations on fresh broken Au-coated fragments has been done. Oxygen, carbon, and strontium isotopes have been chosen for measurement on selected samples.

- Geochemical and isotopic characterisation of fluids.

In addition to field parameters, Eh, Ph, T and conductivity, anion and cations analysis were measured on water samples coupled with the characterisation of gas and hydrocarbons present in

the fluids. Oxygen, carbon, strontium and sulphur isotopes have been chosen for measurement to be comparable with AC.

- Comparison, in terms of mineralogy, geochemistry and isotopic signatures, between carbonates with different morphologies in the same outcrop.
- Comparison among carbonates across the three different outcrops.
- Comparison between stable isotope signatures in AC and the different possible water source: connate waters, nowadays seawater, Pliocene seawater, Pleistocene seawater; depending on the outcrop considered.
- Understand different fluid supply, marine vs connate waters, using oxygen fractionation factor, strontium isotope signature and sulphate isotope.

The results expected from this project can provide powerful tools for regional exploration strategy and a validation of previous works.

1.2 Authigenic Carbonates

The term "Authigenic" refers to a mineral or sedimentary rock that is deposit "in situ", where it is found and observed. In this thesis, the study is limited on a specific type of authigenic carbonates that from in interstitial pores associated to the fluid emission. Authigenic carbonates are, in general, formed by evaporitic deposition or by chemical precipitation in marine and fresh waters. Oceanic authigenic carbonates are classified according to the origin of carbonate carbon source, evaluated through several methods of sedimentary petrography, mineralogy, isotope geochemistry, and microbiology. Aragonite, low magnesium calcite, high magnesium calcite, stoichiometric and non-stocihiometric dolomite predominate among the authigenic carbonates. Their formation is driven by process that must involve a carbon source, from ancient sedimentary rocks, methane and hydrocarbon rich fluids, gas hydrates, organic matter decomposition and bicarbonate-ion of hydrothermal fluids into the modern carbon cycle. The first important study on authigenic carbonates by Strakhov (1951) focused on formation mechanisms of diagenetic carbonates in Black Sea sediments and identified the role of CO_2 coming from organic matter decomposition as carbon source during carbonate formation. After the 1960s the interest about authigenic carbonate formation processes increase with the discover of the methane-derived authigenic carbonates (MDAC) that are related to methane oxidation process in the oceanic sediments and the study on these carbonates in association with gas seeps started (Nissenbaum, 1984). This type of authigenic carbonates is marked by the presence and development of unique biological communities (Sibuet

and Olu, 1998) and by the large variability of their morphologies, including carbonate buildups ("chimneys" or "reefs"), plates, crusts, and so on (Lein, 2004; Magalhães et al., 2012). Their formation is a major process of interaction of organic and inorganic carbon cycles with the calcium cycle. The authigenic carbonates belonging to the three outcrops considered in this thesis originated in marine condition in association with fluid migration, seeping of methane rich fluids and CO_2. Authigenic carbonates that form in marine sediments can be divided in four type, by Lein 2004, according to the geochemistry, mineralogy and isotopic signatures characterising each type.

- Type I: Authigenic diagenetic carbonates formed due to the decay of microbial organic matter in sediments

  These carbonates are characterised in literature by the presence of small anhedral and euhedral crystals and crystalline aggregates of carbonates minerals paragenetically associated with sulphides that can also be found as aggregates forming crusts and nodules (Lein et al., 1986). Usually the mineralogical composition is given by aragonite, low-magnesium calcite, high-magnesian calcite and protodolomite. The signature of the carbon isotope is depleted respect to the normal seawater signature. The formation of authigenic carbonates in a constant paragenesis with sulphide mineralization is related to microbial reduction of sulphate ion in seawater and pore water accompanied by the extraction of isotopically light bicarbonate and hydrogen sulphide according to the reaction:

  (1) $$SO_4^{2-} + 2C_{org} + H_2O \longrightarrow H_2S + 2HCO_3^-$$

  This reaction leads to increase total alkalinity due to the appearance of H_2S, its hydrolysis, and carbonate precipitation. High concentration of bicarbonate ion and precipitation of calcium and magnesium carbonates from the pore water of reduced sediments are documented in sediment cores where active microbial sulphate reduction is observed (Spadafora et al., 2010). The average contribution of dispersed authigenic carbonate minerals to the total carbonate carbon is about 40% (Lein et al., 1986). Nodules and crusts have same mineralogy and same negative signature on $\delta^{13}C$ (Lein, 2004). These carbonates were formed from the carbon dioxide as a result of the decomposition of organic matter (OM) buried in sediments and sulphate reduction (Bontognali et al., 2010). They often served as a hard substrate for oysters and other benthic animals, whose remains occur on the

nodule surface. Reduced sediments from the Gulf of California and the Pacific margin off Mexico are considered a typical model that illustrates the formation of dispersed diagenetic carbonates and carbonate nodules due to active decay of microbial OM and carbon dioxide generation during the reduction of marine sulphate ion (Lein, 2004 and references therein). Reduced sediments of the Black Sea represent another spectacular example of the formation of metabolic carbon dioxide in pore water and dispersed authigenic carbonate in sediments. The upper mud layer, where the contribution of CH_4 carbon to total ΣHCO^{-}_{3} does not exceed 10%, is characterised by a high sulphate reduction rate (Jorgensen et al., 2001; Lein et al., 2002). The formation of this carbonate, due to microbial decomposition of organic matter, has been found mostly in reduced Quaternary terrigenous sediments on shelf and continental slope of ocean and marginal and internal seas.

- Type II: Methane –Derived Authigenic Carbonates (MDAC)

In these carbonates, as the name suggest, biogenic and/or thermogenic methane, serve as main carbon source during the formation. Most of the samples studied in this thesis belong of this type of carbonates with the only exception of the Secchia River globular concretion, that are connected to the methanogenesis instead of methane oxidation. Methane seeps are related to specific tectonic and geomorphological processes of large scale in the marine setting. These carbonates needs a source of methane that permeate the sediments and promote the process. Usually, the source is associated with the seeping phenomenon of methane rich fluids coming from deep reservoirs, methane gas hydrates, mud volcanoes structures and microbial decomposition of organic matter (Hensen et al., 2007; Scholz, et al., 2009, Loyd et al., 2016). The methane seeps studied so far show that microbial activity is mandatory for methane oxidation. The mechanism is anaerobic methane oxidation exerted by different groups of anaerobic microorganisms (Loyd et al., 2016 and references therein). Based on laboratory experiments with pure methanogenetic bacterial cultures the authors demonstrated that if substrates (CO_2) is exhausted and the methane content is high, methanogenesis start to perform methane oxidation, according to the reaction:

(2) $$CH_4 + 2H_2O \longrightarrow CO_2 + 4H_2$$

Since this process proceeds very slowly in pure cultures because of the hydrogen accumulation,(Reeburgh and Alperin, 1988; Valentine and Reeburgh, 2000) the reaction (2) occurs in simultaneous with the sulphate-reduction reaction (3):

(3) $$4H_2 + SO_4^{2-} + H^+ \longrightarrow HS^- + 4H_2O$$

In natural anaerobic ecosystems this implies the involvement of sulphate-reducing bacteria (Reeburgh and Alperin, 1988; Valentine and Reeburgh, 2000). The sum of equations (2) and (3) results in the real mechanism of Anaerobic Methane Oxidation (AOM) coupled with sulphate reduction (SR):

(4) $$CH_4 + SO_4^{2-} \longrightarrow HCO^-_3 + HS^- + H_2O$$

Only methane oxidation coupled with sulphate reduction increases alkalinity. The alkalinity production fostered by eq. 4 sustained by the relatively high concentration of sulphate in seawater promotes extensive carbonate (and sulphide) mineral production near methane seeps. Complex microbial consortia, microflora, including sulphate reducers, aerobic methanotrophs, and large filamentous microorganisms morphologically similar to methanogens, facilitate sulphate reduction-coupled methane oxidation yielding extensive and generally rapid authigenic carbonate production in cold seep environments. The MDAC are characterised by different morphologies, such as crusts, pavements, chimneys, slabs and concretions depending mostly on the fluid flux, sources and porosity. Typical mineral composition of the carbonate fraction depend on the magnitude of the microbial mediation, the flux and the interaction between the fluid source and the seawater, the cementation degree and the diagenesis; the characteristic mineralogical phases are aragonite, calcite, high magnesium calcite and dolomite. The fabric in MDAC is micrite cementing detrital fraction of sandy grains, clay minerals and biological remains. The carbon isotopic composition of carbonate buildups is a mixture of isotopically light carbon formed during the methane oxidation and isotopically heavier bicarbonate carbon of seawater. In those carbonates enrichment of $\delta^{18}O$ respect to the seawater signature is due to the gas hydrates disaggregation interference, the dolomite formation as carbonate facies or to isotopically heavy seeping fluids (Vanneste et al., 2012). When carbonates are found in close paragenesis with authigenic pyrite indicates a reduced formation environment, Eh around -300mV, SO_4

depletion permits carbonate formation in association with this mineral. This is the typical condition of the Sulphate-Methane Transition Zone (Magalhães et al., 2012; Viola et al., 2015 and references therein).

- Type III: Authigenic carbonates formed during the microbial oxidation of hydrothermal methane

Hydrothermal methane fluxes are well known and studied around the world. The precipitation of authigenic carbonates formation can be related to hydrothermal fields (Whiticar, 1999; Campbell et al., 2002; Levin et al., 2012). These AC, like type II, are fine grained carbonates that cements terrigenous sediments. The most abundant mineral phase that characterise type III is aragonite, with minor presence of low and high magnesium calcite. Different morphologies have been found associated to hydrothermal fluid discharge, like chimney, crusts and pavements. The $\delta^{13}C$ values in the fine-grained carbonate, which cements terrigenous material of surface sediments are negative but less depleted with respect to the type II (Ohmoto and Goldaber, 1997). This can be explained by the microbial oxidation of CH_4, SO_4 and other compounds and the influence of chemosynthetic fauna interaction, that colonise the carbonate hard substrata (Kelley et al., 2001). The type III formation could be representative of a large-scale process at site of hydrothermal fluid discharge in mid-oceanic ridges (Olu et al., 1996). Is important to understand that in this case, methane and carbon dioxide of the fluids are not necessarily the carbon sources of the carbonates, they just promote the microbially mediated precipitation process (Lein et al., 2007; Levin et al., 2012 and references therein).

- Type IV: Authigenic carbonates formed during the mixing of hydrothermal fluid with seawater

This type is represented from the new discovered Lost City field. It is located 15km away from the Middle-Atlantic Ridge junction with the Atlantis transform fault. Around 30 light-colored carbonates columnar buildups rising above the carbonate platform. The columns are up to 60m high and 10m of diameter. The mineral composition of the carbonate fraction is mostly aragonite with minor calcite, brucite and Na-Ca carbonates. These columnar carbonates represent a new phenomenon in the ocean, the formation is related to a strongly altered hydrothermal water mixed with normal seawater that discharge at seafloor with very

high flux. This solution is characterised by alkaline pH (over 8), low concentration of Mg^{2+} and SO_4^{2-}, enrichment of Ca^{2+} up to two times normal seawater value and general increase of Cl^-, Na^+, Ba^{2+} ions, also CH_4, H_2S and H_2 are present in solution. Signatures of Sr, H, C and O isotopes prove that the mixing in the formation between this fluid and the normal seawater has a predominance of the last member. At discharge sites of the low-temperature fluid, buildups are overgrown with dense microbial mats composed of various microbial groups dominated by H_2S-oxidizing bacteria (Lein et al., 2002b; Proskurowski et al., 2006 and references therein). Bright white jellylike accumulations of microorganisms and their metabolism products (primarily, mucus) are widespread in the internal part of columns, especially on flat buildup summits with flickering warm water outflows. Active processes of microbial CO2 assimilation and methane oxidation are detected in jellylike clots (Lein 2004; Kelley et al., 2005; Dara et al., 2009). Considerable amounts of CO2, CO and hydrocarbons have been identified in fluid inclusion of the carbonates. The formation process in this case is characterised by the presence of methane rich hydrothermal fluid and high presence of hydrogen. The precipitation of these peculiar carbonates happens when the ascending hot hydrothermal solution, enriched in methane and hydrogen meets the oceanic bottom water and cools down (<100°C). As result, the fluid composition change to form a secondary mixed solution. In this second fluid, metals are mostly absent, but it contains minor Mg2+ and SO42- due to the mix with seawater. Low sulphate concentration in the Lost City solution, respect to the surrounding seawater, means that there is a hydrogen sulphate reduction going on in the mixing zones ad opera of thermophile microbes

(5) $$CaSO_4 + 4H_2 \longrightarrow CaS + 4H_2O$$

Then the hydrolysis of calcium sulphide

(6) $$CaS + 2H_2O \longrightarrow H_2S + Ca(OH)_2$$

and permit to increase the pH and to free Ca^{2+} to have favourable condition for calcium carbonate precipitation (Lein, 2004; Dara et al., 2009 and references therein).

1.3 Isotopes Fractionation Processes

The partitioning of isotopes between two substances or two phases of the same substance with different isotope ratios is called isotope fractionation. The main phenomena producing isotope fractionations are isotope exchange reactions (equilibrium isotope distribution) and kinetic processes that depend primarily on differences in reaction rates of isotopic molecules.

1.3.1 Isotope Exchange

The term isotope exchange is used for all situations, in which there is no net reaction, but the isotope distribution changes between different chemical substances, between different phases, or between individual molecules. Isotope exchange reactions are a special case of general chemical equilibrium. The partition function in this case is temperature controlled. For geologic purposes the dependence of the equilibrium on temperature is the most important property. In principle, isotope fractionation factors for isotope exchange reactions are also slightly pressure-dependent because isotopic substitution makes small change in the molar volume of solids and liquids (Hoefs, 2009 and references therein). Of special interest in stable isotope geochemistry is evaporation–condensation process, because differences in the vapour pressures of isotopic compounds lead to significant isotope fractionations. Lighter molecular species are preferentially enriched in the vapour phase, the extent depending upon the temperature. As condensation or distillation proceeds, the residual vapour or liquid will become progressively depleted or enriched with respect to the heavy isotope (Faure, 1998; Hoefs, 2009 and references therein).

1.3.2 Kinetic Effects

The second main phenomena producing fractionations are kinetic isotope effects, which are associated with incomplete and unidirectional processes like evaporation, dissociation reactions, biologically mediated reactions, and diffusion. The latter process is of special significance for geological purposes (Faure, 1998). A kinetic isotope effect also occurs when the rate of a chemical reaction is sensitive to atomic mass at a particular position in one of the reacting species. Many observed deviations from simple equilibrium processes can be interpreted as consequences of the various isotopic components having different rates of reaction. Isotope measurements taken during unidirectional chemical reactions always show a preferential enrichment of the lighter isotope in the reaction products, this enrichments due

to the kinetic effect in carbonates is detectable thanks to a co-variation of $\delta^{13}C$ and $\delta^{18}O$ (Mickler et al., 2006; Hoefs, 2009 and references therein).

1.3.2.1 Mass Dependent Fractionation

At thermodynamic equilibrium, isotope distributions are strictly governed by relative mass differences among different isotopes of an element. Mass dependent relationships govern many kinetic processes as well. Thus for most natural reactions, isotope effects increase because of isotopic mass differences. This means that for an element with more than two isotopes, such as oxygen or sulphur, the enrichment of ^{18}O relative to ^{16}O or ^{34}S relative to ^{32}S is expected to be approximately twice as large as the enrichment of ^{17}O relative to^{16}O or as the enrichment of ^{33}S relative to ^{32}S. Different mass dependent processes (e.g., diffusion, metabolism, high temperature equilibrium processes) can deviate this rule and follow slightly different mass dependent fractionation laws (Young et al., 2002; Miller, 2002; Farquhar et al., 2003). These very small differences are measurable (Luz et al., 1999; Young et al., 2002; Farquhar et al., 2003).

1.3.3 Diffusion

Diffusion can cause significant isotope fractionations. In general, light isotopes are more mobile and hence diffusion can lead to a separation of light from heavy isotopes. Ideal diffusion isotope effect is more or less limited to ideal gases, where collisions between molecules are infrequent and intermolecular forces are negligible; in natural processes the isotope fractionation is higher (Cerling 1984; Hesterberg and Siegenthaler 1991). Beside ordinary diffusion, thermal diffusion must be considered. Here temperature gradient results in a mass transport; the greater the mass difference, the greater is the tendency of the two species to separate by thermal diffusion, until 1000°C where isotope fractionations appear to be negligible (Hoefs, 2009 and references therein). In solutions and solids, the relationships are much more complicated than in gases. Diffusive-penetration experiments indicate a marked enhancement of diffusion rates along grain boundaries, which are orders of magnitude faster than for volume diffusion. Thus, grain boundaries can act as pathways of rapid exchange. Volume diffusion is driven by the random temperature-dependent motion of an element or isotope within a crystal lattice and it depends on the presence of point defects, such as vacancies or interstitial atoms within the lattice. This solid-state diffusion is yet under exploration and is very difficult to estimate (Hoefs, 2009 and references therein).

1.3.4 Pressure

It is commonly assumed that temperature is the main variable determining the isotopic fractionation and that the effect of pressure is negligible, because molar volumes do not change with isotopic substitution. This assumption is generally fulfilled, except for hydrogen and peculiar natural situation where the pressure is the main factor (Hoefs, 2009).

1.3.5 Chemical Composition

Qualitatively, the isotopic composition of a mineral depends mostly on the nature of the chemical bonds within the mineral and in minor degree upon the atomic mass of the respective elements. In general, bonds to ions with a high ionic potential and small size are associated with high vibrational frequencies and have a tendency to incorporate preferentially the heavy isotope (Chacko et al. 2001).

1.3.6 Crystal Structure

In geochemistry, is important to consider the structural effects affecting the fractionation according to the crystal structure forming. Those are secondary in importance to the ones arising from the primary chemical bonding; the heavy isotope being concentrated in the more closely packed or well-ordered structures. For example the $\delta^{18}O$ and D fractionations between ice and liquid water arise mainly from differences in the degree of hydrogen bonding (order). A relatively large isotope effect associated with structure is observed between graphite and diamond (Bottinga 1969) and in dolomite (Budd, 1997).

Isotopic signatures analysis is very important in this study because this is a quite rare possibility to compare isotopic signatures of fossil authigenic carbonates with the ones from gas and fluids that are still seeping to the surface nowadays. These fluids, in fact, are coming from the same reservoirs that fed the marine basin in the Northern Apennines area during former carbonate formation.

Carbon ($\delta^{13}C$)

Carbon isotopes fractionate depending on temperature, pressure and environment is very well known (Zhang and Krooss, 2001). Carbon isotope is largely used to understand the carbon source linked to the fluid that promoted the carbonate precipitation (organic matter decomposition, thermogenic methane, biogenic methane, gas hydrate melting, etc) and the type of hydrocarbon present in the fluids (methane, butane, ethane, carbon dioxide, etc.)

(Wang et al., 2008; Lapham et al., 2010; Roberts et al., 2010). This is the most important isotope to be considered in this kind of study on seeps associated with carbonate precipitates. There are mainly four carbon phases that should be considered in the environment: CO_2, HCO_3^-, CO_3^{2-} and the C coming from the hydrocarbon-rich fluids, like in our case of study. The temperature, mostly, and pressure, partially, equilibrium dependent variations, allows the formation and the stability of the carbonates in the different mineral phases, with different $\delta^{13}C$ signatures according to the fractionation going on and the carbon source (Hoefs, 2009).

Oxygen ($\delta^{18}O$)

The study of the oxygen stable isotopes is important to understand the formation processes of the rocks and the sources of the oxygen; $\delta^{18}O$ gives information on temperature, the depth of formation, the type of fluids and of mineral phases originated (Vasconcelos et al., 2005; Gabitovet al., 2012; Antler et al., 2013). In marine environment, its fractionation is strictly linked with the fluid composition (Aharon and Fu, 2000; Gabitov et al., 2012) and mineral phase originated, in fact dolomite tend to be enriched in this isotope (Budd, 1997). It is also a very clear indicator for gas hydrates melting events (Magalhães et al., 2009; Demirbas, 2010). Due to the strict dependency to the temperature, this isotope is commonly used to estimate paleo-temperature during carbonate formation (Vasconcelos et al., 2005) and to understand paleo-climatic changes and paleo oceanography (Ravelo and Hillaire-Marcel, 2007).

Radiogenic Strontium ($^{87/86}Sr$)

This element is incorporated as minor element during the formation of the carbonate. Because it is a conservative element, strontium isotopes can be used to characterise the origin of strontium in carbonate because such rocks will generally record the $^{87/86}Sr$ of the source waters (seawater as well as groundwater or meteoric water) at the time of deposition as well as during diagenesis (Paytan et al., 1993; Price and Gröcke, 2002). If the $^{87/86}Sr$ of the present carbonate rocks is significantly different from that of the contemporaneous seawater, the carbonates should have been altered by waters containing $^{87/86}Sr$ derived from outside the actual system, such as different fluids (Burke et al., 1982; Faure, 1986; Armstrong-Altrin et al., 2009). Knowing the signature of $[^{87/86}Sr]_{fluid}$ or the $[^{87/86}Sr]_{carbonate}$ is possible to know the original composition of the water, if there was some additional sources

and estimate the mixing between different fluid sources (Faure, 1998; Ussler, 2001, Armstrong-Altrin et al., 2009). Sr isotopes are particularly useful to assess the interaction between fluids and rocks; especially in marine environment the carbonate formation is in relation to fluid escape, like CO_2 or methane rich, where the Sr in the carbonate reflect the source signature (Joseph et al., 2012).

Sulphur ($\delta^{34}S$)

The sulphur isotope is one of the most interesting isotope to measure when microbial sulphate reduction is going on. Two mechanisms are responsible for S fractionation: microbial processes in which micro-organisms with metabolism based in sulphate reduction fractionate the isotopes of this element; and chemical exchange reactions between sulphate and sulphides in closed and open systems, especially during thermogenic sulphate reduction (Hoefs, 2009). Bacterial sulphate reduction is responsible for the majority of oxidation of organic matter in marine sediments (Kasten and Jørgensen, 2000). In addition, the majority of the methane produced during methanogenesis in marine sediments is oxidised anaerobically by sulphate reduction (Niewöhner et al., 1998; Antler et al., 2013 and references therein). Usually bacterial sulphate reduction is characterised by large and heterogeneous ^{34}S-depletion confined to the bacterial activity areas (Ono et al., 2006, 2007). This magnitude is a function of microbial metabolism and carbon source (Brüchert, 2004 and Sim et al., 2011), amount of sulphate available (Canfield, 2001 and Habicht et al., 2002), and temperature (Canfield et al., 2006). In addition, previous studies also noted a relationship between the magnitude of the sulphur isotope fractionation and the sulphate reduction rate (Antler et al., 2013). This relationship has been shown in pure culture experiments (Canfield et al., 2006), batch culture experiments using natural populations (Stam et al., 2011) and calculated in situ using pore fluids profiles (Antler et al., 2013 and references therein). This isotope can give also indication on of the depth of carbonate formation: over, below or inside the Sulphate-Methane Transition Zone (SMTZ) (Magalhães et al., 2012). According to Borowski et al., (2013), ^{34}S-enriched authigenic sulphide minerals cab be considered as a proxy that should point out elevated methane flux and gas hydrates in the geologic record.

2. Geological setting

The study area belongs to the northwestern Northern Apennines foothills, along the Po Plain side, where fluvial incisions, through Plio-Pleistocene successions, exposed a significant number of authigenic carbonates.

2.1 Northern Apennines

The Northern Apennines are a fold-and-thrust belt resulting from the collision between European and Adriatic Plates.

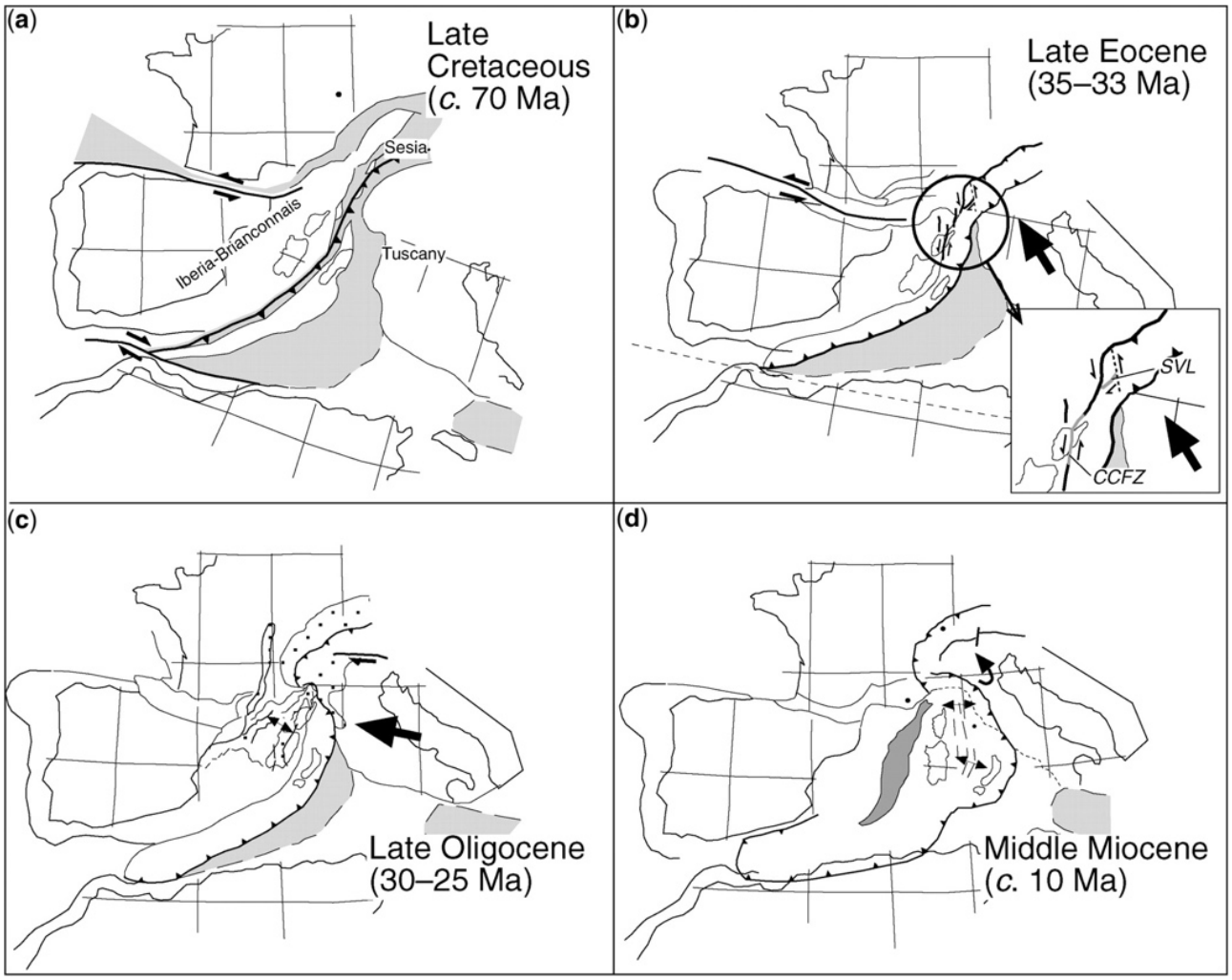

Fig.3: Sketch of the orogenetic evolution of the Apennines (after Molli, 2008).

In the first phase of the chain formation there was the opening of the Balearic Basin (Oligocene) and the rotation of the Corsica-Sardinia Block in the present-day position (Vai and Martini, 2001 and references therein) (Fig. 3). The second phase of the deformation was instead linked with the opening of the Tyrrhenian Sea (Miocene to Pliocene). The tectonic evolution of the area was

controlled by the inversion of the dipping of the subduction plane during middle Eocene: this change in dipping brought the Adriatic plate to subduct below the European lithosphere (Faccenna et al., 2001; Marroni et al., 2010; Molli and Malavieille, 2011; Balestrieri et al., 2011). The Oligo-Miocene collision between Adria and the Corsica-Sardinia block rearranged the Jurassic-Eocene units belonging to the Ligurian deformed oceanic wedge, which progressively thrust over the foredeep successions of Miocene age, forming the Ligurian Nappe (Zattin et al., 2002). In the Po Plain side of the Northern Apennines, the Ligurian Nappe shows a wedge-shaped closure along the foothills with a gravitational reworking at its tip. Today, the exhumed fossil accretionary prism is represented by the Ligurian Units, which occupy the topmost part of the Apennine tectonic pile. Ligurian unit underwent to a first deformation phase, during the the Eocene, which was responsible for the deformation of the Ligurian Meso-Cenozoic accretionary wedge. The inner, southwestern part of the prism is represented by the so-called Internal Ligurian Units, which are composed of ophiolites with their pelagic/hemipelagic and terrigenous turbiditic sedimentary cover (Marroni and Pandolfi, 1996; Marroni et al., 2004, 2010). The northeastern part of the prism is instead formed by the External Ligurian Units, composed of off-scraped and frontally accreted mud-rich sediments with thick piles of calcareous or siliciclastic turbidites of Late Jurassic–Early Cretaceous to early-middle Eocene age (Vannucchi and Bettelli, 2002; Bettelli and Vannucchi, 2003; Marroni et al., 2010). On top of the Ligurian accretionary prism there is a sedimentary cover of marine units, the satellite basin deposits of the Epiligurian successions (Ricci Lucchi and Ori, 1985). The underthrusting Adria plate was composed of the Tuscan and Umbria-Romagna successions (Vannucchi et al., 2008, and references therein) (Fig. 4). The Adriatic slab retreat toward NE led to the formation of a migrating foredeep and the opening of the Tyrrhenian back arc basin (Elter et al., 1975; Malinverno and Ryan, 1986). The foredeep deposits, underlying the Ligurian nappe, have been progressively incorporated into the orogenic belt. Folds and thrusts in the foredeep succession formed during and after the tectonic and gravitational emplacement of the Ligurian Nappe.

The chain deformation slowed down and a diminution of the movement of the Ligurian units above the foredeep until the complete stop mainly during the Messinian age. Recent studies showed that the major parts of the Apennines foothills are affected by recent tectonic activity due high-angle normal faults (Picotti et al., 2009), whereas the chain record the activity of deep thrust that deforms the Ligurian nappe until Holocene continental deposits (Picotti e Pazzaglia, 2008). Plio–Pleistocene marine deposits in which AC fields occur are located at the Northern Apennines foothills.

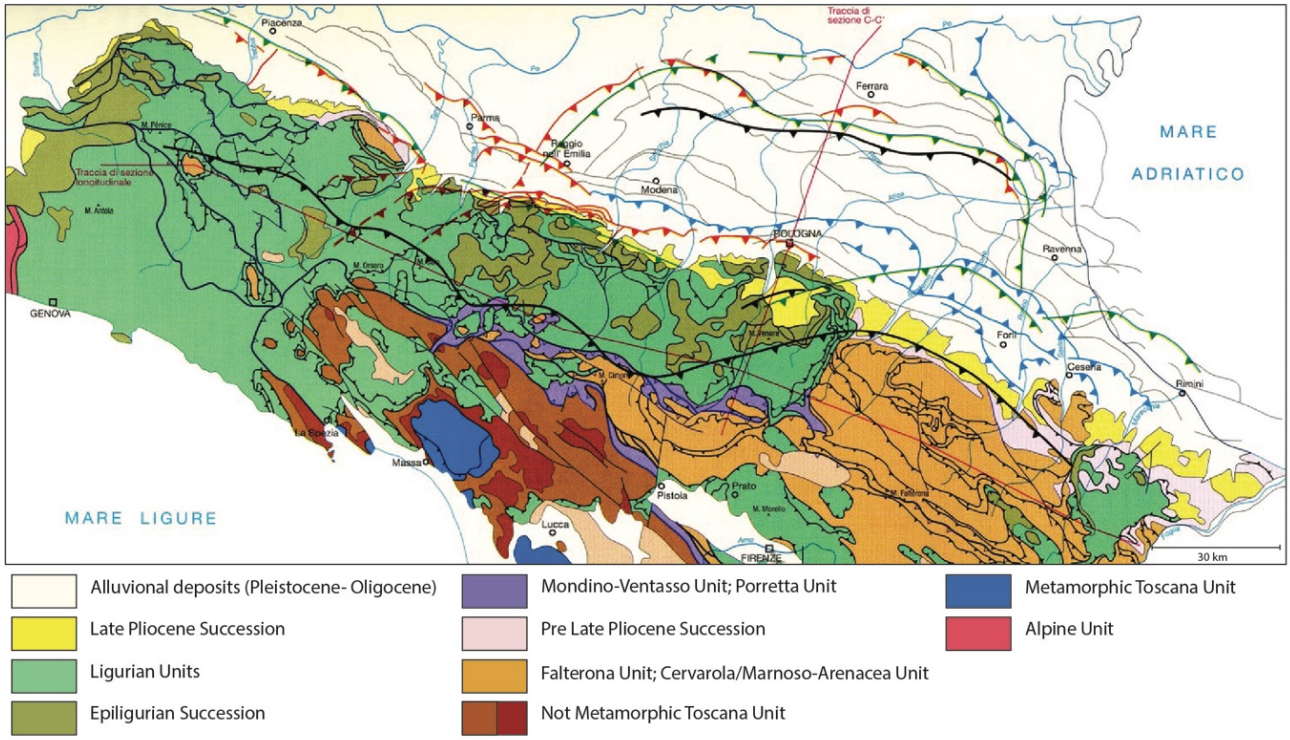

Fig. 4: Geological map of the Northern Apennines and surrounding areas (modified after Boccaletti et al., 2004)

2.2 Northern Apennines Petroleum System

Natural seeps have long been considered as indicators of shallow or deep reservoirs and are very useful for exploration purposes. Fluids seeping occur when favourable condition for tertiary migration has been achieved after expulsion from source rocks, migration and accumulation within stratigraphic and structural traps. The present study focused on active tectonic areas in the Northern Apennines where fluid migration pathways are related to the stratigraphic and structural evolution and it is crucial to understand the different steps of this evolution. To study in detail authigenic carbonate formations, linked to hydrocarbon seepages it was applied a multidisciplinary analytical approach, including petrography, stable isotopic composition, elemental composition and biomarkers, allowing to define the relationships between the present setting and the geologic evolution leading to generation, expulsion and migration of hydrocarbons.

In the Northern Apennines, geochemical analysis on hydrocarbons, saline waters and brines from natural seeps and drilled wells have been carried out in association with the reconstruction of surface and subsurface geology. This study provided new data for the exploration and characterisation of the tectono-thermal evolution of the petroleum system of the Northern Apennines (Picotti et al., 2007; Capozzi and Picotti, 2010; Oppo et al., 2013) that have been poorly explored, due to the insufficient cover or bad results of reflection seismic. The Northern Apennines was usually considered a single petroleum province (e.g. Lindquist, 1999), or as a triple system,

with biogenic gas, thermogenic gas and oil belonging to different geodynamic settings, from the shallower and external (Po Plain) for the biogenic gas, to the deeper and internal ones for the thermogenic gas and oil (Bertello et al., 2008). The recent studies led to identify an extreme variety of the natural settings, where fluids leak out from reservoirs of different ages, which are deformed at different times and as a consequence of different stress regimes (compressional or late-orogenic extensional). A new scenario for the Northern Apennine petroleum system was proposed by Capozzi and Picotti (2010) and Oppo et al. (2013) and a common source rock, located in the deeper Late Cretaceous units, was indicated as feeding the Miocene reservoirs. This deeper source rock can account for the accumulation of the observed hydrocarbons and for their homogeneity in the different reservoir structures and for the generation of significant volumes of hydrocarbons that fed Miocene ages structural traps, buried also in the portion of the Po Plain close to the foothills.

In this study the main focus for understanding the fluids sources at the origin of authigenic carbonate formations was addressed to connate saline waters and gas migrating from the reservoirs. The hydrocarbons and mud volcano fields along the western Northern Apennine foothills are always associated with connate saline waters (Capozzi and Picotti, 2010). The hyper saline water recovered from deep wells in the Salsomaggiore reservoir shows chemical and isotopic characteristics that are consistent with a deep-burial diagenesis, interaction with the solid phase and the microbial activity related to the hydrocarbon occurrence and the exchanges between water and oil (Oppo et al., 2013). On the other hand, the mud volcano waters show a significantly lower salinity due to the filtration mechanism occurring during the migration through the sealing Ligurian Units an through normal faults (Capozzi and Picotti, 2002, 2010). The gas in the Salsomaggiore area is a mixture of biogenic and thermogenic methane, associated with small amounts of C2+ fraction, condensates and oil. The generation of biogenic methane could be ascribed to secondary methanogenesis and to the primary generation from the organic matter dispersed in the reservoirs sediments. The mud volcanoes gas is composed almost entirely by methane, with very small amounts of higher hydrocarbons. The methane $\delta^{13}C$ in the mud volcanoes shows values comparable with those of Salsomaggiore, despite of the higher ^{13}C content in the C2+ fraction, thus supporting the occurrence of alteration processes. The mixing with biogenic methane is also plausible (Oppo et al., 2013).

Associated to these sites, three authigenic carbonate fields have been studied.

2.3 Stirone Field

The Salsomaggiore anticline is the westernmost structure considered in this study. It is formed by a Burdigalian-Serravallian age foredeep succession of turbiditic sandstones and marls. It deformed since the Langhian through the Tortonian as an intrabasinal structure, verging northeast, which was ultimately exposed and eroded at the thrust-top. After a subsidence pulse during the Messinian, the structure was covered and sealed by an olistostrome detached from the Ligurian nappe. A large wave-length folding and erosion phase in the Plio-Pleistocene led to the refolding of the upper thrust sheet with a northwest vergence. The synsedimentary deformation and tectono-thermal evolution governed the leakage of fluids on the anticline flanks since the Serravallian, and caused various episodes of hydrocarbon venting on the seafloor, marked by several seep-related carbonate concretions and chemoherms (Ricci Lucchi and Vai, 1994; Terzi et al., 1994; Monegatti et al., 2001; Taviani, 2001; Cau et al., 2015). The occurrence of seepage-related features is documented on both the flanks of the Salsomaggiore anticline. They are distributed within sediments of various ages comprised between the Middle Miocene and the Late Pliocene (Conti et al., 2007).

Fig. 5: Stirone River Field. Note chimney in center of image. Hammer for scale.

Methane-derived carbonates occurring in the Pliocene hemipelagic succession that overlies the northwestern flank of the Salsomaggiore structure outcrop along the Stirone River (Fig. 5). The deep river incision exposes the upper Messinian to Pleistocene sedimentary succession, whose

upper part documents the transition from marine to continental deposition (Fig. 1 in Cau et al., 2015). The authigenic carbonates investigated in this study are located in a ca. 50 meters-long outcrop formed of hemipelagic clays and silty clays pertaining to the Argille Azzurre Fm., and deposited at the transition between the Zanclean and Piacenzian ages (Monegatti et al., 2001; Cau et al., 2015). The authigenic carbonate concretions are formed by cylindrical chimneys and a few slabs. Moving up-section, various brecciated micritic limestones, Lucinid mudstones and chemoherms occur interspersed within sapropelitic horizons (Cau et al., 2015). The deposition of sapropel-bearing intervals of Piacenzian age was governed by precession cycles (Capozzi et al., 2006) and widespread in the marine basin of the Argille Azzurre Fm. during this time period.

2.4 Enza Field

The occurrence of methane-derived authigenic carbonates outcropping along the Enza riverbanks has been recently documented (Blumenberg et al., 2015; Oppo et al., 2015: Viola et al., 2015). The Enza River field develops at the Northern Apennines foothills in a well-preserved succession that marks the change from shallow marine to transitional sedimentary environments during the Early Pleistocene (Fig. 2 in Gunderson et al., 2014).

Fig.6: View of the Enza field. Chimeys partially buried are coming out from the sediments vertically.

To the south of the authigenic carbonates outcrop, the Quattro Castella ramp anticline, which locally delineates the present-day mountain front, has been generated by the formation of a detachment within the Ligurian Nappe (Gunderson et al., 2014). The Quattro Castella anticline was deforming during the Plio-Pleistocene time, as demonstrated by the growing geometries of the sedimentary

succession overlying the Ligurian Nappe on its forelimb. The Ghiardo plateau is an actively growing E-W trending fold related to blind thrust propagation, which deforms the Miocene foredeep units to the north of the authigenic carbonates outcrop. The anticline growth during the Late Tortonian is shown by the possible erosional truncation at the top, and by the onlap of the Messinian units above the structure (Oppo et al., 2015). The draping of Pliocene sediments within the hanging wall syncline and above the structural high culmination excludes the anticline growth during this time interval. In contrast, the onlap of Pleistocene units, thinning towards the top of the anticline, suggests a new period of fold activity.

The authigenic carbonates field (Fig. 6) is located on the Quattro Castella anticline forelimb, which deforms a fine-grained succession belonging to the Lower Pleistocene Argille Azzurre Fm that represents part of the marine intervals before the transition to continental deposits (Gunderson et al., 2014). The methane-derived carbonates, composed of slabs and chimneys, occur along a 35 meters-thick section formed of continuous inner shelf silty-clays, with intervening cm-thick sandy layers progressively more frequent moving towards the top of the section (Oppo et al., 2015). The top, dated at 1.4 Ma, is marked by a significant angular unconformity and by the deposition of a layer formed by chimney fragments and reworked coarse siliciclastics. This layer is pervaded by dark micritic carbonate concretions and colonised by a corallinaceous assemblage. Southwards to the Enza field, a weakly-cemented body ca. 10 meters high (Enza Hills) occurs within outcropping sand layers. These latter pertain to the upper Argille Azzurre Fm., deposited after the pelitic succession hosting the authigenic carbonates along the Enza riverbanks (Gunderson et al., 2014). These concretions likely formed on the seafloor, as they are rich of benthic fauna and bioturbation.

2.5 Secchia Field

The band of Northern Apennines foothills comprised between the Secchia River and the Nirano mud volcano field (NMVF) shows several features that testify the past and present spontaneous fluid emission. Moreover, the diffuse occurrence of saline water and hydrocarbons in the subsurface is also testified by their extraction in spa activities at Salvarola. In this area, thrusts deforming the Miocene foredeep units create structural traps for the fluids. The Tortonian succession shows elevated thickness, ca. 3 km, and is overlaid by the Messinian units. These latter progressively thin from southwest to northeast, documenting the formation of the structures during this time interval. The thrust growth proceeded during the Pliocene and the deformation in the subsurface appears relevant also in the Quaternary. Later high-angle normal faults along the foothills are likely

providing the main pathways for fluids migration from the deep Miocene reservoirs, and are thus responsible for the present-day fluids emission at the surface (Oppo et al., 2013).

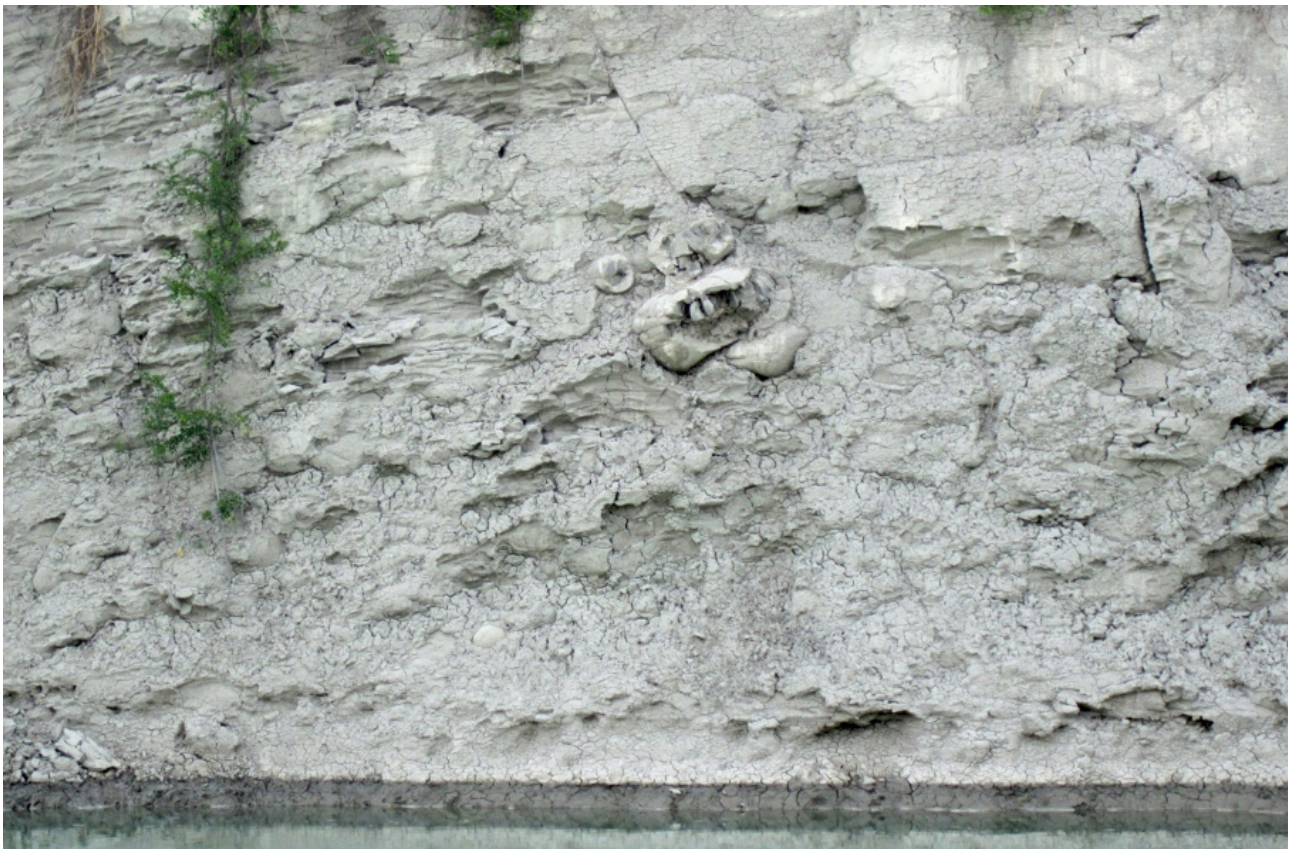

Fig. 7: particular of the Secchia River outcrop where globular concretions and a chimney are visible within the sediments.

Various authigenic carbonate concretions outcrop in the Argille Azzurre Fm. along the Secchia riverbanks (Fig. 7), within the Lower Pleistocene interval, from about 1.7 Ma, similarly to the Enza River site. Carbonates mostly form bulbous and slab-like concretions of meter-size dimension, with a minor presence of smaller chimneys. The slab-like concretions are interlayered in the succession, whereas the orientation of the bulbous features and chimneys is independent from the stratification. Along the riverbanks close to the concretions were also documented some minor normal faults, dipping north-east.

Eastwards of Secchia River, the Nirano mud volcanoes field (NMVF) occurs at the crest of an anticline that forms the fluids reservoir and that is generated by a blind thrust crossing through the sealing Ligurian Nappe down to the Miocene foredeep sediments (Oppo et al., 2013). The mud volcano field develops over an area of ca. 75,000 m^2 into the Plio-Pleistocene Argille Azzurre Fm., and represents one of the largest examples of this features occurring in Italy. The mud volcanoes are

located at the bottom of a caldera-like structure, which is likely the result of a collapse within the pelitic succession as consequence of various paroxysmal fluid emission events. The Nirano mud volcanoes field is formed by four main clusters of vents roughly aligned N55°E, thus probably depicting the trace of a normal fault or a system of secondary fractures developed on top of the underlying anticline. The mud cones and pools at Nirano show the almost constant emission of saline waters and hydrocarbons migrating from the Miocene reservoir. Along a small creek to the west of the NMVF, have been recovered a few carbonate chimney concretions hosted within the Argille Azzurre Formation of Pleistocene age.

3. Materials

3.1 Authigenic Carbonates Samples

Samples from the three representative authigenic carbonates outcrops have been considered in this study. A total number of 73 subsamples, representing various carbonate morphologies, have been selected and analysed. A total number of 28 AC subsamples from the Enza River field have been analysed, belonging to two chimneys (En5 and En10), one tabular slab (Cr2) and one concretion within the upper horizon colonised by the corallinaceous assemblage (Cr3). The En10 chimney shows an open central vent, is 170 cm long and 20 cm in diameter. Only the top and the bottom of the recovered chimney have been analysed. The top has been divided in external (E) and internal (I) portions, whereas only the internal area of the bottom has been analysed. The En5 chimney does not have an open central vent, is 63 cm long and 20 cm in diameter. To investigate possible geochemical variations along the chimney, it has been divided in 8 sections from the bottom (1) to the top (8). Each section, excluding 1 and 8, has been longitudinally separated in internal (I), middle (M) and external (E) parts. The Cr3 sample is a concretion at the top of the Enza section and shows a general dark colour. A dark-grey portion of the sample (Cr3A) has been analysed and compared with light-grey adjacent areas (Cr3B). The Cr2 slab, pertaining to the carbonate concretions stratigraphically below the corallinaceous assemblage layer, shows a general grey colour (Cr2A) with a light-grey area (Cr2B). Two samples from the semi-consolidated carbonate concretions cementing the sandy intervals at Enza Hills, south of the AC field, has been also analysed (ENCO 1 and ENCO 2). At Secchia River the prevalent carbonate morphologies are constituted by bulbous and slab-like concretions, with minor presence of chimneys. Five samples have been collected from globular slab-like concretions (SCH1 to SCH5), show meter-size dimensions. Subsamples have been collected for the external (E) and internal (I) areas of each concretion. One chimney (SCH6) showing a higher degree of cementation has been subsampled: a light-grey layer in the more external area (E), a darker interval forming the bulk of the concretion (M), and a yellowish-grey poorly consolidated infilling of the conduit (I), in total of 13 subsamples. Eastward to the NMVF was recovered a single chimney, ca. 20 cm in diameter and 30 cm long, from which two subsamples of the internal (I) and one of the external (E) areas have been analysed. Eight cylindrical concretions collected at Stirone River (STN1B to STN8) are ca. 50 cm in diameter and 1 m long, and are composed of abundant detrital fraction cemented by authigenic carbonates. The concretions are identified as chimneys without an open central conduit, which is filled with carbonate cements

and sediment arranged in a rose-like morphology. The chimneys have been subsampled in the external (E), middle (M) and internal (I) areas, in total 28 subsamples considered.

3.2 Fluid Samples

Different waters samples and associated hydrocarbons emissions to characterise and understand the fluid migration and the processes that promoted the authigenic carbonates precipitation.

Waters have been collected in:

- Salsomaggiore well 93 and Salsominore well 16 are representative of the brines from the deep reservoirs containing mature hydrocarbon;
- Castel San Pietro Terme wells Ca'Zini1 and Ca'Zini2 are representatives of the Plio-Pleistocene water of the Po Plain foredeep;
- Salvarola Terme Well is representative of the waters coming from the deep Miocene reservoir in the Secchia River area;
- Mud Volcanoes Systems: Nirano, Torre and Rivalta were sampled as representative of seeping water to the surface.

To reconstruct the hydrocarbon source responsible for the authigenic carbonates formation 9 gas samples from the four areas are considered. Three samples have been collected in the deep wells drilled in the Salsomaggiore anticline (Salsomaggiore 7 and 93, and Salsominore 16). Two samples represent the fluids emitted by the Nirano Mud volcanoes, one of which has been sampled during a paroxysmal event. Methane gas has been collected from the Salvarola Terme wells, near the Secchia River field. One single gas sample has been recovered from a small seepage occurring in the authigenic carbonates interval along the Enza riverbed.

4. Methods

The recovered samples have been divided in subsamples, as said before, to have a better characterisation of the geochemical variations. For this process have been used different methods: a hydraulic saw, to cut the chimney and divide it in the subsamples showed in the previous chapter and an agate mortar to powder them, and for Secchia chimney and slabs have been used a micro-driller to obtain the powder for the analysis. After mineralogical, geochemical and petrographic characterisation, only 41 subsamples have been selected for stable isotope analysis and 33 subsamples for the radiogenic strontium isotope analysis.

4.1 X-Ray-Fluorescence (XRF)

To prepare the samples for XRF analysis first have been weight 0.5g of powder rocks and 3g of boric acid. To obtain the pills has been used and hydraulic press at 30bar compression.

Major and trace elements have been determined by X-ray fluorescence (XRF) spectrometry on pressed powered pellets using a Philips PW 1480 automated spectrometer following the methods of Franzini et al. (1972, 1975), Leoni and Saitta (1976) and Leoni et al. (1982) for matrix corrections in XRF Laboratory, BiGeA department, Bologna University. The estimated precision and accuracy for trace element determinations are more than 5% except for the elements at 10 ppm and lower (10 e 15%); the detection limit for most of the trace elements is 3 ppm (Leoni and Saitta, 1976).

4.2 X-Ray-Diffraction (XRD)

The powdered subsamples have been fixed on slides for XRD with MQ water and let it dry overnight. The mineralogy analysis has been done by X-ray Diffraction (XRD) using a Philips PW 1130 (Cu Ka radiation Ni filtered) in the XRD Laboratory of BiGeA department, Bologna University. Powders were pressed into alumina holders in order to avoid preferential orientation of sheet-silicates. Estimates of the relative minerals abundance were determined using MacDiff software packages and carbonate mineral compositional limits defined according to Goldsmith and Graf (1958) and Lumsden (1979).

4.3 Optical Microscope

The petrographic observations were performed using uncovered standard thin sections (45x60 mm2 surface area) at University of Bologna via cathodoluminescence petrography (operating conditions of ca. 20 kV beam voltage and ca. 200 mA beam current).

4.4 Scanning Electronic Microscope - Energy Dispersive X-ray Analysis (SEM-EDX)

Morphological description and chemical elemental composition of the cements were obtained by using a Philips 515 scanning electron microscope (SEM) equipped with an electron back- scattering system and EDX (EDAX DX-4) at the University of Bologna. SEM-EDX investigations were performed on freshly broken samples (Au-coated).

4.5 Carbon and Oxygen Isotope Analysis

Carbon and oxygen isotope values have been analysed in the ETHz using Thermo Fisher DELTA Plus XP Gas Bench mass spectrometer. Between 90 and 140 µg of powder were weighted and insert in vacuum flasks that were sealed and flushed by 99.99% helium gas. After the air was swept out, 100% phosphoric acid was injected to react with the samples. The released CO_2 was purified and analysed. $\delta^{13}C$ and $\delta^{18}O$ values reported relative to the Vienna Pee Dee Belemnite (VPDB) have been corrected using two different standards, IsolabB and MS1, resulting in a precision of ±0.1‰.

4.6 Elemental Quantification for Strontium Isotope Analysis

Between 10 and 30 mg of carbonates have been weight in a 10 ml plastic vials, depending on the Sr ppm concentration detected by XRF. Buffer solution, 5 ml, was added to each sample; vials were shaked by hand first to homogenise the components, then put on the Shaker for 3.5 to 6 hours to digest the carbonate fraction and centrifuged at 3200 rpm for 5 minutes to set the pellet down. 4 ml of suspension were collected with a pipette in 7ml teflon vials to dry overnight on hot plate at 120°C. Once they dry down, was added 1 ml of concentrate nitric acid (HNO_3) then put the samples again on the hot plate closed for 2 hours, the heating will help the dissolution process. After that time some crystals remain so I added 0.33ml of concentrate chlorhydric acid (HCl) to have reverse aqua ragia and put again the vials on the hot plate at 120° and let the sample dry. To convert the reverse aqua ragia in chlorine form, otherwise could affect the mensuration, have been added 0.33 ml of 6M HCl. For the elemental analysis 0.02 ml of each subsample have been taken with a pipette and putted in MS teflon vials together with 9.98 ml of 2% nitric acid. Samples have been analysed with a thermo fisher single collector ICP-MS for the elemental analysis to determine the concentration of ^{86}Sr to prepare each sample for the isotopic measurement.

4.7 Strontium Isotope Analysis

The samples selected for strontium isotope measurement have been purified and extracted

using using double column separation by Deniel and Pin (2001) and de Souza et al. (2010)

- Resin AG50W-X8
- 1ml resin bed

Dissolve the sample in 1ml 1M HCl and put the sample on hot plate at 120°C for at least 1h.

Protocol for AG50W-X8 resin columns:

I. Cleaning: add to the column 7ml 6M HCl
II. conditioning: - 1ml of MQ water
- 2 times 0.7 ml of 1M HCl
III. Load sample: 1ml of dissolved sample
IV. Elution: 3 times 0.1ml of 2.5M HCl 3 ml of 2.5M HCl
V. Collect Sr in new vials: 4ml of 2.5M HCl
VI. Elution of REE: 4ml 6M HCl
VII. Cleaning: 5ml of 6M HCl
- 1ml of 1M HCl

The samples need to dry on hot plate overnight. Once the samples are dried out, proceed with the second purification for Sr extraction with the large teflon columns Sr specific resin. The columns must be filled up with the specific Sr resin. Then dissolve the samples obtained with 0.1 ml of 3M HCl.

1ml resin bed protocol:

I. cleaning: 2ml of MQ water
-2 ml of 6M HCl
-10 ml of MQ water
- 2 ml of 3M HNO_3
- 2ml of MQ water
II. conditioning: 2 ml 3M HNO_3
III. Load the sample: 0.05 ml of the dissolved sample
IV. elute Calcium: 4 times 0.1 ml of 3M HNO_3
V. Elute Barium: 2 times 0.6 ml of 7M HNO_3
-2 times 0.1 ml of 3M HNO_3
VI. Collect Strontium: 1ml of MQ water 0.5 ml of MQ water

Vials with collected strontium need to dry out on hot plate at lower temperature, 80-100°C, to avoid loss by evaporation. Once dry add 0.3 ml of concentrate HNO_3 and put it again on hot plate to oxidase possible residue of resin. Add 0.5 ml of 2% HNO_3 and put the vials

closed on the hotplate for 1h to help dissolution. Once that the dissolution is over, MS vials were prepared with 0,01ml of sample and 0.19 ml of 2% HNO_3. All the measurements have been done with a Neptune Plus, Thermo Fischer Scientific ICP-MCMS at ETH Zurich, between 20 and 25 v. All sample data was renormalised to a Nist SRM 987 literature value of 0.710248 (Thirwall, 1991).

4.8 Sulphur Isotope Analysis

Sulphur isotope on water samples has been analysed on precipitated $BaSO_4$. Sulphate in water samples was precipitated with an acidified barium chloride ($BaCl_2$). Acidification is necessary to avoid carbonate precipitation. First a specific amount of water, depending on sulphate concentration in the water sample, was acidified until pH=3 adding 6M HCl to fast the precipitation process, then was added enough ml of $BaCl_2$ to obtain $BaSO_4$.

The precipitate was recovered by centrifugation, where the supernatant was decanted, and let dry out overnight in stove at 40°C. After dry out, 300 μg of sample was weight and pun in a solid capsule 5x9mm together with the same amount of V_2O_5 to catalyse the reaction. Sulphur isotope measurements were carried out on a Thermo Scientific Flash Elemental Analyser (EA) interfaced to a Delta V Plus Isotope Ratio Mass Spectrometer. $\delta^{34}S$ value resulting are reported in Vienna-Canyon Diablo Troilite (V-CDT) and was corrected by NBS 127, IAEA SO 5 and IAEA SO 6 standards resulting in a precision of ±0.4‰.

5. Manuscripts

The following three manuscripts summarise the research performed during my three-year PhD thesis:

- **Paper 1:** *Mineralogy, geochemistry and petrography of methane-derived authigenic carbonates from Enza River, Northern Apennines (Italy)*. In this paper is presented an exhaustive characterisation of AC of the Enza River field. Based on geochemical and field evidences, their genesis has been attributed to microbial-governed carbonate precipitation from hydrocarbon-enriched fluids. Mineralogical and petrographic analyses of some chimneys and slabs document that the dominant cement is dolomite with calcite presence in the external areas. $\delta^{13}C$ indicate AOM-SR process as the promoter of carbonate precipitation. The occurrence of sulphide minerals in the stratigraphically upper samples indicates possible renewal of fluids leakage after a major erosive event.

  Personal contribution to the paper: I have performed all fieldwork, personally collected three samples of the four considered, performed all analytical work on samples En10, Cr2 and Cr3 for XRD and XRF. I interpreted all the data present in the paper beside petrography. I participate to the ideation, interpretation and writing to the 80% of the manuscript and sketched all the geochemical figures.

- **Paper 2:** *Carbon, oxygen and strontium isotopic constraints on fluid sources, temperatures and biogeochemical processes during the formation of seep carbonates - Secchia River site, Northern Apennines*. This paper is the first study on the new discovered Secchia River AC field. During 2014 and 2015, winter floods and river incisions exposed a new field of authigenic carbonates. Globular concretions (GC) and carbonate chimney are interspersed along the strata beds in the whole thickness of the section. The samples are composed by microcristalline dolomite, that cement remaining silicoclastic grains. Carbon, oxygen and strontium isotope signatures have been analysed on all the samples and on Salvarola Terme Well water, as representatives of the deep Miocene reservoir water still migrating in the area. The $\delta^{13}C$ signatures identified two groups of formation processes: globular concretions suffered influence of CO_2 associated to methanogenesis; whereas chimney precipitation is promoted by anaerobic oxidation of methane coupled with sulphate reduction processes. The sources of fluids in AC formation are often identified with sea water. In order to clarify this

aspect, I estimate the $\delta^{18}O$ and $^{87/86}Sr$ in dolomite cements. The results indicate that marine pore water is not always the main source of oxygen and a contribution of connate waters can be stressed. The mixing models permitted to quantify the mixing factor and the amount of seawater and connate water for each subsamples, emphasising the changes in feeding of the area.

Personal contribution to the paper: I have performed all fieldwork, personally collected the samples, performed all analytical work present in the paper. I participate to the ideation, interpretation and writing to the 80% of the manuscript and drew all figures.

- **Paper 3:** *Fluid sources and stable isotope signatures in Authigenic Carbonates from the Northern Apennines, Italy.* To Understand the relationship between fluids involved in their formation and the isotopic signals recorded in the carbonate cements is crucial in the study of AC. The selected outcrops of dolomitic authigenic carbonates were analysed to compare signature of seeping fluids with fractionation of stable carbon and oxygen isotopes recorded in the carbonate. Deep methane-rich fluids migrate to the surface through mud volcanoes or are exploited in wells drilled nearby to the authigenic carbonates outcrops. $\delta^{13}C$ indicate that gas composition from the deep hydrocarbon reservoirs is relatively uniform along the foothills. On the contrary, $\delta^{13}C$ in fossil authigenic carbonates strongly varies among different areas and also within the same outcrop. The different carbon sources that fed the investigated carbonates were identified and include: thermogenic methane from the deep Miocene reservoirs, ^{13}C-enriched CO_2 derived from secondary methanogenesis and microbial methane from Pliocene successions buried in the Po Plain. The $\delta^{13}C$ variability documented in the single outcrop testifies that the authigenic carbonates seems to record variation in biogeochemical processes happening in the hydrocarbon reservoirs. Oxygen isotopic fractionation in the dolomite cements of considered samples indicates that marine pore water couldn't be the sole source of oxygen, providing preliminary evidences that deep waters are involved in carbonates precipitation. The concomitant occurrence of active cold seepages and fossil record of ancient plumbing systems suggests that generation and migration of hydrocarbons are long-lasting and very effective processes along the Northern Apennines foothills.

  Personal contribution to the paper: I have performed all the field work in Secchia and Enza fields and participate to the field work in Stirone and Nirano mud volcanoes fields, collected

the samples. I performed all the analytical work presented beside the hydrocarbon analysis. I participate to the ideation, interpretation and writing equally to other authors.

PAPER 1

Mineralogy, geochemistry and petrography of methane-derived authigenic carbonates from Enza River, Northern Apennines (Italy).

Viola Irene, Oppo Davide, Franchi Fulvio, Capozzi Rossella, Dinelli Enrico, Liverani Barbara, and Taviani Marco.

Marine and Petroleum Geology, Volume 66 (2015), pp. 556-588

Marine and Petroleum Geology 66 (2015) 566–581

Contents lists available at ScienceDirect

Marine and Petroleum Geology

journal homepage: www.elsevier.com/locate/marpetgeo

Research paper

Mineralogy, geochemistry and petrography of methane-derived authigenic carbonates from Enza River, Northern Apennines (Italy)

I. Viola [a, *], D. Oppo [a], F. Franchi [b, c], R. Capozzi [a], E. Dinelli [a], B. Liverani [a], M. Taviani [b]

[a] Department of Biological, Geological and Environmental Sciences, University of Bologna, Via Zamboni 67, 40126 Bologna, Italy
[b] Institute of Marine Sciences (ISMAR)-CNR, Via Gobetti 101, 40129 Bologna, Italy
[c] Department of Earth and Environmental Sciences, BIUST, Private Bag 16, Palapye, Botswana

ARTICLE INFO

Article history:
Received 3 December 2014
Received in revised form
9 March 2015
Accepted 12 March 2015
Available online 20 March 2015

Keywords:
Carbonate chimneys
Hydrocarbon migration
Anaerobic methane oxidation
Apennine chain

ABSTRACT

A remarkable exposure of carbonate pipe-like and slab concretions occurs along the Enza riverbanks on the Northern Apennines foothills (Italy). Based upon geochemical and field evidences, their genesis has been attributed to microbial-governed carbonate precipitation from hydrocarbon-enriched fluids. The pipe-like concretions are thus interpreted as former conduits (chimneys) marking sites of methane ascent onto the seafloor. The resulting Enza River chimney field is arranged in a palisade fashion, a rare example of such. Mineralogical and petrographic analyses of some chimneys and slabs document that the dominant cement is dolomite. Although the chimneys show a rather homogeneous texture, a clear zonation is observed in the relative distribution of major and minor elements in their internal and external parts. The occurrence of sulphide minerals in the stratigraphically upper samples indicates possible renewal of fluids leakage after a major erosive event.

© 2015 Elsevier Ltd. All rights reserved.

1. Introduction

The formation of authigenic carbonates linked to hydrocarbon-enriched fluids seepage onto the seafloor is a well-known phenomenon. It is documented in modern and ancient marine sedimentary basins worldwide particularly, but not exclusively, in compressive tectonic regimes at convergent margins (e.g., Taviani, 2001; Pinheiro et al., 2003; Nyman et al., 2010; Capozzi et al., 2012). Microbially mediated anaerobic oxidation of methane (AOM) and sulphate reduction (SR) increase the pore water alkalinity, favouring the precipitation of methane-derived authigenic carbonates (MDAC) (e.g. Boetius et al., 2000; Peckmann and Thiel, 2004; Teichert et al., 2005). Their various morphologies include slabs and crusts, cylindrical and pipe-like conduits, and irregularly shaped bodies (e.g. Taviani, 2001; Clari et al., 2004; Lein, 2004; Magalhães et al., 2012). Pipe-like conduits are the less reported in literature and their formation mechanisms are still under debate (e.g. Nyman et al., 2010; Magalhães et al., 2012; Oppo et al., in this issue).

Increasing attention is presently devoted to understanding pipe-like concretions characteristics and formative processes (e.g., Orpin, 1997; Díaz-del-Rio et al., 2001, 2003; Somoza et al., 2003; De Boever et al., 2006a,b; Nyman et al., 2010; Magalhães et al., 2012; Oppo et al., in this issue; Angeletti et al., in this issue). The seep carbonates show characteristic mineralogy and geochemistry, as the authigenic carbonate minerals, such as dolomite, calcite and aragonite, which compose the MDAC concretions, are usually over than 50% bulk weight. Their relative amounts depend on the formation environment and on the fluids involved in the precipitation (e.g. Peckmann and Thiel, 2004; Magalhães et al., 2012; Vanneste et al., 2012). Being considered as indicators of hydrocarbon seepages, authigenic carbonates testify the present-day or past occurrence of petroleum generation systems (Capozzi et al., 2012; Oppo et al., 2013; Unterseh, 2013).

This study provides first detailed mineralogical, geochemical and petrographic information on hydrocarbon-imprinted carbonates, from the Enza River succession (Capozzi et al., 2013; Gunderson et al., 2014; Oppo et al., in this issue). In addition, we also provide some compositional data on the host marine sediments for a better characterization of the genetic environments of carbonates. At this site, the formation of methane-derived authigenic carbonates is strictly connected with the geologic evolution of the basin (see Oppo et al., in this issue).

2. Geological setting

Intense flooding events over the last few years resulted in a pronounced fluvial incision of the Enza riverbanks in the Northern Apennines foothills (Fig. 1).

* Corresponding author.
E-mail address: irene.viola3@unibo.it (I. Viola).

http://dx.doi.org/10.1016/j.marpetgeo.2015.03.011
0264-8172/© 2015 Elsevier Ltd. All rights reserved.

Such erosive processes resulted in the exposure downstream the city of San Polo d'Enza of a marine succession punctuated by a number of slab and pipe-like carbonate concretions (Fig. 2).

The foothills deformation in the Enza River area started in the Late Miocene and continued until the Pleistocene, resulting in the formation of the Quattro Castella anticline (Boccaletti et al., 2010; Ponza et al., 2010; Gunderson et al., 2014). The Enza River succession belongs to the forelimb of the Quattro Castella anticline and represents a full transition, from muddy shelfal deposits (Argille Azzurre Fm.) to the transitional coastal system (Sabbie Gialle Fm.) (Gunderson et al., 2014, and references therein). The synsedimentary tilting of the anticline led to the variation of strata dip along the 65 m-thick studied succession, which progressively changes from 55° at the base to 42° at the top. A corallinaceous rhodolith-rich bed, which dips 35°, represents the top of the studied section and identifies an angular unconformity (Gunderson et al., 2014) that marks an erosional discontinuity. The recovering of deposition started with the colonization by benthic epifauna (Oppo et al., in this issue).

The carbonate concretions are enclosed in the Lower Pleistocene Argille Azzurre Fm., which is composed of blue-grey silty clays deposited in external continental shelf environment. The carbonate pipe-like concretions, in this paper defined as chimneys, and slabs occur between 30 and 65 m of the Enza section (Oppo et al., in this issue). The chimneys have often sub-vertical orientation with respect to horizontal and are arranged in a sort of pipe palisade, a rare occurrence seldom seen in outcrop (e.g. De Boever et al., 2006a; Cau et al., in this issue) and submerged situations (e.g. Taviani, 2014) whilst slabs conform to stratification. Morphologies and dimensions vary: pipe-like and cylindrical chimneys range from few cm to almost 2 m high, with up to 40 cm in diameter; slabs are few cm to 30 cm thick and up to several metres long (Fig. 2) (see also Capozzi et al., 2013; Gunderson et al., 2014; Oppo et al., in this issue).

3. Materials and methods

Fieldwork was conducted in May 2010 and May 2013 to sample chimneys, slabs and host sediment for their mineralogical, geochemical and petrographical comparative characterization. 31 samples of Argille Azzurre Fm. have been recovered and analysed, together with 4 samples of carbonate concretions: two chimneys (En5 and En10) and two carbonate bodies, one tabular slab (Cr2) and a concretion within the rhodolith-rich layer (Cr3) (Fig. 3).

The carbonate concretions have been divided in 29 sub-samples to be analysed (Fig. 4).

The En5 chimney does not have an open central vent and is 63 cm long and 20 cm in diameter (Fig. 4a). To investigate eventual geochemical variations along the chimney, it has been cut in 8 sections from the bottom (1) to the top (8). Each section, excluding 1 and 8, has been longitudinally divided in 3 subsamples: internal part (A), central part (B) and external part (C). The En10 chimney is

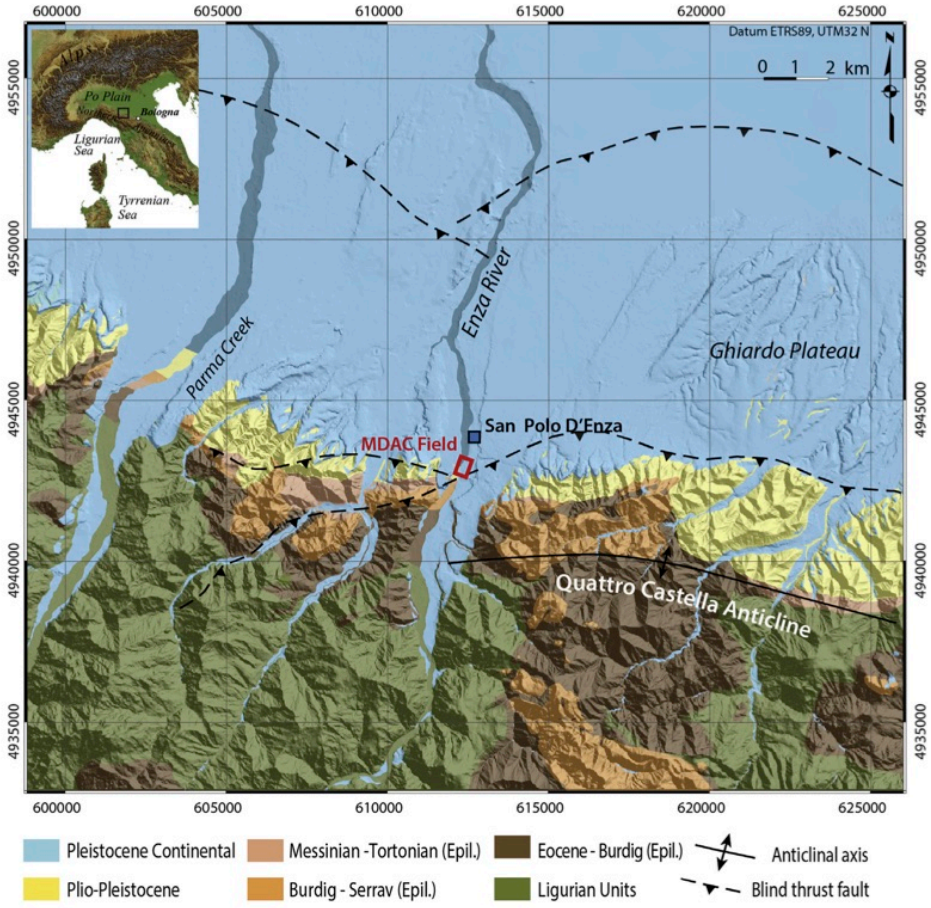

Figure 1. Geological map of the investigated area of the Northern Apennines. The Enza carbonate field (red square) is located along the Enza River near the town of San Polo d'Enza (modified from Oppo et al., in this issue). (For interpretation of the references to colour in this figure legend, the reader is referred to the web version of this article.)

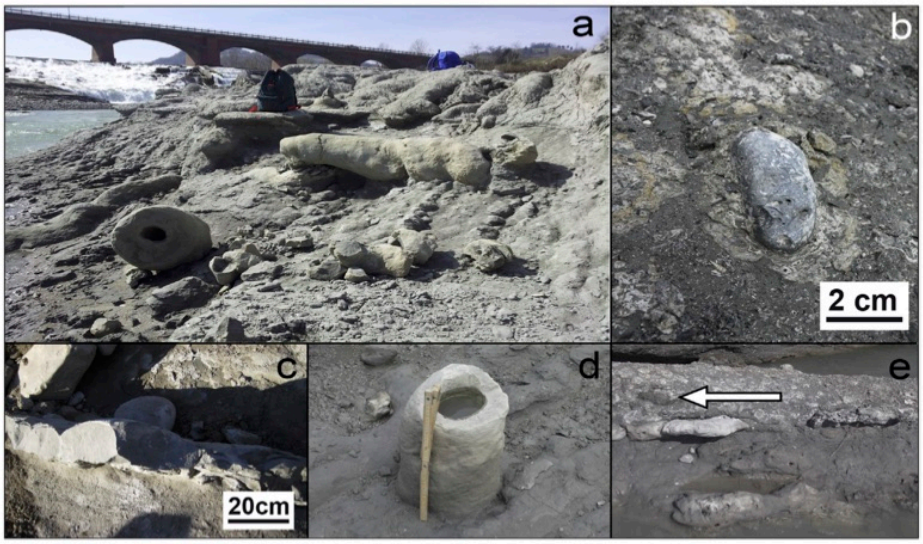

Figure 2. Example of the carbonate concretions occurring along the Enza riverbanks. a) Various concretions have been exposed by the erosion. The observed chimneys reached up to 2 m in length. b) Detail of the rhodolith-rich layer. A fine-grained cemented matrix contains numerous rhodolites and biogenic structures. A dark-grey carbonate pebble is encrusted by red algae. c) Outcropping slab. d) Pipe-like chimney with sub vertical orientation respect to the horizontal. e) The rhodolith-rich bed directly overlies a carbonate slab. Arrow points to dark-grey carbonate enclosed in the bed.

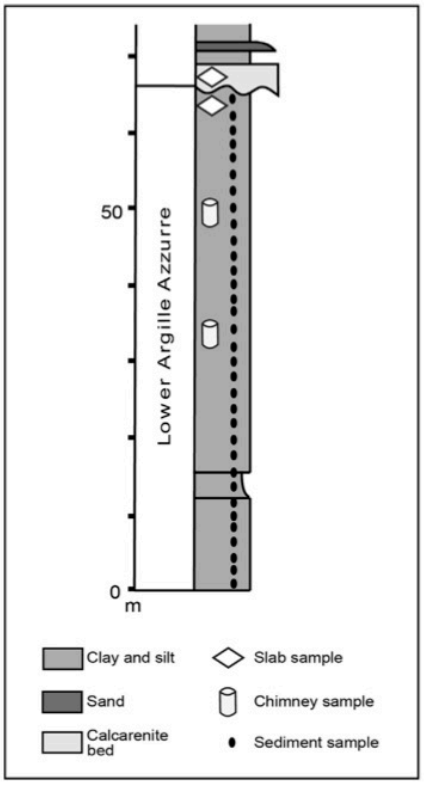

Figure 3. Simplified stratigraphic column of the studied succession along the Enza River. The rhodolith-rich layer marks an erosional unconformity, separating the interval hosting the concretions from the underlying Lower Pleistocene succession. The position of samples discussed in text is marked. Sediments are sampled from 4 to 64 m bottom–top; chimney En5 is the lower one, En10 the upper one; slab Cr2 is the one just below the corallinaceus bed, while Cr3 is the one collected inside the corallinaceus bed.

170 cm long and 20 cm in diameter; only the top and the bottom have been analysed (Fig. 4 b and c, respectively). The top subsample has been divided in external (B) and internal (A) portions.

The Cr3 sample is a concretion within the rhodolith-rich layer; it shows a dark colour and is well cemented. A dark-grey area (Cr3A, Fig. 4d) was analysed and compared with the light-grey matrix (Cr3B, Fig. 4e). The Cr2 slab pertained to the carbonate concretions stratigraphically below the rhodolith-rich layer; it shows a grey colour with a light-grey area (Cr2b in Fig. 4f).

The samples have been powdered, homogenized in agate mortar and analysed for mineralogy by X-ray diffractometry (XRD) using a Philips PW 1130 (Cu Kα radiation Ni filtered) in the XRD Laboratory of BiGeA department, Bologna University. Powders were pressed into alumina holders in order to avoid preferential orientation of sheet-silicates. Estimates of the relative minerals abundance were determined using MacDiff software packages and carbonate mineral compositional limits defined according to Goldsmith and Graf (1958) and Lumsden (1979).

Nitrogen and Total Organic Carbon (TOC) have been analysed with CHNS pre-treating 10 mg of powdered sample in 40 μl of HCl 1.5 N for 2 h in the oven, this procedure have been repeated two times to eliminate all the inorganic carbon traces. The resulting compounds have been analysed to estimate TOC and Nitrogen by CHNS- Analizer Flash 2000 Thermo Scientific Gas Chromatographer in Pedology Laboratory, BiGeA department, Ravenna, Bologna University. This analysis was performed only on En5 samples and hosting sediments because the higher number of samples from En5 gives a better representation of the carbonates bodies in all its parts (internal, central and external) and were more accurate for a comparison with the hosting sediments samples.

Major and trace elements have been determined by X-ray fluorescence (XRF) spectrometry on pressed powered pellets using a Philips PW 1480 automated spectrometer following the methods of Franzini et al. (1972, 1975), Leoni and Saitta (1976) and Leoni et al. (1982) for matrix corrections in XRF Laboratory, BiGeA department, Bologna University. The estimated precision and accuracy for trace element determinations are more than 5% except for the elements at 10 ppm and lower (10–15%); the detection limit for most of the trace elements is 3 ppm (Leoni and Saitta, 1976).

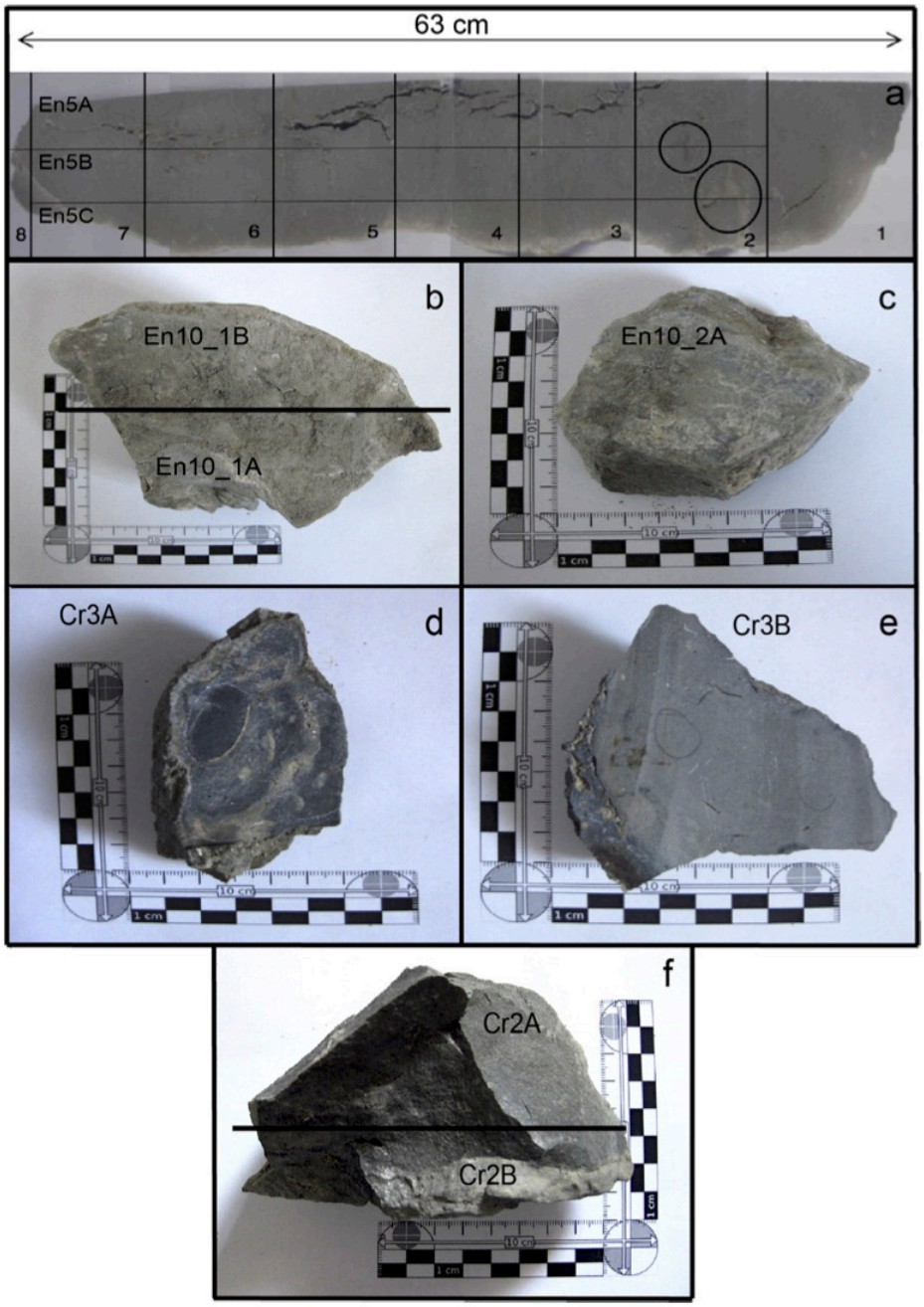

Figure 4. Carbonate samples analysed in this study. a) The En5 chimney that has been divided in 8 sections from bottom to top. Horizontal lines separate the internal (En5A), central (En5B) and external (En5C) subsamples. b) The top of En10 chimney has been divided in external (En10_1B) and internal (En10_1A) portions. c) Bottom of the En10 chimney. d) Cr3A concretion. The dark-grey colour, mainly due to the high sulphide minerals content, can be observed. e) Grey portion of the Cr3 concretion. Along the left edge of the sample can be observed a dark-grey thrombolytic layering. f) The Cr2 slab has been divided in two samples to differentiate the darker part of the concretion (Cr2A) from the lighter-colour of the external area (Cr2B). (For interpretation of the references to colour in this figure legend, the reader is referred to the web version of this article.)

The petrographic and microfacies-based analyses were performed on. 80 uncovered thin sections (45 × 60 mm^2 surface area, 30 μm thickness) at the ISMAR-CNR, U.O.S. Bologna. Cathodoluminescence petrography was conducted using a CL 8200 MK3 optical equipment (operating conditions: 20 kV beam voltage and 200 μÅ beam current) at the University of Padua. Morphological description and chemical elemental composition of microscopic features were obtained by using a Philips 515 scanning electron microscope (SEM) equipped with an electron back-scattering system and EDX (EDAX DX-4) at the SEM Laboratory, BiGeA department University of Bologna. SEM-EDX investigations (SEM operating conditions: 15 and 25 kV accelerating voltage) were performed on freshly broken samples (Au-coated) and thin sections (C-coated).

Carbon and oxygen isotopic analyses have been performed on carbonate samples from Enza River in this study at CNR-Institute

Table 1
Mineral abundances in the sediment. Samples position starts from the base of the Enza section.

Samples	Position	Quartz	Chlorite	Muscovite	Calcite	Dolomite	Feldspars	Pladgioclase	Clay minerals	Others
	(m)	(%)	(%)	(%)	(%)	(%)	(%)	(%)	(%)	(%)
4	1.2	20	6	9	21	2	15	10	15	2
12	4.4	27	7	9	18	0	13	6	19	1
17	6.4	23	9	8	19	0	11	10	17	3
22	8.4	16	6	6	28	2	7	11	23	1
27	10.4	11	5	8	31	0	6	14	23	2
32	12.4	24	8	10	19	0	9	15	11	4
37	14.4	15	7	8	25	0	8	5	30	2
42	16.4	21	9	10	20	0	11	6	20	3
47	18.4	18	7	7	22	2	13	11	16	4
52	20.4	17	5	6	28	2	8	9	23	2
57	22.4	24	8	8	17	0	17	4	19	3
62	24.4	16	5	7	29	0	8	6	25	4
67	26.4	26	6	9	19	0	12	11	15	2
72	28.4	17	7	6	26	1	9	13	19	2
77	30.4	23	6	7	21	3	12	10	15	3
82	32.4	18	7	7	22	3	13	8	16	6
88	34.8	25	7	10	14	0	20	12	11	1
92	36.4	24	9	11	15	4	9	8	17	3
97	38.4	21	6	8	15	2	24	7	15	2
102	40.4	13	10	7	23	2	9	10	24	2
107	42.4	21	8	8	20	3	9	9	19	3
113	44.8	12	5	5	31	2	8	14	21	2
117	46.4	25	7	10	17	2	13	12	10	4
122	48.4	14	7	7	25	1	10	4	29	3
127	50.4	25	7	7	20	2	12	9	17	1
132	52.4	13	11	6	23	2	10	12	20	3
137	54.4	20	8	9	21	0	12	10	19	1
142	56.4	25	5	8	17	2	17	8	16	2
147	58.4	32	10	9	13	0	14	6	12	4
152	60.4	16	4	4	30	1	9	14	19	3
157	62.4	24	8	7	18	2	17	7	15	2
162	64.4	21	6	9	20	2	12	7	21	2

Table 2
Major oxides in the sediment. Samples position starts from the base of the Enza section.

Sample	Position	SiO_2	TiO_2	Al_2O_3	Fe_2O_3	MnO	MgO	CaO	Na_2O	K_2O	P_2O_5	LOI	Mg/Ca	Sr/Ca
	(m)	(wt %)	(wt %)	(wt %)	(wt %)	(wt %)	(wt %)	(wt %)	(wt %)	(wt %)	(wt %)	(wt %)		
4	1.20	44.70	0.60	12.25	5.20	0.12	3.31	15.28	0.98	2.11	0.11	15.36	0.1828	0.0041
12	4.40	45.93	0.58	12.67	4.83	0.12	3.41	14.42	1.04	2.16	0.07	14.78	0.1996	0.0042
17	6.40	45.29	0.58	12.25	4.90	0.12	3.39	15.50	1.07	2.12	0.06	14.70	0.1846	0.0043
22	8.40	40.64	0.56	11.88	4.63	0.11	2.94	17.90	0.98	1.96	0.05	18.34	0.1386	0.0041
27	10.40	40.55	0.57	12.34	4.81	0.11	2.77	16.72	0.93	2.15	0.08	18.97	0.1398	0.0048
32	12.40	45.94	0.58	12.84	5.02	0.12	3.31	14.06	1.12	2.13	0.07	14.81	0.1987	0.0046
37	14.40	45.99	0.56	12.45	4.57	0.12	3.17	15.00	1.05	2.07	0.07	14.95	0.1783	0.0049
42	16.40	46.12	0.57	12.60	4.64	0.12	3.35	14.16	0.95	2.11	0.07	15.30	0.1996	0.0037
47	18.40	46.57	0.58	12.80	4.59	0.11	3.28	13.95	0.97	2.14	0.07	14.93	0.1984	0.0044
52	20.40	45.54	0.58	12.92	4.76	0.11	3.36	14.29	1.00	2.15	0.07	15.22	0.1984	0.0036
57	22.40	45.88	0.58	12.85	4.92	0.12	3.39	14.60	0.98	2.14	0.12	14.43	0.1959	0.0040
62	24.40	46.64	0.54	12.07	4.09	0.12	3.45	15.08	1.01	1.96	0.08	14.95	0.1931	0.0029
67	26.40	47.06	0.57	12.65	4.77	0.12	3.43	13.99	1.06	2.15	0.05	14.16	0.2069	0.0041
72	28.40	46.45	0.58	13.19	4.75	0.11	3.51	13.46	0.96	2.22	0.09	14.69	0.2201	0.0040
77	30.40	45.97	0.58	12.60	4.63	0.11	3.68	14.32	1.00	2.12	0.06	14.92	0.2169	0.0037
82	32.40	45.20	0.60	12.77	4.77	0.11	3.75	14.69	1.01	2.14	0.07	14.88	0.2154	0.0046
88	34.80	48.54	0.62	13.67	4.87	0.11	3.71	12.11	1.05	2.26	0.10	12.96	0.2585	0.0043
92	36.40	48.06	0.57	12.59	4.54	0.11	3.55	13.65	1.08	2.11	0.07	13.68	0.2195	0.0042
97	38.40	48.36	0.60	13.31	4.99	0.11	3.50	12.41	1.02	2.25	0.10	13.34	0.2380	0.0041
102	40.40	46.55	0.62	13.40	5.13	0.11	3.46	12.97	1.00	2.31	0.12	14.33	0.2251	0.0044
107	42.40	46.05	0.60	13.13	4.87	0.12	3.47	13.62	1.01	2.22	0.09	14.82	0.2150	0.0044
113	44.80	47.17	0.57	12.88	4.70	0.12	3.56	14.05	1.10	2.08	0.06	13.72	0.2138	0.0040
117	46.40	47.44	0.59	13.13	4.77	0.11	3.42	13.20	1.03	2.19	0.11	14.00	0.2186	0.0043
122	48.40	48.12	0.63	14.28	5.21	0.11	3.37	11.37	1.00	2.35	0.08	13.49	0.2501	0.0039
127	50.40	47.73	0.61	12.51	4.77	0.11	3.54	13.77	1.10	2.20	0.08	13.57	0.2169	0.0042
132	52.40	47.93	0.59	12.36	4.85	0.12	3.54	13.59	1.14	2.10	0.11	13.68	0.2198	0.0038
137	54.40	47.93	0.59	12.91	4.65	0.11	3.33	13.29	1.06	2.12	0.08	13.93	0.2114	0.0040
142	56.40	48.28	0.56	12.34	4.57	0.13	3.49	14.28	1.27	2.01	0.13	12.93	0.2062	0.0037
147	58.40	46.38	0.59	12.58	4.73	0.12	3.37	14.43	0.89	2.09	0.09	14.74	0.1971	0.0036
152	60.40	48.07	0.58	12.56	4.54	0.11	3.28	13.79	1.00	2.05	0.09	13.93	0.2007	0.0038
157	62.40	49.09	0.54	12.05	4.30	0.12	3.32	14.46	1.24	1.94	0.09	13.25	0.1937	0.0041
162	64.40	50.63	0.55	12.50	4.32	0.11	3.29	13.19	1.17	1.97	0.10	12.17	0.2105	0.0038

Table 3
Minor elements in the sediment. Samples position starts from the base of the Enza section.

Sample	Position	Sc	V	Cr	Co	Ni	Cu	Zn	As	Rb	Sr	Y	Zr	Nb	Ba	La	Ce	Pb	Th	S	Br	Mo	TOC
	(m)	(ppm)	(ppm)	(ppm)	(ppm)	(ppm)	(ppm)	(ppm)	(ppm)	(ppm)	(ppm)	(ppm)	(ppm)	(ppm)	(ppm)	(ppm)	(ppm)	(ppm)	(ppm)	(ppm)	(ppm)	(ppm)	(%)
4	1.2	9	94	138	16	80	19	74	7	113	451	19	110	10	281	15	61	14	2	2250	<20	<3	0.56
12	4.4	11	101	143	14	88	35	93	7	114	429	18	96	10	287	22	67	6	2	770	<20	<3	0.52
17	6.4	7	98	134	11	80	18	70	10	114	473	20	105	11	313	35	62	3	9	1910	<20	3	0.5
22	8.4	2	100	114	12	74	23	95	5	103	531	16	67	10	261	38	69	4	12	1430	<20	<3	0.68
27	10.4	10	104	108	11	74	29	103	10	131	578	22	53	13	293	26	62	11	12	750	<20	3	0.69
32	12.4	11	94	136	16	80	22	96	5	118	464	22	128	13	286	24	62	8	10	670	<20	<3	0.46
37	14.4	7	95	132	13	77	33	94	14	131	522	24	106	13	318	22	50	7	7	2890	<20	<3	0.57
42	16.4	9	100	124	11	80	22	94	<3	104	379	17	88	8	266	13	58	7	10	1600	<20	<3	0.67
47	18.4	9	98	128	10	79	23	101	11	120	435	21	101	9	282	21	60	9	15	2990	<20	<3	0.58
52	20.4	4	101	138	11	85	25	100	<3	103	366	14	84	10	290	22	75	9	12	610	<20	3	0.62
57	22.4	12	104	136	16	87	34	98	20	111	419	20	79	9	280	31	60	7	14	3310	<20	3	0.61
62	24.4	16	87	134	14	74	23	82	11	71	317	14	67	9	251	26	56	2	11	1670	<20	<3	0.5
67	26.4	13	102	147	11	87	19	93	21	111	415	18	102	10	280	19	58	2	7	2800	<20	<3	0.46
72	28.4	10	106	141	15	98	23	96	2	115	385	19	93	11	275	25	50	7	12	2580	<20	<3	0.44
77	30.4	7	104	158	13	96	22	99	9	99	374	18	88	12	274	28	69	7	6	2600	<20	<3	0.38
82	32.4	12	106	165	13	88	16	97	13	122	488	23	122	12	283	20	68	10	9	2830	<20	<3	0.42
88	34.8	12	105	166	13	87	19	95	6	114	371	23	165	11	280	29	87	8	9	1590	<20	<3	0.35
92	36.4	13	102	139	10	76	17	88	<3	111	405	23	141	8	297	13	61	11	14	1980	<20	3	0.41
97	38.4	14	109	148	14	85	32	96	5	109	360	22	118	10	318	21	59	4	16	2760	<20	<3	0.41
102	40.4	11	106	126	11	76	17	82	<3	129	407	21	104	13	286	28	81	9	16	1750	<20	3	0.44
107	42.4	11	111	142	13	77	24	101	11	118	429	20	102	10	318	29	73	8	12	1590	<20	<3	0.43
113	44.8	8	101	132	13	71	19	88	16	111	403	21	143	11	289	17	82	10	7	2260	<20	<3	0.39
117	46.4	13	101	132	10	74	17	74	4	122	403	20	129	12	263	29	72	5	10	1600	<20	<3	0.43
122	48.4	13	113	158	12	87	19	101	6	108	313	18	94	10	294	28	75	13	10	2860	<20	<3	0.42
127	50.4	8	100	137	13	79	14	100	9	116	414	26	136	13	321	15	46	11	6	3660	<20	<3	0.39
132	52.4	16	99	139	13	79	19	97	23	103	370	20	107	12	285	28	72	13	7	1890	<20	3	0.44
137	54.4	12	105	141	14	80	22	99	<3	107	384	22	113	10	301	29	58	12	8	2190	<20	3	0.58
142	56.4	13	84	145	10	71	16	60	20	93	377	19	148	12	303	19	67	6	11	3400	<20	<3	0.52
147	58.4	11	96	130	11	72	18	72	13	98	374	16	82	10	275	44	60	10	14	2330	<20	<3	0.48
152	60.4	11	95	137	10	74	28	90	18	99	375	19	118	9	312	41	60	7	2	2610	<20	4	0.48
157	62.4	10	85	154	11	73	27	81	<3	96	425	23	160	8	304	22	70	8	14	5570	<20	3	0.52
162	64.4	13	86	141	10	73	12	61	16	90	361	18	132	10	273	9	73	2	3	4950	<20	4	0.34

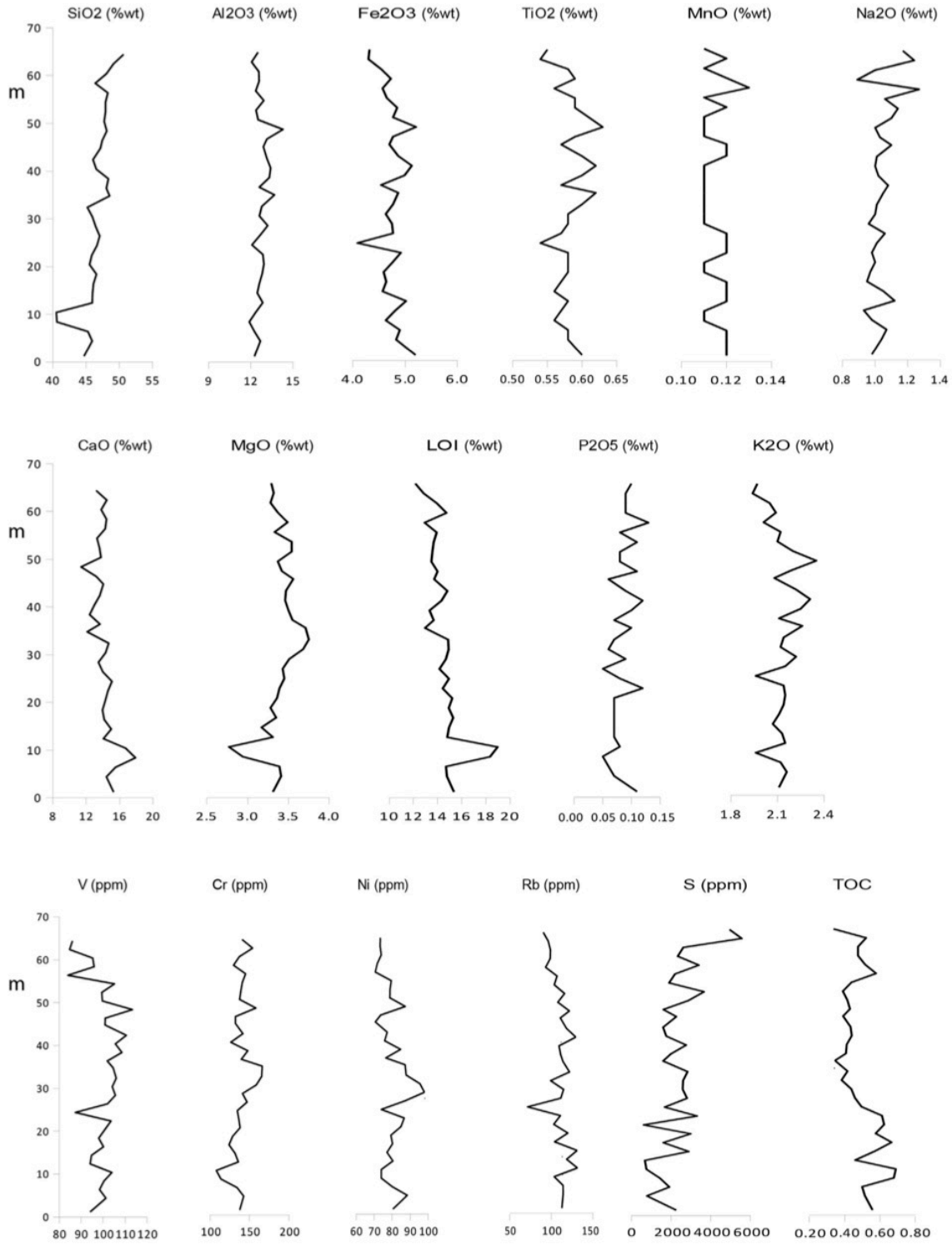

Figure 5. Along-section profiles of major oxides, LOI and minor elements in the sediment of the investigated succession, from the base (1.2 m) to the top (64 m).

of Geosciences and Georesources (CNR-IGG) of Pisa and by J. Reitner (personal communication). The sampling for these analyses has been done slicing the carbonates and using a micro-driller to collect the sub-samples, in order to have precise measuring of the isotopes in the different areas. The powdered sub-samples (100–200 μg) were reacted for 10 min at 90 °C with 100% phosphoric acid on an automated carbonate device connected to a VG-PRISM mass spectrometer calibrated with NBS18,

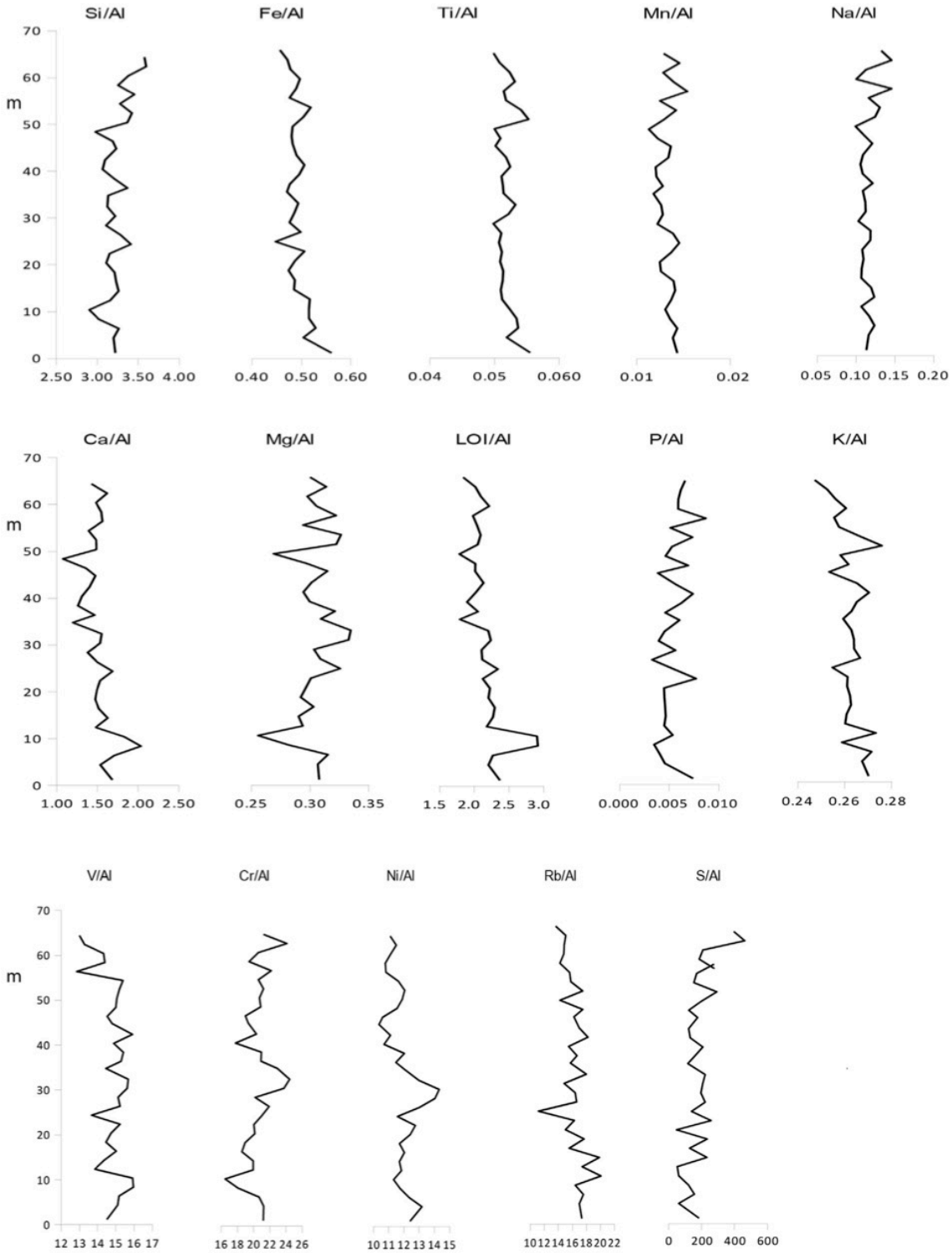

Figure 6. Along-section profiles of elements occurring in the sediment normalized respect to Aluminium.

NBS19 and NBS20 standards. The results are reported in the conventional δ‰ notation with reference to VPDB (Vienna Pee-dee Belemnite). For the dolomite samples (sample with N 20% of dolomite) $\delta^{18}O$ values were calculated with the Rosenbaum and Sheppard fractionation factor. Analytical reproducibility of the method, based on repeated analysis of standards is better than ±0.1‰ for both carbon and oxygen (Rosenbaum, 1994; Rosenbaum and Sheppard, 1986).

Table 4
Mineral abundances in the carbonates concretions.

Sample	Calcite (%)	Dolomite (%)	Detrital (%)
En5 8A	0	65	35
En5 8B	6	57	37
En5 7A	12	61	27
En5 7B	0	66	34
En5 7C	0	73	27
En5 6A	5	58	37
En5 6B	1	65	34
En5 6C	5	60	35
En5 5A	0	75	25
En5 5B	0	74	26
En5 5C	10	55	35
En5 4A	0	78	22
En5 4B	0	71	29
En5 4C	13	46	41
En5 3A	0	80	20
En5 3B	0	80	20
En5 3C	11	50	39
En5 2A	0	82	18
En5 2B	1	75	23
En5 2C	6	60	34
En5 1A	0	71	29
En10 1A	0	76	24
En10 1B	2	75	22
En10 2A	0	81	19
Cr2A	0	80	20
Cr2B	4	71	25
Cr3A	0	65	35
Cr3B	11	52	37

4. Results

4.1. Hosting sediments geochemistry and mineralogy

XRD analyses (Table 1) show ca. 21% content of carbonate minerals in the sediments, mainly formed of calcite, dolomite is also present (1%) but just in few samples located between 28.4 m and 64.4 m along the section, coupled with the appearance of protodolomite.

The bulk of these carbonates is made of biogenic residuals, mainly foraminifera and calcareous nannoplancton. The other minerals in the Argille Azzurre Fm. sediments of the Enza section are quartz (ca. 20%), clay minerals as smectite and illite (ca. 18%), feldspars (ca. 12%), plagioclase (ca. 9%); muscovite (ca. 8%) and chlorite (ca. 7%). The along-section chemical profiles show a clear perturbation around 10 m (Tables 2 and 3; Fig. 5) where a positive peak of CaO, LOI and in part TOC is matched by a negative peak of to SiO_2, Al_2O_3, Fe_2O_3, and K_2O. This is the most evident occurrence, but as other minor peaks in the logs of these elements, reflect the biogenic carbonate/silicate proportion.

MgO displays a peculiar trend with a maxima in the central portion of the log (between 30 and 35 m) and an increasing trend up-section. Cr and Ni show a similar trend. TOC has a variable distribution with concentrations around 0.6% up to 22 m, then a decrease around 0.4% up to 52 m and then an increase at the top of the section. The normalisation with respect to Al (Fig. 6) shows that the peaks of SiO_2, Al_2O_3, Fe_2O_3, K_2O, Cr and Ni persist at 10, 25 and 50 m.

Figure 6 shows peaks in the normalized profiles of Cr, Ni and Mg between 30 and 40 m.

4.2. Carbonate geochemistry and mineralogy

Carbonate bodies are mainly composed of dolomite (in average 68% bulk weight) with low and variable amounts of calcite (up to 13%) (Table 4).

The detrital fraction (up to 41%) is similar in all the samples: major components are quartz, feldspars, plagioclase, clay minerals and micas. The concretion Cr3A has also high content of pyrite and arsenopyrite (5%) and is the only sample where strontianite is present (1%).

Table 5
Major oxides in the carbonate concretions.

Sample	SiO_2 (wt %)	TiO_2 (wt %)	Al_2O_3 (wt %)	Fe_2O_3 (wt %)	MnO (wt %)	MgO (wt %)	CaO (wt %)	Na_2O (wt %)	K_2O (wt %)	P_2O_5 (wt %)	LOI (wt %)	Mg/Ca	Sr/Ca
En5 8A	12.94	0.17	3.46	1.83	0.09	17.98	25.26	0.55	0.58	0.09	37.06	0.6007	0.0018
En5 8B	21.53	0.26	6.04	2.68	0.13	13.32	23.47	0.66	0.94	0.09	30.87	0.4789	0.0018
En5 7A	14.95	0.18	3.72	1.86	0.09	17.34	24.01	0.60	0.63	0.09	36.53	0.6094	0.0021
En5 7B	14.47	0.18	4.02	1.78	0.10	17.52	24.56	0.60	0.62	0.08	36.08	0.6020	0.0016
En5 7C	16.60	0.23	4.75	2.18	0.11	15.36	25.54	0.57	0.77	0.11	34.77	0.5075	0.0018
En5 6A	13.34	0.19	3.67	1.84	0.09	18.02	24.91	0.52	0.63	0.06	36.73	0.6104	0.0017
En5 6B	12.74	0.18	3.75	1.73	0.09	17.97	25.07	0.53	0.60	0.07	37.27	0.6049	0.0018
En5 6C	16.94	0.20	4.22	2.16	0.11	15.63	24.59	0.60	0.72	0.10	34.73	0.5364	0.0023
En5 5A	14.91	0.19	3.89	1.87	0.10	17.47	24.40	0.58	0.66	0.10	35.83	0.6042	0.0020
En5 5B	16.54	0.21	4.24	2.00	0.10	16.82	24.05	0.59	0.74	0.12	34.58	0.5902	0.0022
En5 5C	23.32	0.27	6.05	2.95	0.13	12.92	22.96	0.66	0.98	0.08	29.68	0.4748	0.0023
En5 4A	14.52	0.18	3.72	1.81	0.10	17.65	24.67	0.54	0.63	0.11	36.07	0.6037	0.0018
En5 4B	15.40	0.18	3.81	1.77	0.10	17.37	24.41	0.58	0.66	0.10	35.61	0.6005	0.0023
En5 4C	24.95	0.29	6.41	3.23	0.15	11.84	23.08	0.72	1.03	0.14	28.15	0.4329	0.0019
En5 3A	15.00	0.19	4.08	1.84	0.10	17.41	24.47	0.61	0.63	0.10	35.58	0.6004	0.0022
En5 3B	17.01	0.19	3.92	1.89	0.10	16.80	24.32	0.66	0.68	0.11	34.33	0.5829	0.0019
En5 3C	25.96	0.29	6.62	3.12	0.14	11.50	22.68	0.74	1.07	0.10	27.78	0.4279	0.0017
En5 2A	13.08	0.18	3.77	1.69	0.09	17.80	25.11	0.54	0.62	0.08	37.03	0.5982	0.0020
En5 2B	15.62	0.19	3.93	1.70	0.09	17.20	24.46	0.66	0.65	0.11	35.40	0.5934	0.0022
En5 2C	22.81	0.26	5.92	2.80	0.14	12.48	24.01	0.74	0.94	0.09	29.84	0.4386	0.0020
En5 1A	19.66	0.26	5.62	2.56	0.12	14.00	23.46	0.62	0.90	0.10	32.70	0.5036	0.0014
En10 1A	14.79	0.20	4.36	1.78	0.10	17.13	23.90	0.37	0.57	0.21	36.59	0.5680	15.2939
En10 1B	21.75	0.27	6.08	2.40	0.11	13.45	22.31	0.50	0.85	0.20	32.07	0.6585	11.1116
En10 2A	16.78	0.21	4.59	2.05	0.11	16.07	23.85	0.45	0.61	0.23	35.05	0.4833	21.6196
Cr2A	25.40	0.28	6.04	2.46	0.15	12.95	22.80	0.68	0.84	0.14	28.26	0.6379	6.0197
Cr2B	26.93	0.24	5.80	2.12	0.11	14.04	21.32	0.82	0.73	0.23	27.66	0.7167	15.6611
Cr3A	14.14	0.27	5.60	8.94	0.26	13.19	27.29	0.92	0.78	1.30	27.33	0.6029	18.8705
Cr3B	25.47	0.27	5.27	2.60	0.14	16.86	26.43	0.73	0.75	0.32	21.16	0.6738	19.5430

Dolomite content increases toward the internal parts of the chimneys, whereas in the external portion the calcite cement and the detrital fraction are more abundant. Terrigenous components, such as SiO_2, Al_2O_3 and Fe_2O_3, increase towards the external areas; whereas, elements pertaining to the carbonate phases have their maximum in the middle and internal parts (Table 5; Fig. 7).

The trace elements Cr, V, Ni and Rb show maximum concentrations in the external parts of the chimney, while S has a small

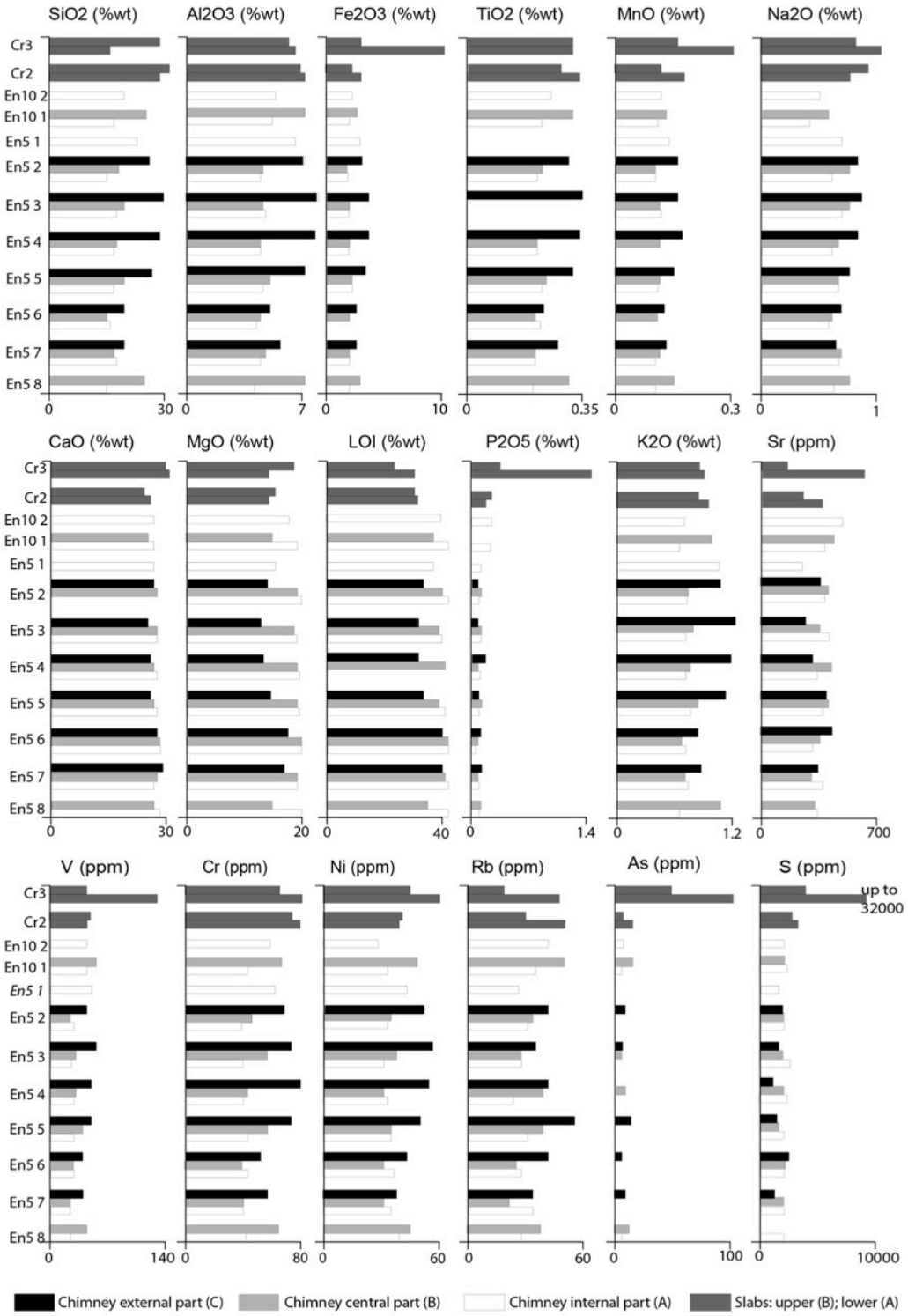

Figure 7. Major oxides concentration, LOI and minor elements of the carbonate chimneys (En5–En10), slab (Cr2) and the concretion (Cr3).

Table 6
Minor elements in the carbonate concretions.

Sample	V (ppm)	Cr (ppm)	Co (ppm)	Ni (ppm)	Cu (ppm)	Zn (ppm)	As (ppm)	Rb (ppm)	Sr (ppm)	Y (ppm)	Zr (ppm)	Nb (ppm)	Ba (ppm)	La (ppm)	Ce (ppm)	Pb (ppm)	Th (ppm)	S (ppm)	TOC (%)
En5 8A	24	35	<3	34	6	34	5	23	320	2	2	2	223	12	23	<3	<3	1950	0.48
En5 8B	40	56	<3	39	4	26	10	32	308	3	17	7	300	12	40	<3	<3	1060	0.60
En5 7A	22	36	<3	30	4	32	<3	30	356	3	2	6	264	<3	22	<3	6	2330	0.24
En5 7B	21	36	<3	27	12	29	<3	18	286	3	2	5	235	11	47	<3	7	2150	0.22
En5 7C	36	51	<3	33	12	40	10	29	332	2	2	6	269	4	39	<3	5	1380	1.00
En5 6A	26	39	<3	32	7	34	<3	25	301	2	2	8	250	<3	25	<3	<3	2250	0.45
En5 6B	24	35	<3	27	14	33	<3	22	331	2	2	5	258	11	31	<3	<3	2450	0.93
En5 6C	33	43	<3	38	10	39	5	36	413	2	2	6	250	10	53	<3	7	2660	0.36
En5 5A	27	37	<3	31	9	38	<3	26	349	5	2	5	245	9	44	<3	3	2160	0.67
En5 5B	32	50	<3	30	14	37	<3	33	384	4	2	6	273	9	37	<3	4	1850	0.26
En5 5C	44	65	4	45	10	51	13	48	380	7	19	9	278	18	37	<3	7	1590	0.40
En5 4A	26	35	<3	29	10	35	<3	21	310	4	2	6	243	<3	28	<3	4	2590	1.13
En5 4B	27	38	<3	27	6	35	7	34	397	3	2	6	259	4	25	<3	5	2061	0.77
En5 4C	45	70	<3	47	17	50	<3	36	310	3	6	5	296	13	33	<3	7	1340	0.29
En5 3A	23	35	<3	27	8	31	<3	24	376	5	2	4	272	9	25	<3	<3	2880	0.20
En5 3B	27	48	<3	33	6	36	4	24	334	5	2	3	258	<3	33	<3	5	2280	0.22
En5 3C	50	64	4	49	19	51	7	30	269	6	16	5	259	6	54	<3	8	1830	0.35
En5 2A	26	34	<3	29	10	35	<3	26	365	2	2	6	223	<3	31	<3	<3	2390	1.02
En5 2B	20	40	<3	30	6	33	<3	29	388	2	4	4	251	3	32	<3	10	1940	0.22
En5 2C	40	61	4	44	21	47	8	36	352	10	13	6	284	26	43	<3	4	1910	1.39
En5 1A	42	55	<3	37	17	44	<3	23	239	5	2	4	255	12	37	<3	<3	1750	0.49
En10 1A	39	36	<3	30	14	16	4	30	374	6	17	5	202	10	32	12	4	2520	
En10 1B	49	58	<3	42	13	25	13	44	421	10	39	7	253	3	26	15	<3	2270	
En10 2A	37	52	<3	25	9	16	5	36	466	10	34	5	251	9	13	11	<3	2380	
Cr2A	41	71	<3	34	8	23	14	45	349	11	73	4	284	<3	3	13	<3	3560	
Cr2B	46	67	<3	35	8	22	5	27	237	7	65	3	201	3	26	10	<3	3070	
Cr3A	116	71	22	53	15	42	87	42	590	21	20	7	241	4	35	92	<3	32,000	
Cr3B	40	58	4	39	12	20	41	17	159	3	36	<3	202	<3	<3	20	<3	4390	

increase in the internal areas. The overall content of trace elements is higher in samples En5 with respect to samples En10.

The slab (sample Cr2) and the concretion (Cr3) consist of dolomite (up to 80% wt), whereas calcite is present in correspondence of the white zone of Cr2B (4% wt) and in the carbonate fraction of Cr3B (11% wt) (Table 4). MgO is usually higher in the chimneys than in the slabs. These latter, on the other hand, show higher concentrations of V, Cr, and S.

Cr3A shows higher concentrations of trace elements than Cr2 and Cr3B (Fig. 7). For instance S reaches the concentration of 32,000 ppm in Cr3A (Table 6). Furthermore, this sample has the lowest concentration of SiO_2.

4.3. Carbonate stable isotopes

In Table 7 are presented the results for the $\delta^{13}C$ and $\delta^{18}O$ for carbonate samples. The slabs show carbon isotope values more depleted than chimneys, in particular Cr3A is the most negative with −40.13‰ VPDB.

$\delta^{13}C$ values are generally more negatives toward the internal parts (A) of the En5 chimney, ranging between −17.07 and −20.06‰ VPDB, respect to the $\delta^{13}C$ of −8.6‰ VPDB, detected in the externals parts in the sample En5_3C. A further variation of ^{13}C has been observed from the top (En5_8) to the bottom (En5_1) of the chimney showing less negative $\delta^{13}C$ values. The $\delta^{18}O$ isotope values range between 4.37‰ and 6.24‰ VPDB. In this case the slabs values, ranging between 4.4‰ and 6.24‰ VPDB, are close to those from the chimneys, which are between 4.37‰ and 6.21‰ VPDB.

4.4. Carbonate petrography

Petrographic observation of thin sections was performed along En5 chimney, on the Cr3A dark concretion and on the carbonate breccia enclosed in the rhodolith-rich layer.

- The EN5 chimney is cemented by dolomitic micrite (hereafter referred to as dolomicrite) and microsparite (Figs. 8A and 9A) with abundant angular to sub-angular quartz clasts (up to 35% vol., 50–150 μm). SEM-EDS analyses revealed the presence of clusters of framboidal pyrite engulfed within the dolomitic cements (Fig. 9B). The chimney shows clear zonation probably due to dissolution–cementation cycles (Fig. 8 B–C). This zonation is marked by corrosion surfaces often lined by a thin generation (ca. 10 μm) of isopachous scalenohedral calcite (Fig. 8B–C). Locally, the chimneys are made of alternating peloidal micrite and dolomicrite. Peloids are 250–500 μm ovoidal to circular in shape, organized in clotted fabric (Fig. 8D); inter-peloids porosity is filled with microcrystalline cements and sand-sized clasts of quartz. Thin levels (ca. 500 μm) of sandy dolomicrite are breached by sigmoidal fractures (Fig. 8 E–F). Well-rounded clasts of glauconite (Figs. 8C and 9C) are sparse in the matrix as well as poorly rounded mica and plagioclase crystals. The chimneys are often breached by systems of radial and longitudinal fractures partially filled by microsparite (Fig. 8F). Some of those networks show geometrical intersections that suggest a likely affinity with tension cracks structures (Fig. 8G).
- *Dark limestone* (sample Cr3A), which stratigraphically overlies the chimneys, is made of micrite with clasts of quartz (>50% vol., 50–150 μm) and mottled micrite that shows peloidal fabric. Toward the upper surface of the slab, this facies is bounded by red coralline algae (Fig. 8H). Rhodalgal-coated chips of fossil-barren mudstone together with foraminifera and coral remains are shown in Figure 8I.
- *In situ carbonate breccia* is made of millimetre-sized pebbles of micrite, micrite with abundant sand-sized clasts of quartz and red algae fragments. Several centimetre-sized rhodolithes were described within this facies (Fig. 8J). This facies show high voids ratio; sometimes voids are filled by mesosparite and botryoids of acicular aragonite (Fig. 8J). An isopachous generation of scalenohedral calcite growth on the carbonatic pebbles. Macroborings are restricted to the rhodolithes, indicating lithification before the settlement of macroborers (Fig. 8 K–L). Macroborings are filled with bright luminescence micrite, with sand-sized clasts of quartz and probably feldspar (Fig. 8 K–L)

5. Discussion

The chemical composition of the Argille Azzurre Fm. that hosts the seep carbonates reflects the mineralogy of the eroded rocks supplying sediments to the continental shelf during the Pleistocene (Capozzi and Picotti, 2010; Capozzi et al., 2012; Dinelli et al., 2012). Elements linked with quartz, plagioclase, micas, clay minerals and feldspars are abundant. The enrichment of Ni and Cr indicates the presence of mafic and ultramafic minerals, derived from the contribution of local magmatic rocks occurring within the drainage area in the emerging Northern Apennines chain (Picotti et al., 2007; Ghielmi et al., 2010; Gunderson et al., 2014). The enrichment in CaO, LOI and TOC matched by a negative peak of SiO_2, Al_2O_3, Fe_2O_3, and K_2O at 10 m seems to be associated to the presence of a thin horizon probably corresponding to a peak of primary productivity, linked to calcareous phytoplankton and associated with organic carbon. Negative peaks of Al_2O_3, Fe_2O_3, K_2O, TiO_2, V and Rb (Fig. 5), coupled with the positive peak of Si/Al (Fig. 6) at 25 m suggest a grain-size increase, corresponding to the occurrence of thin sandy and silty-sand layers in the succession, coupled with the first occurrence of carbonate concretions. The same variations can be found at 50 m, where the sandy layers are well developed and thicker slabs occur along the bedding planes (Oppo et al., in this isue). The carbonate minerals in the sediments are mainly attributed to the presence of fossil tests. However, dolomite and protodolomite occur only in the upper 35 m of the section, suggesting an origin linked to the same processes that generated the associated carbonate concretions.

The concretions are mainly composed of authigenic dolomite (>60% wt), variable amounts of calcite (<15% wt) and detrital fraction. The cements petrography frequently shows clotted peloidal micrite. This microfabric has been widely observed in methane-derived authigenic carbonates (MDAC) found in active or fossil cold seep systems (e.g. Peckmann et al., 2001; Magalhães,

Table 7
Stable isotopes in the carbonate concretions. The symbol * indicates the measurements performed at CNR-IGG in Pisa.

Sample	$\delta^{13}C$ (vpdb)	$\delta^{18}O$ (vpdb)
En5 8A	−20.06	5.86
En5 8B	−19.49	5.47
En5 6A	−19.31	6.2
En5 6B	−18.97	6.13
En5 4A*	−18.22	6.08
En5 3A	−18.61	6.21
En5 3C	−8.60	4.37
En5 1A	−17.07	5.59
En5 1B	−16.07	5.49
Cr2A*	−28.56	6.12
Cr3A	−35.42	4.49
Cr3A	−40.13	4.44
Cr3A*	−30.69	5.10
Cr3B* (calcite)	−30.91	5.44
Cr3B*	−35.39	6.13
Cr3B* (calcite + dolomite)	−35.07	6.24

2007; Capozzi et al., 2012). The peloids are interpreted as the product of intense and widespread microbial activity during carbonate precipitation (Peckmann et al., 2001; Peckmann and Thiel, 2004; Peckmann et al., 2007; Feng et al., 2008). Sulphur is particularly abundant in Cr3A and reflects the occurrence of pyrite and arsenopyrite. Further evidence of AOM can be found in the stable isotope ratios of the carbonate cements (Table 7). In the chimneys of Enza River, the $\delta^{13}C$ ranges between −8.60‰ and −20.06‰ (VPDB), whereas the slabs have lower values, ranging between −28.56‰ and −40.13‰ VPDB. These values are indicative of AOM processes, as described for MDAC elsewhere (e.g. Rodriguez et al., 2000; Diaz-del-Rio et al., 2003; Hensen et al., 2007; Capozzi et al., 2012; Magalhães et al., 2012). The $\delta^{18}O$ in our samples vary from 4.4‰ VPDB and 6.2‰ VPDB meaning that they are significantly enriched in ^{18}O with respect to carbonates precipitated in a nowadays seawater conditions where $\delta^{18}O$ is usually between 0‰ and 1‰ VPDB (Magalhães, 2007). This enrichment could be explained by the fact that carbonate dolomite phase shows usually an increase of 2–4‰ in $\delta^{18}O$ composition respect to the ambient water (Budd, 1997; Aloisi et al., 2000; Oppo et al., in this issue); moreover according to Zachos et al., 2001 the values of $\delta^{18}O$ during the Early Pleistocene were around 3‰ VPDB (Oppo et al., in this

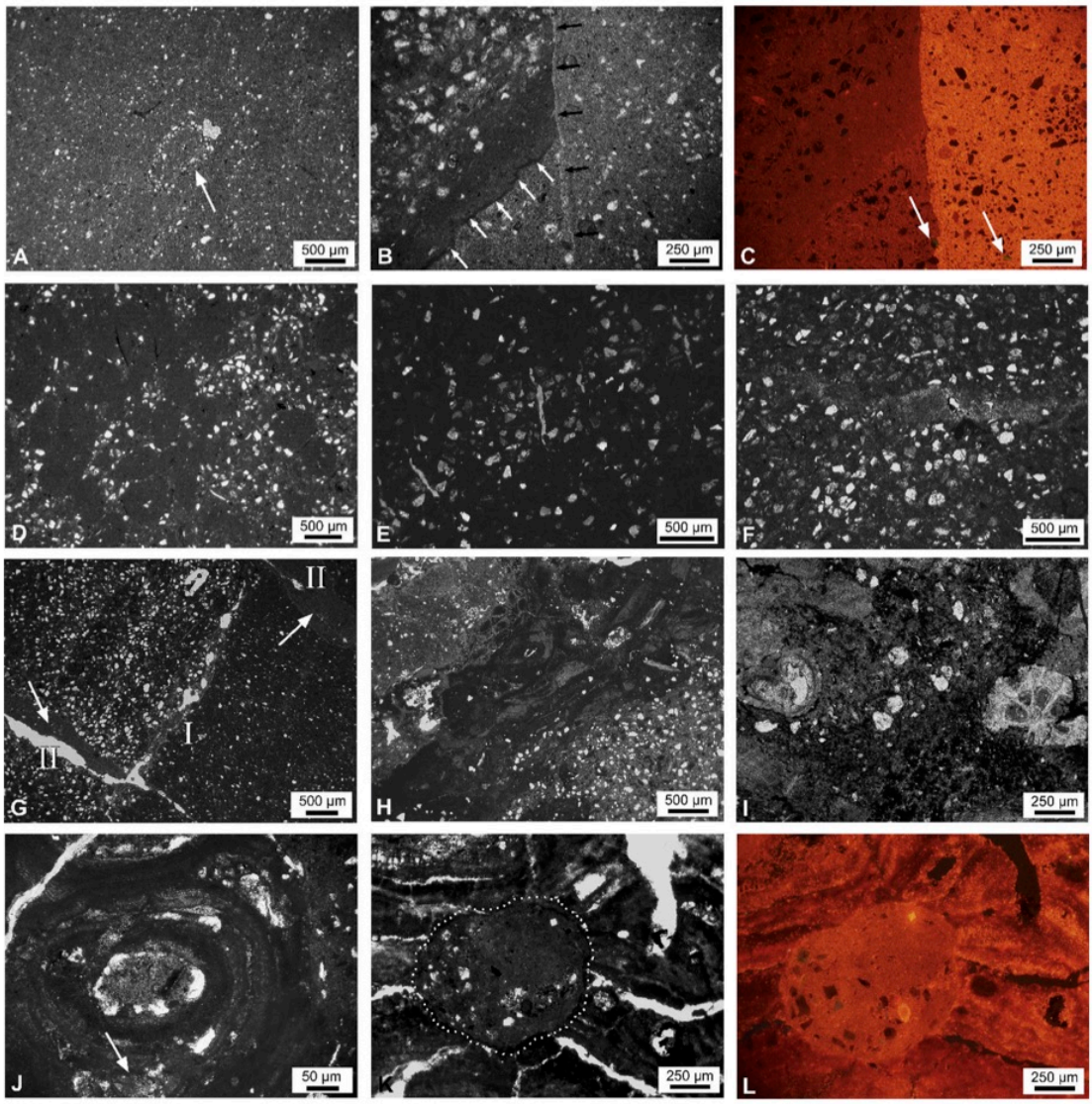

Figure 8. Photomicrographs of the studied carbonates. A) Mottled micrite/microsparite with abundant angular to sub-angular quartz clasts. The arrow point to a rounded carbonate intraclast fouled by angular quartz clasts. B) Fractures (bright cements) breaching the chimney dolomicrite (darker cements). Often fracture walls are lined by dark layers of organic matter-rich micrite (with arrows) or thin isopachous generation of calcite cements (black arrows). C) Cathodoluminescence photomicrograph (same as B) showing two dominant phases: bright luminescent fracture fills, dominated by calcitic micrite; dark red dolomicrite. Arrows point to glauconite clasts. D) Peloidal fabric within chimney wall. Note that peloids are avoid of quartz clasts. E) Thin layer of angular quartz clasts breached perpendicularly by hollow fractures. F) Fractures filled by microcrystalline cements. G) Two perpendicular systems of fractures: first system (I), parallel to the chimney's wall, mark the contact between dolomitic sandstone (upper left) and dolomicrite (lower right); the second system (II), perpendicular to the first one, is partially filled by micrite (arrows). H, I) Topmost part of the dark concreted slab showing red algae bounding dolomitic sands. Red algae level is covered by thin bioclastic mud with rare quartz clasts (upper left in H). J) Red algal rhodoids. Large voids within the thallus (conceptacles) are locally filled with aragonite (arrow). K–L) Macroboring (dotted line) within red algal rhodoids is infilled with bright luminescence sandy micrite (L). (For interpretation of the references to colour in this figure legend, the reader is referred to the web version of this article.)

issue). Petrographic analyses revealed that the chimneys are breached by expansion and sigmoidal fractures that have been described elsewhere within gas saturated sediments (Mazzini et al., 2005) and might be related to fluids expulsions-related processes. This fracture network would represent the main mechanism of gas diffusion in fine-grained sediments as observed in the model of Choi et al. (2011).

The progressive increase of carbonate cements is observed toward the internal parts of the chimneys, which is mainly made of dolomite (up to 82% bulk rock in the sample En5_2A). Otherwise, authigenic calcite increases in the external parts. The higher content of calcite toward the edges reflects the increased influence of pore water rich of SO_4^{2-}, which inhibits the dolomite precipitation in anaerobic environment and favours the formation of calcite (e.g. Douglas, 2005).

Higher concentration of SiO_2 and Al_2O_3 in the external areas of the EN5 evidence the gradual increase of siliciclastics from the internal to external areas, as suggested by the changes in mineralogy.

The chimneys form due to the focused fluids flow through a narrow discontinuity in the sediment interval consistent with the increase of sand within sedimentary record. The continued and vigorous flow progressively displaces the sediment particles and creates an open central vent that in some cases has been fully closed. The mainly dolomitic phase in cements suggests that all carbonate concretions so far analysed formed within the sediment pile near the Sulphate–Methane Interface (SMI) where the interstitial water is quite depleted in the sulphate component (Magalhães, 2007; Magalhães et al., 2012 and references therein).

The enrichment of Fe, S, Ni and Cr, involved in the formation of sulphide minerals in the Cr3A, could indicate precipitation/

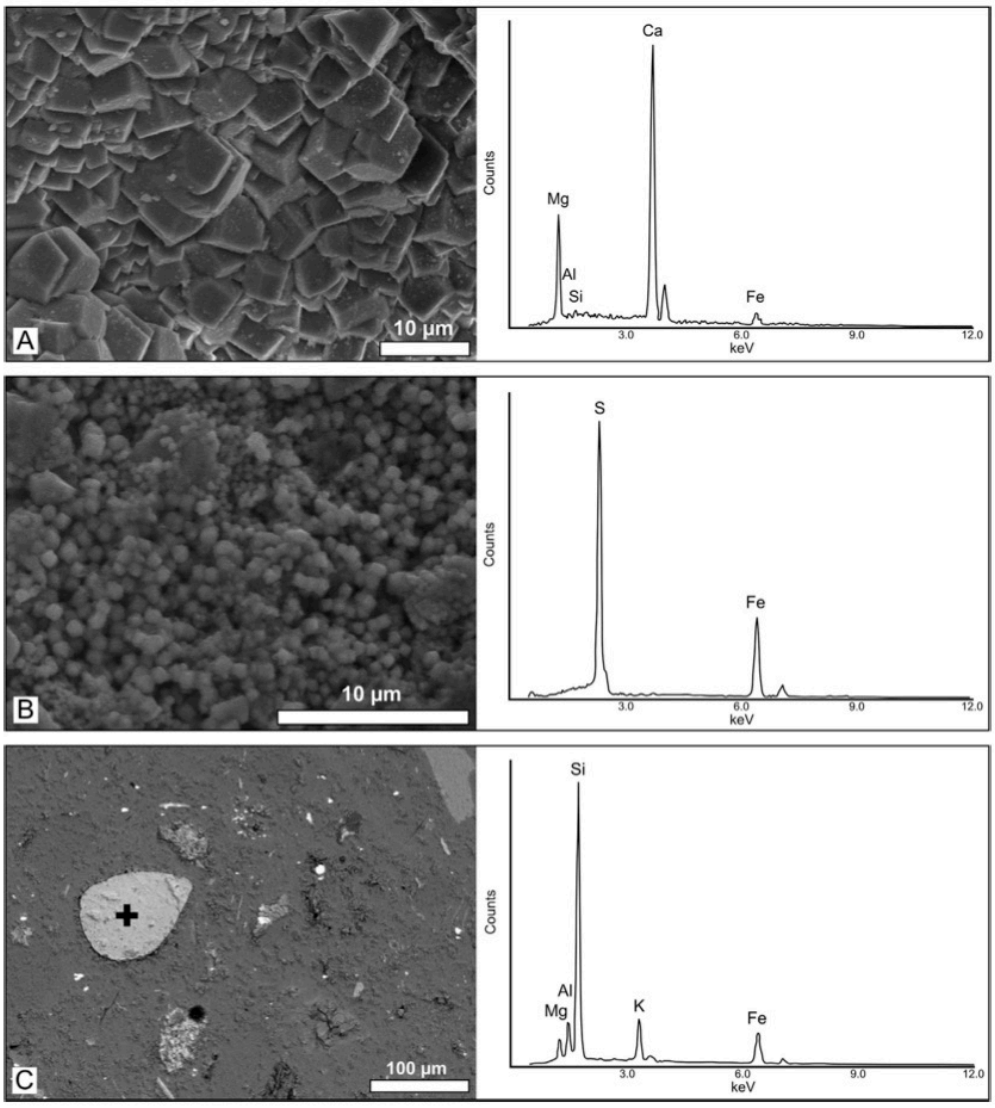

Figure 9. Scanning electron microscope (SEM) photomicrographs and EDX analyses of the dolomitic chimneys from the Enza river. A) Microcrystalline euhedral rhombs of dolomite and EDX spectrum collected with 15 keV accelerating voltage from the entire area. B) Loose euhedral S–Fe-rich microcrystals (pyrite). EDX spectrum collected with 15 keV accelerating voltage from the entire area. C) Back scattered (BEI) photomicrograph of chimney dolomicrite showing well rounded clast of glaukonite. EDX spectrum collected with 15 keV accelerating voltage from the bright rounded clast (cross).

alteration of the carbonate by a renewed fluids leakage, permeating the rhodolith-enriched layer, after a period of non-deposition or erosion at the seafloor. The mottled micrite with its peloidal fabric indicates a renewed bacterial activity that possibly developed near the seafloor. In fact, in situ carbonate breccia also shows high voids ratio in same cases filled by mesosparite and botryoids of acicular aragonite that are very similar to those reported in methane-derived authigenic carbonates recovered at the seafloor in the Black Sea and Adriatic Sea (Naudts et al., 2008; Capozzi et al., 2012).

6. Conclusions

Geochemical analyses on the Argille Azzurre Fm. sediments that host the carbonate concretions revealed their dominant siliciclastic composition, with small contents of biogenic calcite. Dispersed dolomite and protodolomite occur in the upper half of the section in association with the carbonate concretions.

Dolomite cement represents the 60–80 % weight of the studied carbonate concretions. Therefore, the chimney palisade share compositional similarities with analogue dolomitic pipes identified in the Gulf of Cadiz (Magalhães et al., 2012), southern New Zealand continental slope (Orpin, 1997), offshore Brazil (Wirsig et al., 2012), Black Sea (Reitner et al., 2005), Mediterranean Sea (Angeletti et al., in this issue) and other localities on land (e.g. De Boever et al., 2006a; Cau et al., in this issue).

Petrographic observations support the role of methane-enriched fluids in the genesis of the carbonate chimneys and slabs. The occurrence of clotted and peloidal microfabric, which commonly represents bacterially induced precipitates, is frequently observed in methane derived authigenic carbonates. Moreover, stable carbon isotope ratios in cements indicate anaerobic oxidation of methane and sulphate reduction during the carbonate precipitation.

The dolomite increase in the internal zone of chimneys reflects the progressive isolation from the SO_4-rich pore water, which instead favours the calcite precipitation in the external area. The siliciclastic content increases moving from the internal to external zones due to the sediment displacement operated by the fluid flow along the central emission vent.

Pyrite, arsenopyrite and strontianite together with aragonite botryoids, possibly indicate secondary carbonate dissolution/precipitation within the rhodolith-rich bed. The presence of this sulphide within carbonates points to a change in fluid leakage conditions within more permeable sediments saturated by SO_4-rich marine water. These carbonates probably deposited after a period of seabed erosion in the Early Pleistocene shelf environment. The fluid leakage persists in present-day, after the emersion of the Apennine foothills.

Acknowledgements

Funding was provided by the national project PRIN 2009 "Carbonate conduits linked to hydrocarbons enriched seepages" (PI R. Capozzi) of the Italian Ministry of University and Research (MIUR). Thanks are due to C. Mazzoli (University of Padua) for the access at the cathodoluminescence facilities. The authors are indebted with two anonymous reviewers for their constructive criticism. This is ISMAR-Bologna scientific contribution number 1851.

References

Aloisi, G., Pierre, C., Rouchy, J.-M., Foucher, J.-P., Woodside, J., 2000. Methane-related authigenic carbonates of eastern Mediterranean Sea mud volcanoes and their possible relation to gas hydrate destabilisation. Earth Planet. Sci. Lett. 184, 321–338.

Angeletti, L., Canese, S., Franchi, F., Montagna, P., Reitner, J., Walliser, E.O., Taviani, M., 2015. The chimney forest of the deep Montenegrin margin, south-eastern Adriatic Sea. In: Capozzi, R., Negri, A., Reithner, J., Taviani, M. (Eds.), Carbonate Conduits Linked to Hydrocarbon-enriched Fluid Escape. Special Issue of Mar. and Petr. Geo.

Boccaletti, M., Corti, G., Martelli, L., 2010. Recent and active tectonics of the external zone of the Northern Apennines (Italy). Earth Sci. 100, 1331–1348.

Boetius, A., Ravenschlag, K., Schubert, C.J., Rickert, D., Widdel, F., Giesecke, A., Amann, R., Jorgensen, B.B., Witte, U., Pfannkuche, O., 2000. A marine microbial consortium apparently mediating anaerobic oxidation of methane. Nature 407, 623–626.

Budd, D.A., 1997. Cenozoic dolomites of carbonate islands: their attributes and origin. Earth Sci. Rev. 42, 1–47.

Capozzi, R., Picotti, V., 2010. Spontaneous fluid emissions in the Northern Apennines: geochemistry, structures and implications for the petroleum system. In: Goffey, G.P., Craig, J., Needham, T., Scott, R. (Eds.), Hydrocarbons in Contractional Belts, Geol. Soc London Spec. Publ. 348, London, pp. 115–135.

Capozzi, R., Guido, F.L., Oppo, D., Gabbianelli, G., 2012. Methane-Derived Authigenic Carbonates (MDAC) in northern-central Adriatic Sea: relationships between reservoir and methane seepages. Mar. Geol. 332–334, 174–188.

Capozzi, R., Negri, A., Reitner, J., Taviani, M., Franchi, F., Oppo, D. (Eds.), 2013. Carbonate Conduits Linked to Hydrocarbon-enriched Fluid Escape, Workshop and Field Seminar, Bologna, June 28th– July 1st, 2013, Field Guide and Abstracts with Program, Bologna, pp. 1–51.

Cau, S., Franchi, F., Roveri, M., Taviani, M., 2015. The Pliocene-age Stirone river hydrocarbon chemoherm complex (Northern Apennines, Italy). In: Capozzi, R., Negri, A., Reithner, J., Taviani, M. (Eds.), Carbonate Conduits Linked to Hydrocarbon-enriched Fluid Escape. Special Issue of Marine and Petroleum Geology.

Choi, J., Mouillesseaux, K., Wang, Z., Fiji, H.D., Kinderman, S.S., Otto, G.W., Geisler, R., Kwon, O., Chen, J.N., 2011. Aplexone targets the HMG-CoA reductase pathway and differentially regulates arteriovenous angiogenesis. Development 138, 1173–1181.

Clari, P., Cavagna, S., Martire, L., Hunziker, J., 2004. A miocene mud volcano and its plumbing system: a chaotic complex revised (Monferrato, NW Italy). J. Sediment. Res. 74, 662–676.

De Boever, E., Swennen, R., Dimitrov, L., 2006a. Lower Eocene carbonate-cemented "chimney" structures (Varna, Bulgaria) - control of seepage rates on their formation and stable isotopic signature. J. Geochem. Explor. 89, 78–82.

De Boever, E., Swennen, R., Dimitrov, L., 2006b. Lower Eocene carbonate cemented chimneys (Varna, NE Bulgaria): formation mechanisms and the (a)biological mediation of chimney growth? Sediment. Geol. 185, 159–173.

Díaz-del-Rio, V., Somoza, L., Martinez-Frias, J., Hernandez-Molina, F.J., Lunar, R., Fernandez-Puga, M.C., Maestro, A., Terrinha, P., Llave, E., Garcia, A., Garcia, A.C., Vazquez, J.T., 2001. Carbonate chimneys in the Gulf of Cadiz: initial report of their petrography and geochemistry. In: Akhmanov, G., Suzyumov, A. (Eds.), Geological Processes on Deep-water European Margins. IOC-UNESCO Workshop Report 175, pp. 53–54.

Díaz-del-Río, V., Somoza, L., Martínez-Frías, J., Mata, P., Delgado, A., Hernández-Molina, F.J., Lunar, R., Martín-Rubí, J.A., Maestro, A., Fernández-Puga, M.C., León, R., Llave, E., Medialdea, T., Vázquez, J.T., Hernández-Molina, F.J., 2003. Vast fields of hydrocarbon derived carbonate chimneys related to the accretionary wedge/olistostrome of the Gulf of Cadiz. Mar. Geol. 195, 177–200.

Dinelli, E., Ghosh, A., Rossi, V., Vaiani, S.C., 2012. Multiproxy reconstruction of Late Pleistocene-Holocene environmental changes in coastal successions: microfossil and geochemical evidences from the Po Plain (Northern Italy). Stratigraphy 9, 153–167.

Douglas, S., 2005. Mineralogical footprints of microbial life. Am. J. Sci. 305, 503–525.

Feng, D., Chen, D.F., Qi, L., Roberts, H., 2008. Petrographic and geochemical characterization of seep carbonate from Alaminos Canyon, Gulf of Mexico. Chin. Sci. Bull. SP Science in China Press 53 (11), 1716–1724.

Franzini, M., Leoni, L., Saitta, M., 1972. A simple method to evaluate the matrix effects in X-Ray fluorescence analysis. X-Ray Spectrom. 1, 151–154.

Franzini, M., Leoni, L., Saitta, M., 1975. Revisione di una metodologia analitica per fluorescenza-X, basata sulla correzione completa degli effetti di matrice. Rend. Soc. Ital. Mineral. Petrol. 31, 365–378.

Ghielmi, M., Minervini, M., Nini, C., Rogledi, S., Rossi, M., Vignolo, A., 2010. Sedimentary and tectonic evolution in the eastern Po-Plain and northern Adriatic Sea area from Messinian to Middle Pleistocene (Italy). Rend. Lincei 21, S131–S166.

Goldsmith, J.R., Graf, D.L., 1958. Relation between lattice constants and composition of the Ca–Mg carbonates. Am. Mineral. 43, 84–101.

Gunderson, K.L., Pazzaglia, F.J., Picotti, V., Anastasio, D.A., Kodama, K.P., Rittenour, T., Frankel, K.F., Ponza, A., Berti, C., Negri, A., Sabbatini, A., 2014. Unraveling tectonic and climatic controls on synorogenic stratigraphy (Northern Apennines, Italy). GSA Bull. 126, 532–552.

Hensen, C., Nuzzo, M., Hornibrook, E., Pinheiro, L.M., Bock, B., Magalhaes, V.H., Bruckmann, W., 2007. Sources of mud volcano fluids in the Gulf of Cadiz—indications for hydrothermal imprint. Geochim. Cosmochim. Acta 71 (5), 1232–1248.

Lein, A. Yu, 2004. Authigenic carbonate formation in the ocean. Lithol. Miner. Resour. 39 (1), 1–30. Translated from Litologiya i Poleznye Iskopaemye 1, 2004: 3-35.

Leoni, L., Saitta, M., 1976. X-ray fluorescence analysis of 29 trace elements in rock and mineral standards. Rend. Soc. Ital. Mineral. Petrol. 32, 497–510.
Leoni, L., Menichini, M., Saitta, M., 1982. Determination of S, Cl, and F in silicate rocks by X-Ray fluorescence analyses. X-Ray Spectrom. 11, 156–158.
Lumsden, D.N., 1979. Discrepancy between thin-section and X-ray estimates of dolomite in limestone. J. Sediment. Res. 49, 429–435.
Magalhães, V.H., 2006–2007. Carbonates autigénicos e estruturas de escape de fluidos no Golfo de Cádis. Unpubl. Thesis (Tese apresentada do grau de Doutor em Geocencias.) Departamento de Geocencias, Universidade de Aveiro. a.a.
Magalhães, V.H., Pinheiro, L.M., Ivanov, M.K., Kozlova, E., Blinova, V., Kolganova, J., Vasconcelos, C., McKenzie, J.A., Bernasconi, S.M., Kopf, A.J., Díaz-del-Río, V., González, F.J., Somoza, L., 2012. Formation processes of methane-derived authigenic carbonates from the Gulf of Cadiz. Sediment. Geol. 243–244, 155–168.
Mazzini, A., Aloisi, G., Akhmanov, G.G., Parnell, J., Cronin, B.T., Murphy, P., 2005. Integrated petrographic and geochemical record of hydrocarbon seepage on the Vøring Plateau. J. Geol. Soc. Lond. 162, 815–827.
Naudts, L., Greinert, J., Artemov, Y., Beaubien, S.E., Borowski, C., Batist, M.D., 2008. Anomalous sea-floor backscatter patterns in methane venting areas, Dnepr paleo-delta, NW Black Sea. Mar. Geol. 251, 253–267.
Nyman, S.L., Nelson, C.S., Campbell, K.A., 2010. Miocene tubular concretions in East Coast Basin, New Zealand: analogue for the subsurface plumbing of cold seeps. Mar. Geol. 272, 319–336.
Oppo, D., Capozzi, R., Picotti, V., 2013. A new model of the petroleum system in the Northern Apennines, Italy. Mar. Pet. Geol. 48, 57–76.
Oppo, D., Capozzi, R., Picotti, V., Ponza, A., 2015. A genetic model of hydrocarbon-derived carbonate chimneys in shelfal fine grained sediments: the Enza River field, Northern Apennines (Italy). In: Capozzi, R., Negri, A., Reithner, J., Taviani, M. (Eds.), Carbonate Conduits Linked to Hydrocarbon-enriched Fluid Escape. Special Issue of Marine and Petroleum Geology.
Orpin, A.R., 1997. Dolomite chimneys as possible evidence of coastal fluid expulsion, uppermost Otago continental slope, southern New Zealand. Mar. Geol. 138, 51–67.
Peckmann, J., Reimer, A., Luth, U., Luth, C., Hansen, B.T., Heinicke, C., Hoefs, J., Reitner, J., 2001. Methane-derived carbonates and authigenic pyrite from the northwestern Black Sea. Mar. Geol. 177, 129–150.
Peckmann, J., Thiel, V., 2004. Carbon cycling at ancient methane-seeps. Chem. Geol. 205, 443–467.
Peckmann, J., Campbell, K.A., Walliser, O.H., Reitner, J., 2007. A Late Devonian hydrocarbon-seep deposit dominated by dimerreloid brachiopods, Morocco. Palaios 22, 114–122.
Picotti, V., Capozzi, R., Bertozzi, G., Mosca, F., Sitta, A., Tornaghi, M., 2007. The Miocene petroleum system of the Northern Apennines in the central Po Plain (Italy). In: Lacombe, O., Lavé, J., Roure, F., Vergés, J. (Eds.), Thrust Belts and Foreland Basins, from Fold Kinematics to Hydrocarbon System. Springer Verlag, Berlin, pp. 117–131.
Pinheiro, L.M., Ivanov, M.K., Sautkin, A., Akhmanov, G., Magalhaes, V.H., Volkonskaya, A., Cunha, M.R., 2003. Mud volcanism in the Gulf of Cadiz: results from the TTR-10 cruise. Mar. Geol. 195, 131–151.
Ponza, A., Pazzaglia, F.J., Picotti, V., 2010. Thrust-fold activity at the mountain front of the Northern Apennines (Italy) from quantitative landscape analysis. Geomorphology 123, 211–223.
Reitner, J., Peckmann, J., Reimer, A., Schumann, G., Thiel, V., 2005. Methane-derived carbonate build-ups and associated microbial communities at cold seeps on the lower Crimean shelf (Black Sea). Facies 51, 66–79.
Rodriguez, N.M., Paull, C.K., Borowski, W.S., 2000. Zonation of authigenic carbonates within gas hydrate-bearing sedimentary sections on the Blake Ridge: offshore southeastern North America. Proc. ODP Sci. Results 164, 301–312.
Rosenbaum, J., Sheppard, S.M.F., 1986. An isotopic study of siderites, dolomites and ankerites at high-temperatures. Geochim. Cosmochim. Acta 50 (6), 1147–1150.
Rosenbaum, J.M., 1994. Stable-isotope fractionation between carbon-dioxide and calcite at 900 °C. Geochim. Cosmochim. Acta 58 (17), 3747–3753.
Somoza, L., Díaz-del-Rio, V., Léon, R., Ivanov, M.K., Fernández-Puga, M.C., Lobato, A., Maestro, A., Hernández-Molina, F.J., Gardner, J.M., Rodero, J., Pinheiro, L.M., Vásquez, J.T., Medialdea, T., Fernández-Salas, L.M., 2003. Seabed morphology and hydrocarbon seepage in the Gulf of Cadiz mud volcano area: imagery of multibeam data and ultra-high resolution data. Mar. Geol. 195, 153–176.
Taviani, M., 2001. Fluid venting and associated processes. In: Vai, G.B., Maltini, I.P. (Eds.), Anatomy of an Orogen: the Apennines and Adjacent Mediterranean Basins. Kluwer Academic Publisher, Great Britain, pp. 351–366.
Taviani, M., 2014. Marine chemosynthesis in the Mediterranean Sea. In: Goffredo, S., Baader, H., Dubinsky, Z. (Eds.), The Mediterranean Sea: Its History and Present Challenges. Springer, Science + Business Media Dordrecht, pp. 69–83.
Teichert, B.M.A., Bohrmann, G., Suess, E., 2005. Chemoherms on Hydrate Ridge: unique microbially mediated carbonate build-ups growing into the water column. Palaeogeogr. Palaeoclimatol. Palaeoecol. 227, 67–85.
Unterseh, S.L., 2013, May 6. Early Recognition of Seabed and Sub-seabed Natural Hydrocarbon Seeps in Deep Offshore Angola. Offshore Technology Conference.
Vanneste, H., Kastner, M., James, R.H., Connelly, D.P., Fisher, R.E., Kelly-Gerreyn, B.A., Heeschen, K., Haeckel, M., Mills, R.A., 2012. Authigenic carbonates from the Darwin Mud Volcano, Gulf of Cadiz: a record of palaeo-seepage of hydrocarbon bearing fluids. Chem. Geol. 300–301, 24–39.
Wirsig, C., Kowsmann, R.O., Miller, D.J., de Oliveira Godoy, J.M., Mangini, A., 2012. U/Th dating and post-depositional alteration of a cold seep carbonate chimney from the Campos Basin offshore Brazil. Mar. Geol. 329–331, 24–33.
Zachos, J., Pagani, M., Sloan, L., Thomas, E., Billups, K., 2001. Trends, rhythms, and aberrations in global climate 65 Ma to present. Science 292, 686–693.

PAPER 2

Carbon, oxygen and strontium isotopic constraints on fluid sources, temperatures and biogeochemical processes during the formation of seep carbonates - Secchia River site, Northern Apennines

Irene Viola, Rossella Capozzi, Stefano M. Bernasconi and Jörg Rickli

Submitted to Sedimentary Geology on March 28, 2017

Carbon, oxygen and strontium isotopic constraints on fluid sources, temperatures and biogeochemical processes during the formation of seep carbonates - Secchia River site, Northern Apennines

Irene Viola[1*], Rossella Capozzi[1], Stefano M. Bernasconi[2] and Jörg Rickli[3]

1 - Department of Biological, Geological and Environmental Sciences, University of Bologna, Via Zamboni 67, 40127 Bologna, Italy.

2 - Geological Institute, ETH Zurich, Sonneggstrasse 5, 8092 Zurich, Switzerland.

3 - Institute of Geochemistry and Petrology, ETH Zurich, Clausiusstrasse 25, 8092 Zurich, Switzerland.

*corresponding author: irene.viola3@unibo.it

Abstract

Understanding seep authigenic carbonate formation provides clues for hydrocarbon exploration and insights into contributions to gas budgets of marine environments and the atmosphere. Seep carbonates discovered in the outcropping succession along the Secchia riverbanks (near Modena, Italy) belong to the Argille Azzurre Formation of Early Pleistocene age deposited in an upper shelf environment overlying the Miocene foredeep successions, which include hydrocarbon fields. The fluid migration form the hydrocarbon fields up to the surface is presently active on land and started in the marine succession during the Late Miocene.

Authigenic globular carbonate concretions and carbonate chimneys are interspersed along the strata throughout the section. A comprehensive geochemical characterisation of the carbonates has been carried out to understand the processes leading to their formation. The carbonate concretions are the record of past hydrocarbon vents linked to the Miocene petroleum system of the Northern Apennines. The samples are composed of more than 50% microcristalline dolomite. The $\delta^{13}C$ signatures identify two groups in the samples according to different type of formation processes. Globular concretions have positive values that suggest an influence of CO_2 associated to secondary methanogenesis due to microbial degradation of higher hydrocarbons. The analysed chimney, with negative $\delta^{13}C$ values, is interpreted as former conduit where carbonate precipitation is promoted by anaerobic oxidation of methane coupled with sulphate reduction. The $\delta^{18}O$ range, coupled with $^{87/86}Sr$ signatures, indicate that the contribution of deep connate water from the Miocene reservoirs

is up to 23% during the formation of the globular concretions. The connate water occurrence is also documented by higher ambient temperatures. The different isotope signatures in seep carbonates result from the relative contribution of the recognised gas and water components, linked to different plumbing systems and fluid supply from a well-defined hydrocarbon field. The seep carbonate characteristics have enlightened variations in biogeochemical processes, which can be rarely quantified in ancient and present-day marine environments.

Key Words: Stable isotope, Strontium isotope, authigenic carbonates, fluid mixing, formation processes.

1.Introduction

The formation of seep authigenic carbonates linked to hydrocarbon-enriched fluid at the seafloor is a well-known phenomenon. It is documented in modern and ancient marine sedimentary basins worldwide and linked to different tectonic regimes at convergent and passive margins (e.g. Taviani, 2001; Pinheiro et al., 2003; Ge et al., 2010; Nyman et al., 2010; Capozzi et al., 2012; Van Landeghem et al., 2015 and references therein; Marzec et al., 2016; Mazzini et al., 2016 and references therein; Roy et al., 2016). The occurrence of seep carbonates corresponds to present and past hydrocarbon vents, which contribute to the gas budget of the marine environment and the atmosphere. In addition, the seepages are used as indicators of deep hydrocarbon fields and provide clues for hydrocarbon exploration and prospect evaluation (e.g. Abrams, 2005). One of the main processes promoting carbonate precipitation is the microbially mediated Anaerobic Oxidation of Methane (AOM) coupled to Sulphate Reduction (SR), which increase pore water alkalinity, hence, inducing the precipitation of Methane-Derived Authigenic Carbonates (MDAC) (e.g. Boetius et al., 2000; Peckmann and Thiel, 2004; Teichert et al., 2005; Van Landeghem et al 2015; Loyd et al., 2016 and references therein; Mazzini et al 2016). Methane is not always the only carbon source: CO_2 originating from organic matter oxidation or methanogenesis also promotes the precipitation of carbonate minerals in sulphate reduced environments (e.g. Whiticar, 1999; Formolo et al. 2004, Lein, 2004; Tong et al., 2013; Saitoh et al., 2015; Wang et al., 2015; Liang et al., 2016, Loyd et al., 2016). The morphologies of authigenic carbonates include slabs and crusts, cylindrical and pipe-like conduits, and irregularly shaped bodies (e.g. Taviani, 2001; Clari et al., 2004; Lein, 2004; Magalhães et al., 2012; Talukder 2012; Wang et al., 2015). Pipe-like conduits, also named

chimneys, are less commonly reported in the literature and their formation mechanisms are still under debate (e.g. Nyman et al., 2010; Magalhães et al., 2012; Talukder 2012; Oppo et al., 2015; Reitner et al., 2015; Andrews et al., 2016). The case study from the Secchia River succession provides new insights into the relationships between the formation of authigenic carbonates, which occurred in a shelf environment during the Early Pleistocene, the geologic evolution of the marine basin and the concurrent hydrocarbon migration processes in the petroleum system of the Northern Apennines. The relative contribution of ambient seawater and fluids migrating form deep hydrocarbon fields are estimated by means of C, O and Sr isotopic signatures. The results are combined with a mineralogical and geochemical characterisation of the carbonates for a better understanding of their formation processes.

2. Geological settings

Intense flooding and seasonal erosive events during 2014 and 2015 in the Secchia River near Sassuolo (province of Modena, Italy) resulted in a pronounced incision of the riverbanks in the Northern Apennines foothills exposing a succession of 200 m of marine sediments (Lower

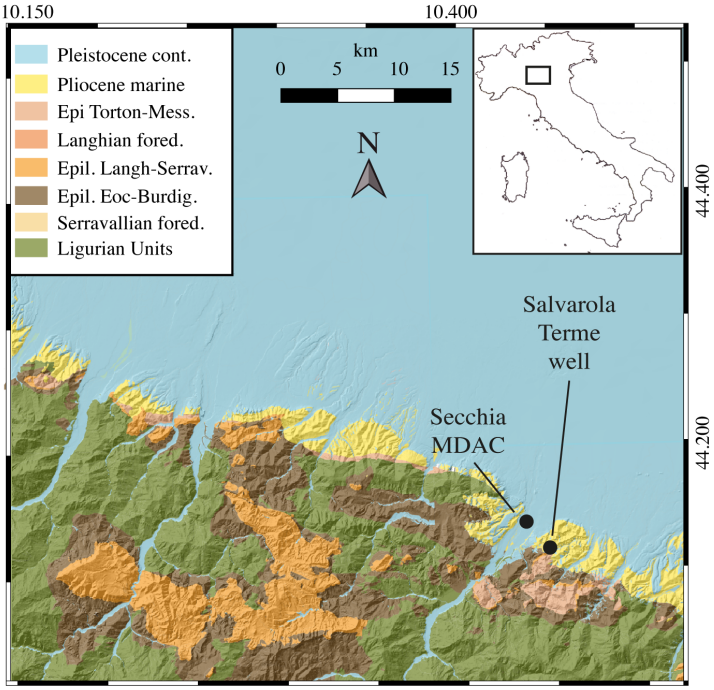

Fig. 1: *Geological map of the Northern Apennines surrounding the study area. The location of authigenic carbonate outcrops and the Salvarola Terme well are indicated.*

Pleistocene, Argille Azzurre Formation) whi ch hosts several globular and pipe-like carbonate concretions (Fig. 1). In this area, Pliocene and Pleistocene successions are marine deposits, which overlie the units of the Ligurian Nappe and the Miocene foredeep units. The Ligurian Nappe

consists of rearranged Jurassic-Eocene deformed oceanic wedge of the Ligurian ocean, which progressively was thrusted over the foredeep successions of Miocene age (Zattin et al., 2002). The foredeep deposits form a fold-and-thrust belt that has been progressively incorporated into the Apennine orogeny. The Miocene deformed foredeep provides the structural traps for the hydrocarbon accumulation in the subsurface of the Northern Apennines and of the Po Plain, whereas the Ligurian Units provide the seal for the in chain reservoirs (e.g. Capozzi and Picotti, 2010; Oppo et al., 2013 and references therein). The main hydrocarbon reservoir in the Secchia River area is of Tortonian to Messinian age and has a thickness of ca. 3 km. The Messinian units are progressively thinning from southwest to northeast, documenting the growth of anticlinal ramp structures in the Po Plain subsurface during this time interval (Oppo et al., 2013).

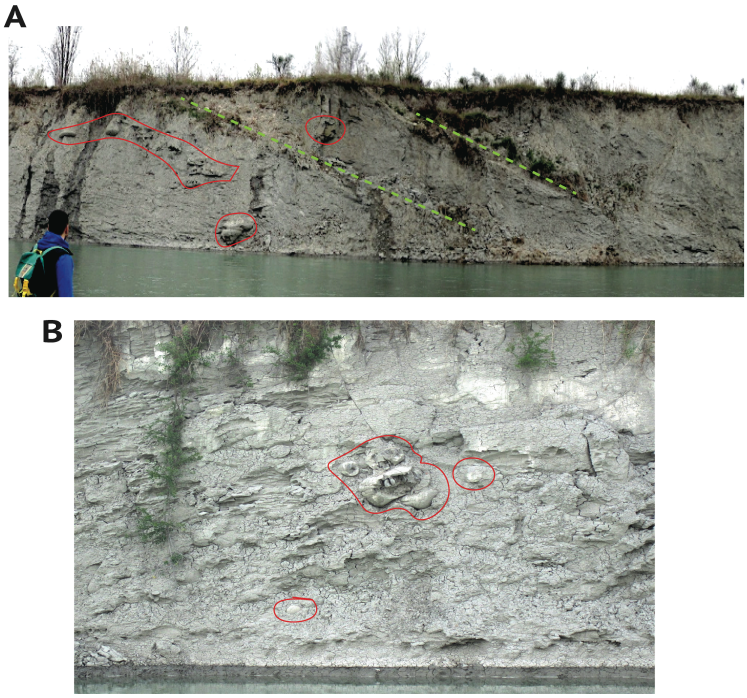

Fig. 2: *(A) Part of the Secchia River outcropping section showing stratified sediments, including authigenic carbonate concretions (in red) distributed along the dipping of small fractures (in green). (B) Close up of some globular carbonates (GCs).*

Further compressive deformation is also documented in Pliocene and Lower Pleistocene sedimentary units (Oppo et al., 2013). In the area, hydrocarbons and connate waters are exploited from deep wells and their leakages from the deep reservoirs feed active mud volcanoes. The outcropping marine Upper Pliocene to Lower Pleistocene succession along the foothills shows geometries indicating a decrease of thrust activity and a transition towards continental deposition prior to the emersion in the Middle Pleistocene (e.g. Oppo et al., 2013; Gunderson et al., 2014). The Lower Pleistocene succession along the Secchia River (Figs. 1, 2) has been sampled and

Gephirocapsa Oceanica has been found at the bottom of the succession, dating it to 1.7 M.a. (de Kaenel et al., 1999 and references therein). The authigenic carbonates mostly form globular concretions (GCs) with dimensions up to one meter, in some cases presenting a large void in the internal part, but occasionally also include smaller chimneys. The orientation of the globular concretion features and chimneys is at some sites along bedding planes and at other sites independent from the stratification. Along the riverbanks where the concretions occur are also small normal faults dipping northeast.

3. Materials and Methods

3.1 Samples

Along the Secchia River outcrop two carbonate morphologies have been recognised. Globular concretions are more abundant meanwhile chimneys are rare. Five sampled concretions are slab-like and about one meter in size (SCH1 to SCH5, Fig. 3A). Subsamples have been collected for the external (E) and internal (I) areas of each sample (Fig. 3C).

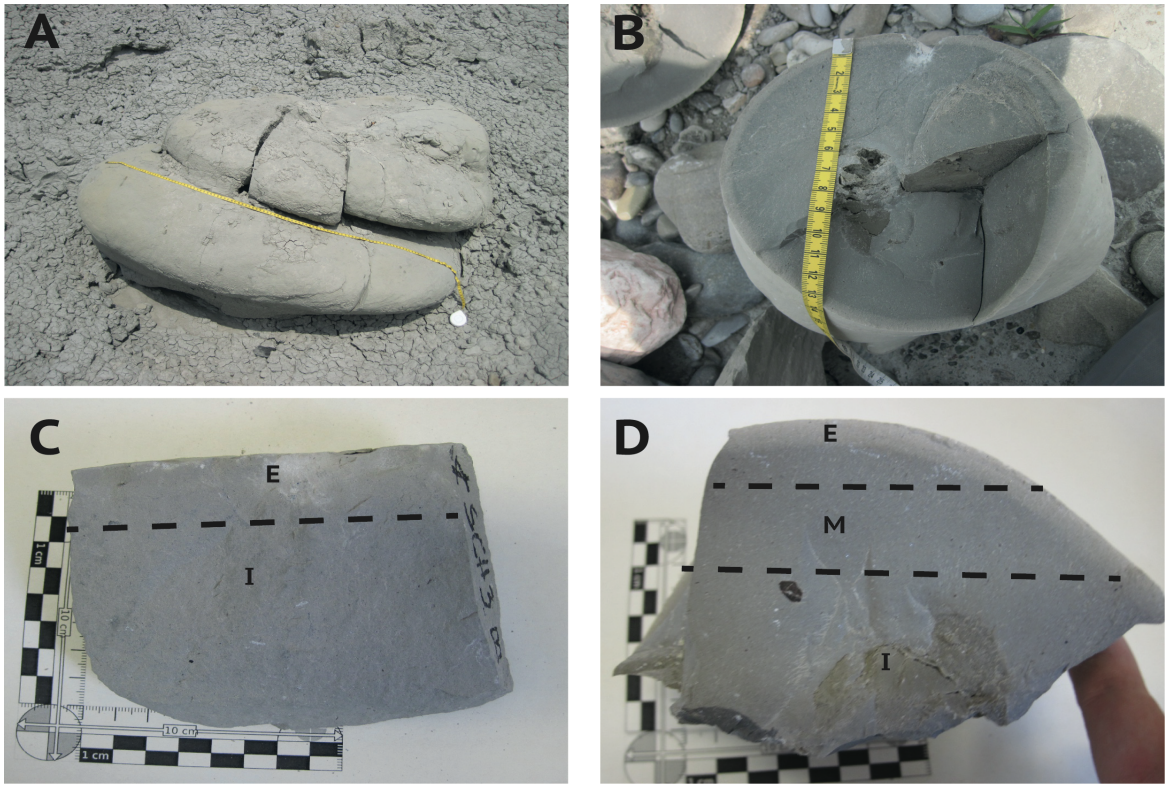

Fig. 3: *Examples of carbonate concretions investigated in this study: Globular concretions SCH3 and SCH5 are shown in A and C. Each sample has been divided into external (E) and internal (I) areas. The chimney SCH6 from Secchia River is shown in B and the three analyzed subsamples, representative of external (E), internal (C) and middle (M) portions in D.*

One chimney (SCH6, Fig. 3B), shows a higher degree of cementation, and has also been subsampled based on visual criteria: A light-grey layer in the more external area (E), a darker

interval forming the bulk of the concretion (M), and the yellowish-grey conduit filling (C) (Fig. 3D). In order to understand the formation process and the signature of the fluids involved during the precipitation of the authigenic carbonates, samples of connate water from the Salvarola Terme wells have been analysed. This water derives from the Miocene reservoir, and the fluid migration that fed the area is still active today. The geochemical characteristics indicate that it undergoes a reverse osmosis process along the migration pathway and is not mixed with meteoric groundwater (e.g. Capozzi and Picotti, 2010). The gas component seeping in the same area is mainly thermogenic methane mixed with secondary biogenic methane due to bacterial degradation of the heavy hydrocarbons in the reservoir (e.g. Oppo et al., 2013, Oppo et al., in press). Fifteen sediment samples from within the Argille Azzurre succession, from the top (S15) to the bottom (S1), in which the carbonates were recovered, have been analysed for Total Organic Carbon (TOC) at the Institute of Marine Science labs of the National Research Council (ISMAR-CNR) in Bologna.

3.2 Methods

The carbonate subsamples have been collected by micro-drilling in order to have a precise characterisation of the various areas of the carbonates concretions. The drilled subsamples have been homogenised in agate mortar and analysed for mineralogy by X-ray diffractometry (XRD) using a Philips PW 1130 (Cu Ka radiation Ni filtered) in the XRD Laboratory of Biological, Geological and Environmental Sciences (BiGeA) Department, University of Bologna. Powders were pressed into alumina holders in order to avoid preferential orientation of sheet-silicates. Estimates of the relative mineral abundances were determined using the MacDiff software packages considering the six major peaks, representing the relative abundance of mineral species indicated in table 1. Carbonate mineral compositional limits are defined according to Goldsmith and Graf (1958) and Lumsden (1979).

Major and trace elements have been determined by X-ray fluorescence (XRF) spectrometry on pressed powered pellets using a Philips PW 1480 automated spectrometer following the methods of Franzini et al. (1972, 1975), Leoni and Saitta (1976) and Leoni et al. (1982) for matrix corrections in the XRF Laboratory, BiGeA Department, Bologna University. The estimated precision and accuracy for trace element determinations is ~5% except for elements < 10 ppm, where it corresponds to 10-15%. The detection limit for most trace elements is 3 ppm (Leoni and Saitta, 1976).

The petrographic observations were made using uncovered standard thin sections (45 x 60 mm) at

the University of Bologna via cathodoluminescence petrography (operating conditions of ca. 20 kV beam voltage and ca. 200 mA beam current). Morphological descriptions and chemical elemental compositions of the cements were obtained using a Philips 515 scanning electron microscope (SEM) equipped with an electron back- scattering system and EDX (EDAX DX-4) at the University of Bologna. SEM-EDX investigations were performed on fresh Au-coated rock surfaces.

Physical and chemical parameters of Salvarola Terme water were measured in the field (Eh, pH, Temperature, Salinity) and concentrations of cations and anions were determined on a filtered aliquot in the Environmental Study Center Research Institute (GRUPPO C.S.A. S.p.A.) in Rimini by ionic chromatography.

$\delta^{13}C$ and $\delta^{18}O$ on micro-drilled carbonate sub-samples and $\delta^{13}C$ on dissolved inorganic carbon (DIC) of the Salvarola Terme well water have been measured using a Thermo Fisher DELTA V mass spectrometer coupled to a Gas Bench II device (at the Department of Earth Sciences, ETH Zurich). Between 90 and 140 μg of carbonate powder, and 200 μl of sample water, were inserted into flasks, sealed and flushed with 99.99% helium gas. Subsequently, concentrated phosphoric acid was injected to react with the samples. The released CO_2 was purified and analysed. Carbon and oxygen isotopes are reported in the conventional delta notation relative to the Vienna Pee-Dee Belemnite (VPDB). Reproducibility is better than ±0.1‰ for both $\delta^{13}C$ and $\delta^{18}O$. $\delta^{18}O$ of water was measured on a Picarro L3120 analyser, with a reproducibility of ±0.1‰ and is reported on the VSMOW scale.

Sulphur isotopes in water of the Salvarola Terme well have been analysed by quantitatively precipitating sulphate as $BaSO_4$ by the addition of $BaCl_2$ to acidified water (pH=3). Acidification is necessary to avoid carbonate precipitation. After drying, 300 μg of precipitated $BaSO_4$ was weight into a tin capsule together with the same amount of V_2O_5. The sulphur isotope measurement was carried out on a Thermo Scientific Flash Elemental Analyser (EA) interfaced to a Delta V Plus Isotope Ratio Mass Spectrometer. The $\delta^{34}S$ value is reported relative to the Vienna-Canyon Diablo Troilite (V-CDT) and is corrected by NBS 127, IAEA SO 5 and IAEA SO 6 standards resulting in a reproducibility of ±0.04‰.

For Sr isotopic analysis, 10 to 30 mg of micro-drilled carbonate sub-samples were leached in buffered acetic acid for 2.5 hours to dissolve the carbonate fraction (0.5 M acetic acid / 0.5 M sodium acetate). Strontium in the leached carbonate and well water was purified based on methods by Deniel and Pin (2001) and de Souza et al. (2010). The procedural blank through chemical

separation was < 30 pg. Samples were measured at total Sr beams between 7.7 and 32 V by MC-ICP-MS (Neptune Plus, Thermo Fischer Scientific at ETH Zurich) comprising 50 ratios of 4.2 s integration time in static mode. The exponential law was applied to correct for instrumental mass fractionation and all $^{87}Sr/^{86}Sr$ ratios were normalised to $^{86}Sr/^{88}Sr = 0.11940$. ^{85}Rb was monitored to correct for minute Rb interferences on ^{87}Sr. In both sessions Nist SRM 987 was repeatedly run to estimate the external reproducibility of the measurements yielding values of 0.710236 ± 0.000011 and 0.710234 ±0.000014, respectively (2 SD, n = 16 in both sessions). All sample data was renormalised to a Nist SRM 987 literature value of 0.710248 (Thirlwall, 1991).

4. Results

4.1 Mineralogy

The carbonate bodies are composed of dolomite (on average 56 wt.%) and a detrital fraction (on average 44 wt.%) (Tab. 1, Fig. 4). Abundant detrital minerals comprise quartz, feldspars, clay minerals and micas. In addition, gypsum (4-11 wt.%), pyroxenes (0-2 wt.%) and oxides (2-7 wt.%) have been found. The percentage of dolomite is lower in GCs (SCH1 to SCH5, average of 54 wt.%) than in the chimney sample (average of 61 wt.%). Dolomite content increases toward the internal parts of the chimney, whereas in the external portion the detrital fraction is more abundant (Table 1).

***Table 1**: Secchia carbonates mineralogy.*

	Dolomite	Feldspar	Silicates	Sulfates	Pyroxens	Clay Minerals	Micas	Oxydes	Others
SCH1E	51%	4%	20%	10%		5%	7%	3%	
SCH1I	70%		6%	10%		4%	6%	4%	
SCH2E	52%	11%	15%	9%		4%	6%	3%	
SCH2I	51%	16%	11%	8%		4%	7%	3%	
SCH3E	47%	9%	21%	7%	2%	3%	7%	3%	1%
SCH3I	56%	11%	18%	2%			5%	7%	1%
SCH4E	59%	11%	7%	11%		2%	5%	4%	
SCH4I	47%	9%	20%	11%		3%	6%	4%	
SCH5E	50%	11%	17%	9%			6%	7%	
SCH5I	57%	10%	8%	9%	2%	2%	6%	7%	
SCH6E	59%	12%	8%	9%		2%	4%	4%	
SCH6M	62%	11%	13%	4%		4%	4%	2%	
SCH6C	63%	9%	6%	7%	2%	4%	4%	4%	

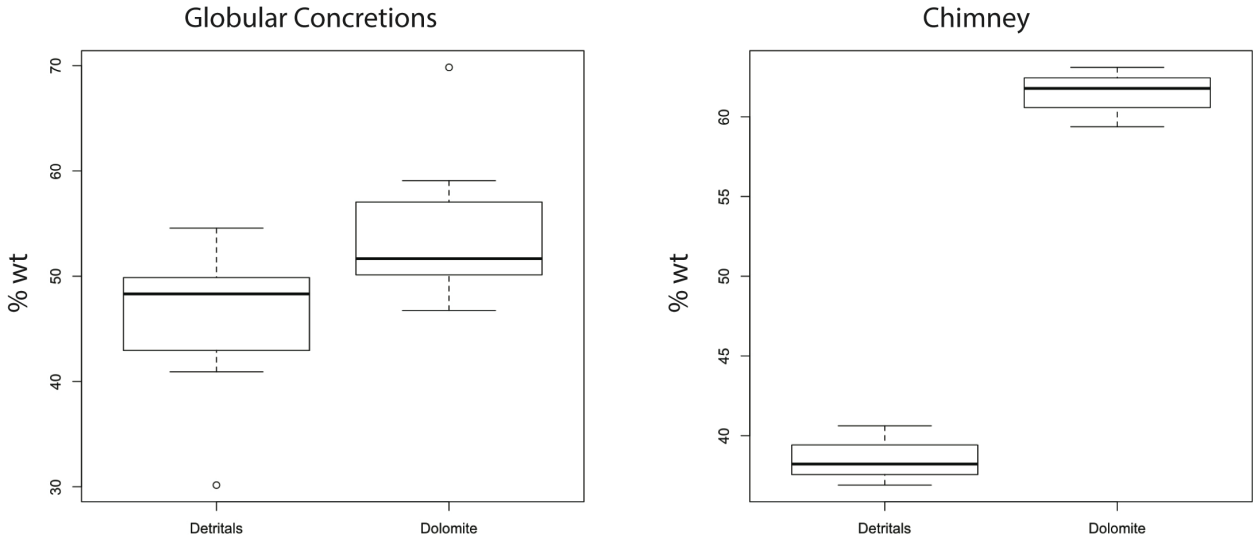

Fig. 4: *Box-plot for globular concretions and the chimney sub-samples showing the relative abundance of dolomite and detrital components.*

4.2 Geochemistry

Major elemental oxides associated with the terrigenous component, in particular SiO_2, Al_2O_3 and Fe_2O_3, are enriched in GCs relative to the chimney (Tab. 2). The concentrations have been normalised to TiO_2, since Ti is the least mobile element in this system. Most of the major oxides have their maximum in SCH1E and their minimum in SCH1I. Differences in Fe_2O_3 between GCs and the chimney are small. Typically, it varies between 3.55 wt.% and 2.15 wt.%, although SCH5I and SCH5E yield even lower values of 1.79 wt.% and 1.93 wt.%. Major elements related to the carbonate phases, MgO and CaO, reflect the trend of the mineralogy: their concentrations are elevated in the internal subsamples (I) relative to the external ones (E) with the exception of SCH4 and SCH5 where both MgO and CaO are very similar in the internal and external subsamples (Tab. 2, Fig. 5A). On average, Ca and Mg are enriched in the chimney consistent with its mineralogy. Moving to trace elements, As, Sr, Y, Ba, Pb and S are on average higher in the chimney than in the GCs, whereas all the other elements and the LOI are higher in GCs. Strontium concentrations in our samples vary between 185 and 452 ppm in GCs and between 342 and 470 ppm in the chimney. Total organic carbon (TOC) has been analysed in 15 samples representative of all the section from the top (S15) to the bottom (S1) and varies between 0.5and 0.86 wt.% (Fig. 5C).

4.3 Petrography

The chimney (SCH 6) shows abundant clasts cemented by dolomitic micrite in which clusters of sulphides occur as black spots (Fig. 6A). Locally, the chimney matrix is made of spotted peloidal

Table 2: *Secchia carbonates geochemistry*

	SiO_2	TiO_2	Al_2O_3	Fe_2O_3	MnO	MgO	CaO	Na_2O	K_2O	P_2O_5	LOI	Mg/Ca	Sc	V	Cr	Co	Ni	Cu	Zn	As	Rb	Sr	Y	Zr	Nb	Ba	La	Ce	Pb	Th	S
						(wt %)																*(ppm)*									
SCH1E	24.36	0.32	7	3.75	0.16	10.92	18.33	0.64	1.07	0.1	33.35	0.60	na	46	73	6	27	10	48	4	44	185	13	73	6	305	11	14	8	11	1290
SCH1I	14.66	0.19	3.73	1.16	0.1	22.94	23.51	0.32	0.61	0.11	32.68	0.98	na	21	23	<2	14	3	6	4	16	452	5	55	3	242	4	9	4	3	1120
SCH2E	22.36	0.28	6.08	3.36	0.08	13.58	18.23	0.58	0.98	0.09	34.38	0.75	4	44	62	4	22	13	37	3	37	198	10	68	8	253	15	21	7	<3	1120
SCH2I	21.18	0.28	5.78	2.92	0.08	16.21	20.38	0.58	0.91	0.09	31.6	0.80	<3	37	54	5	18	11	32	3	33	199	10	61	7	256	7	20	7	<3	750
SCH3E	22.75	0.30	6.33	3.55	0.09	15.32	20.28	0.59	1.03	0.11	29.67	0.76	<3	39	57	6	22	9	35	3	35	222	12	68	7	253	11	24	7	<3	890
SCH3I	22.80	0.29	6.07	2.15	0.06	18.10	20.55	0.67	0.94	0.10	28.28	0.88	<3	36	54	3	19	10	34	<3	36	233	10	70	7	248	19	21	7	<3	900
SCH4E	17.11	0.23	4.76	3.41	0.18	19.50	22.68	0.37	0.77	0.10	30.9	0.86	<3	31	46	3	14	7	28	3	26	210	7	53	6	227	6	21	5	<3	710
SCH4I	19.01	0.25	5.25	3.15	0.15	18.66	21.93	0.39	0.82	0.10	30.27	0.85	<3	31	51	<3	15	8	28	3	30	193	8	51	6	242	17	27	7	<3	730
SCH5E	17.40	0.25	5.25	1.79	0.05	21.84	20.88	0.39	0.73	0.10	31.33	1.05	4	33	49	<3	16	9	30	3	30	279	9	61	6	243	14	24	6	<3	910
SCH5I	17.99	0.26	5.36	1.93	0.05	21.01	22.79	0.42	0.74	0.12	29.33	0.92	<3	31	49	<3	15	9	28	3	31	264	7	56	6	229	8	18	6	<3	750
SCH6E	18.6	0.25	5.04	2.09	0.12	18.88	22.03	0.95	0.79	0.07	31.18	0.86	na	34	54	<2	19	7	25	7	27	470	22	62	3	386	12	25	7	5	1600
SCH6M	17.13	0.21	4.67	1.61	0.1	21.21	23.75	0.39	0.69	0.07	30.18	0.89	na	23	32	<2	16	7	15	4	17	415	5	56	3	294	6	12	6	6	1210
SCH6C	15.71	0.18	4.14	1.38	0.1	21.62	26.03	0.36	0.61	0.08	29.79	0.83	na	24	15	<2	15	6	5	8	11	342	4	45	2	240	5	11	6	2	1000

micrite and dolomicrite. Peloids are ovoidal to circular in shape, organised in clotted fabric.

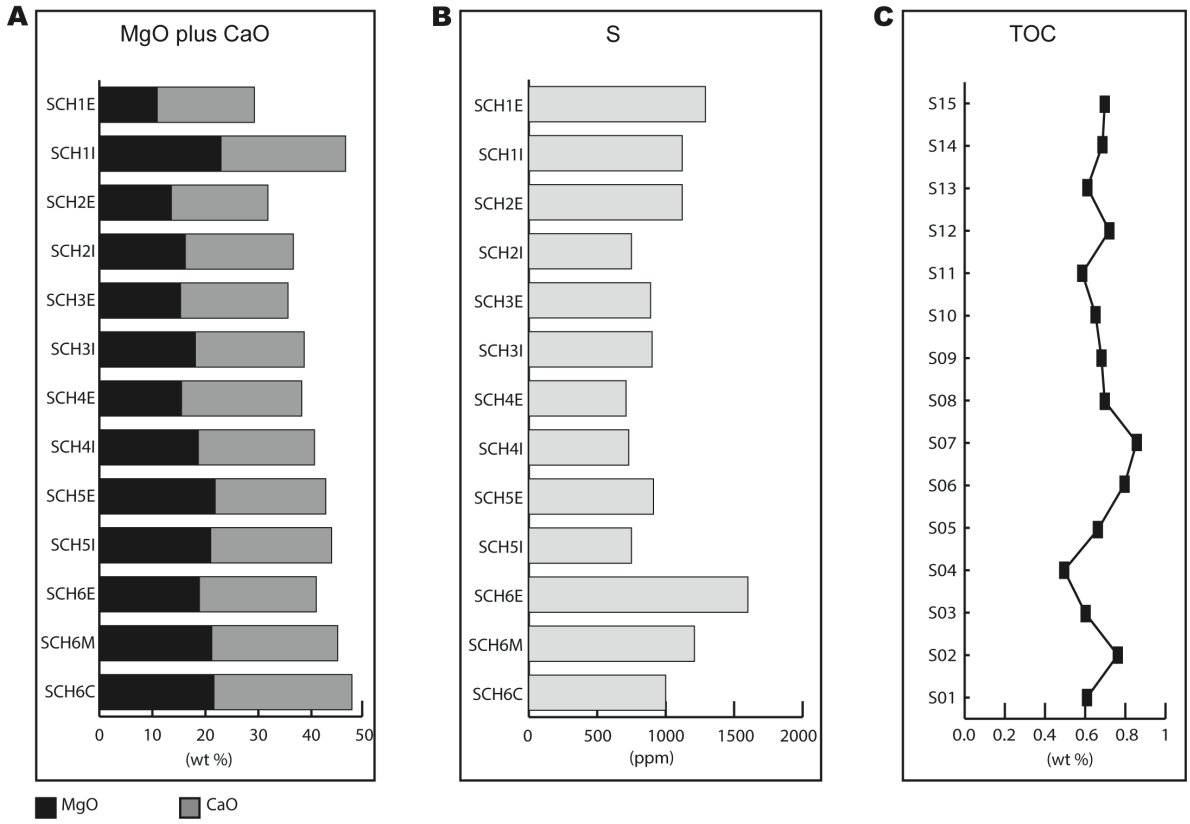

Fig. 5: *XRF plots. (A) represents the sum of the major oxides related to the carbonate fraction, MgO and CaO, to highlight their relative abundances in each sub-sample. (B) Sulfur concentration that shows a decreasing abundance from external to internal portions of each sample. (C) TOC log profile across the sedimentary section, where S01 is at the base of the measured section and S15 is at the top.*

Thin levels of sand-sized grains (Fig. 6A) and foraminifera are evident and the foraminifera's chambers are filled with crystals of microsparite, of unknown composition, and sulphides (Fig. 6B). Sponge spiculae as well as poorly rounded mica and plagioclase crystals are occasionally observed in the texture. Carbonate GCs show dolomitic micrite with abundant sand-sized quartz crystals and poorly rounded mica and plagioclase. Some foraminifera and sponge spiculae are observed also in these samples (Fig. 6D). Figure 7A shows a SEM photograph of the matrix and a dolomite crystal. The spectrum of the shell fragment in Fig. 7B indicates that it is made of calcite and surrounded by a dolomite matrix (Fig. 7C). The calcite of bioclastic components is evidently very low as it was not detectable in the XRD analysis.

4.4 Stable isotopes

Table 3 and Fig. 8 present the results of the $\delta^{13}C$ and $\delta^{18}O$ analysis. The majority of the GC sub-samples show positive $\delta^{13}C$ values contrasting with the negative values of the chimney and SCH1I. Specifically in GCs, the carbon isotope compositions are generally more positive in the external

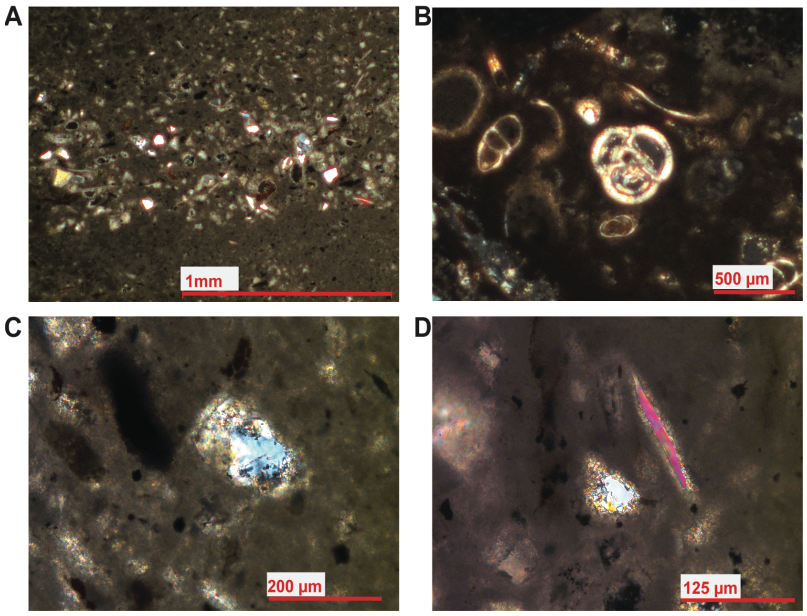

Fig. 6: *Photomicrographs of thin sections of (A): chimney cement with dense, clotted cement, sulphides (black spots), and fine siliciclastics grains; (B) foraminifera with partial recrystallisation (see text); (C) quartz grain, which shows partial dissolution likely due to fluid interaction; (D) relic of spicule of sponges frequently associated with disoxic conditions.*

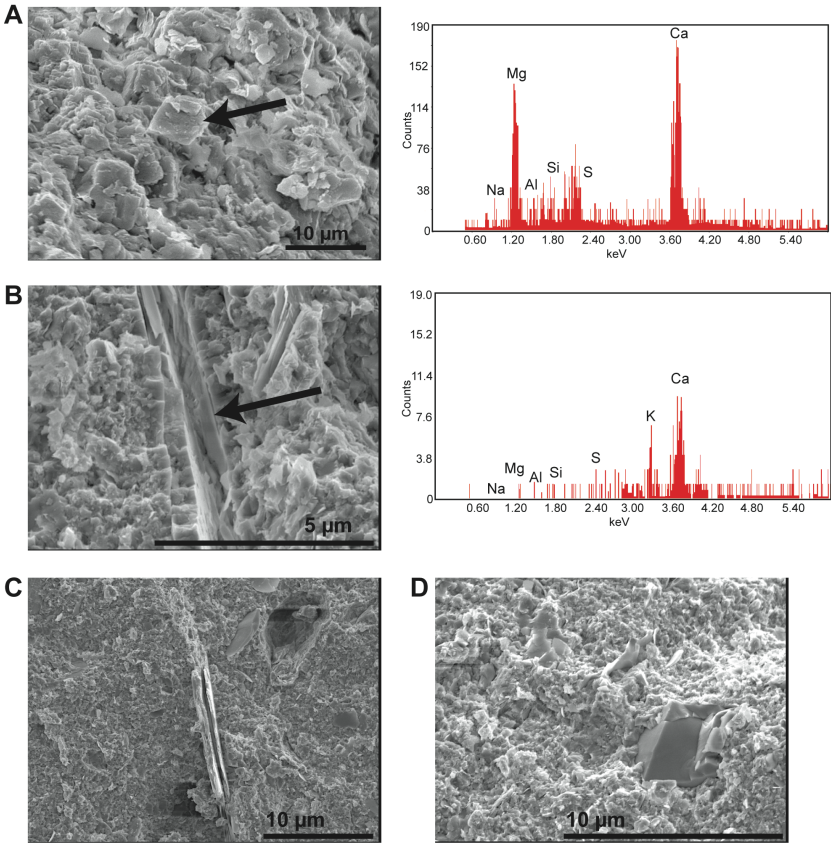

Fig. 7: *Scanning Electron Microscope (SEM) photomicrographs and relative EDX spectrum of the carbonate cement forming the analyzed samples. All spectra have been collected with 15keV accelerating voltage. The arrows indicate the areas and crystals selected for EDX analysis. (A) Carbonate cement in the Secchia River samples where dolomite crystals are clearly visible. (B) A calcite shell fragment trapped in the dolomitic cement. (C) A siliceous spicule trapped in the dolomitic cement. (D) Quartz grain within the dolomitic matrix.*

Table 3: *Stable and radiogenic isotopes of Secchia carbonates and connate water from Salvarola Terme well.*

	$\delta^{13}C$	$\delta^{18}O$	$^{87/86}Sr$	$\delta^{34}S$
	(‰ VPDB)	*(‰ VPDB)*	ratios	*(‰ V-CTD)*
SCH1E	6.87	5.49	0.70894	-
SCH1I	-9.42	5.36	0.70903	-
SCH2E	6.40	5.34	0.70891	-
SCH2I	7.48	5.50	0.70912	-
SCH3E	6.47	5.18	0.70892	-
SCH3I	9.70	5.12	0.70892	-
SCH4E	10.60	5.06	0.70893	-
SCH4I	10.72	5.15	0.70886	-
SCH5E	11.91	5.73	0.70889	-
SCH5I	11.77	5.66	0.70892	-
SCH6E	-12.32	5.12	0.70903	-
SCH6M	-9.30	5.20	0.70905	-
SCH6C	-8.30	5.18	0.70904	-
Salvarola Terme Well	16.45	5.16	0.70866	22.07

part of the concretions. The values vary mostly between 6.4‰ and 11.91‰ but also include a value of -9.42‰ (SCH1I). In the chimney, the $\delta^{13}C$ values are between -8.30‰ and -12.32‰ moving from the sub-sample SCH6C to SCH6E. $\delta^{18}O$ (VPDB) values in the GCs vary between 5.06‰ and 5.73‰ and encompass those from the chimney ranging between 5.12‰ and 5.20‰ (Tab. 3, Fig. 8).

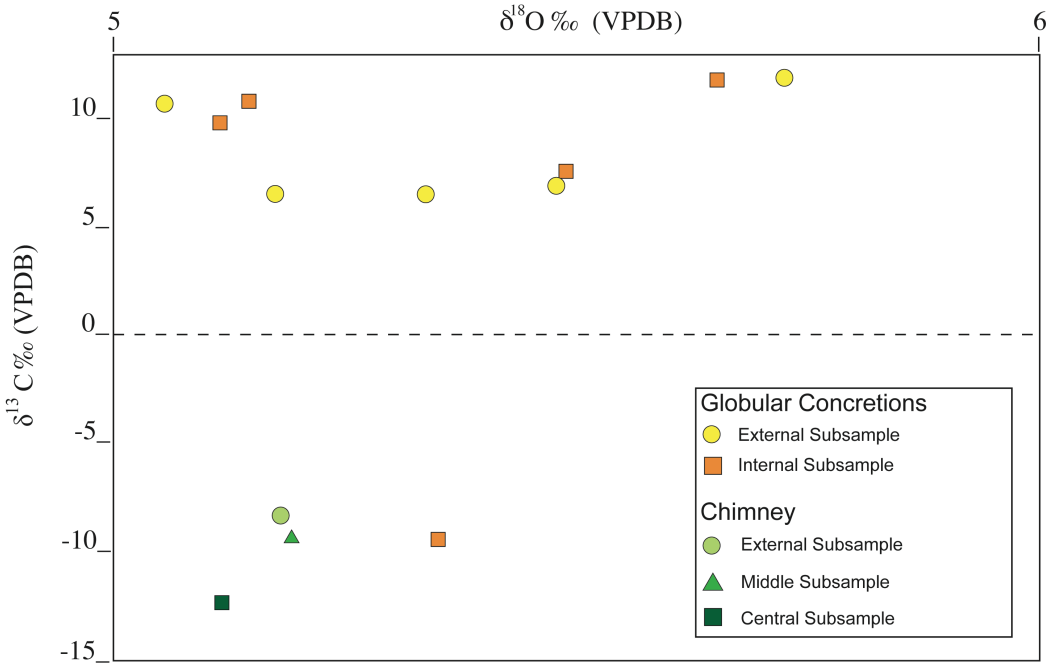

Fig. 8: *$\delta^{13}C$ vs. $\delta^{18}O$ diagram for the AC concretions considered in this study. Two groups are well identified: GCs have positive $\delta^{13}C$ values with the exception of SCH1I, whereas chimney sub-samples show negative values. $\delta^{18}O$ values show more homogeneous values with respect to $\delta^{13}C$.*

The connate water and methane from the Salvarola Terme well are considered as representative of the fluids migrating from the deep Miocene reservoir (Oppo et al., 2013). The $\delta^{13}C$ of the DIC is 16.45‰ and $\delta^{18}O$ is 5.16‰ (SMOW) respectively. The $\delta^{34}S$ of dissolved SO_4^{2-} is 22.7‰.

4.5 Radiogenic strontium isotope

Table 3 and Fig. 9 present the measured radiogenic Sr isotope compositions of leached carbonate from rock subsamples as well as from water from the Salvarola Terme. The $^{87}/^{86}Sr$ isotope ratios vary between 0.70886 and 0.70912; 8 subsamples of GCs are similar and show a ratio between 0.70886 and 0.70894. SCH1E and SCH2E yield a higher value of 0.70903 and 0.70912 respectively. The chimney is isotopically homogeneous with values between 0.70903 and 0.70905. The deep connate water from the Salvarola Terme well is representative of the still migrating fluids from the Miocene reservoir and shows a ratio of 0.708664.

5. Discussion

5.1 Mineralogy, geochemistry and petrography

The carbonate bodies considered in this study are mainly composed of dolomite (>56 wt.%) cementing a subordinate detrital fraction. This detrital fraction reflects the typical mineralogy of the Argille Azzurre formation (e.g. Viola et al., 2015, for a comparison with the coeval succession along the Enza River). The dolomite concretions were linked to hydrocarbon leakages and are, therefore, authigenic in origin (Wang et al., 2015). The increase of dolomite cements towards the interior of the GCs and the chimney could be related to very low or absent SO_4^{2-} in pore water that usually favor dolomite precipitation and inhibit calcite formation (Douglas, 2005; Magalhães et al., 2012). The dolomite formation is due to the mediation of microbial mats for carbonate nucleation and magnesium incorporation at low temperature (Douglas, 2005; Bontognali et al., 2014). In addition, the presence of authigenic sulfides (pyrite and arsenopyrite) indicates that the sulfate reduction process was active and the sulfate concentration in the water was decreasing during carbonate precipitation.

Total organic carbon values measured in the sediments and the high concentration of Mn, V, Co, Ni indicate that the carbonates mainly formed in a reducing environment (Algeo and Maynard, 2004; Sabatino et al., 2011; Neumeuster et al., 2016). This is an indication that, locally, condition prone to the precipitation of authigenic dolomite, via AOM, could be achieved. In fact, kinetic barriers to the precipitation of this mineral are overcome by the consumption of sulfate by AOM-SR, allowing Mg^{2+} to enter the carbonate lattice and leading to the formation of dolomite in marine sediments

influenced by hydrocarbon migration processes (Greinert et al., 2001; Peckmann et al., 2001).

5.2 Carbon isotope signature

The precipitation process of authigenic carbonates incorporates dissolved inorganic carbon (DIC) from the pore water without a significant fractionation of its isotopic composition (Diaz-Del-Rio et al., 2003). Generally, in this type of carbonates a negative value of $\delta^{13}C$ is associated with methane oxidation, whereas positive values are mostly associated to organic matter decomposition by acetoclastic methoanogenesis or CO_2 reduction, which both lead to an enrichment in ^{13}C in the residual CO_2 (Whiticar, 1999; Formolo et al., 2004). In the study area of the Northern Apennines it has been observed that mainly thermogenic methane from depth is mixed with secondary biogenic methane associated to ^{13}C- enriched CO_2 (Oppo et al., 2013; Oppo et al., in press). The samples from the chimney have negative $\delta^{13}C$ signatures, whereas the GC sub-samples have positive values, with the exception of SCH1E. Several studies have reported $\delta^{13}C > 5‰$ in authigenic carbonates associated with the occurrence of microbial methane during their precipitation (Peckmann and Thiel, 2004 and references therein; Roberts et al., 2010). The occurrence of secondary methanogenesis via CO_2 reduction is likely responsible for the positive $\delta^{13}C$ in GCs, as the residual CO_2 is highly enriched in ^{13}C. The process of microbial methanogenesis is still active in the present-day seepages and in the fluids of the Salvarola well (Heller et al., 2011). This condition could have been active also during the Early Pleistocene because the structural setting for the migration and entrapment of deep fluids was just attained (Oppo et al., 2013). Variations of fluid flow intensity or gas composition are likely responsible of some negative values as recorded in subsample SCH1I.

5.3 Oxygen isotope signature

The $\delta^{18}O$ of carbonates depends on the temperature and the $\delta^{18}O$ of the ambient water from which the carbonates precipitate (Vasconcelos et al., 2005; Tong et al., 2013). The precipitation of dolomite in AC cements usually enriches $\delta^{18}O$ by up to 2-3.4‰ than the ambient water (e.g. Budd, 1997; Aloisi et al., 2000; Oppo et al., 2015) and hints a further supply of heavy oxygen to achieve the higher values measured in the Secchia samples. Another important process that strongly influences the oxygen signature recorded in carbonate samples is the formation-dissociation of methane hydrates. Specifically, the formation of gas hydrates (GHys) reduces the $\delta^{18}O$ in the water whereas the dissociation has the opposite effect. Several studies report enrichments in ^{18}O in waters and carbonates as a consequence of GHy dissociation (e.g. Aloisi et al., 2000; Pierre and Rouchy, 2004; De la Pierre et al., 2010; Pierre et al., 2014). In the context of this study, it is important to

stress that hydrates could not form as the Secchia River Argille Azzurre succession was not in the gas hydrates stability zone: it is a shelf succession, deposited at ca. 80 m water depth with waters possibly only a little bit colder than today at comparable depth in the Adriatic basin.

5.4 Strontium isotope signature

Secular variations in the radiogenic strontium isotope composition of seawater have been widely examined (e.g. Elderfield, 1986; Paytan et al., 1993; Farrell et al., 1995; Naehr et al., 2007). The strontium isotopic composition of carbonate minerals reflects the composition of the ambient water during their formation (e.g. Hess et al., 1986, Naehr et al., 2007) and can, therefore, be used to characterize the possible source of fluids for authigenic carbonate precipitation (e.g. Sample and Reid, 1998; Payton et al., 1993; Naehr et al., 2000; Naehr et al 2007 and references therein). According to biostratigraphy the carbonate samples from the Secchia River are Pleistocene in age and should, hence, yield a $^{87/86}Sr$ ratio of 0.7091-0.7092 if they precipitated from pure contemporaneous seawater (e.g. Paytan et al.,1993; Naehr et al., 2007). If, instead, the only fluid source during carbonate precipitation was connate water, the Sr isotope composition of a carbonate sample should reflect this composition. Salvarola Terme water representing connate water yields a signature of 0.70866, which is typical for the Early Miocene (Paytan et al., 1993) and consistent with the age of the foredeep reservoir (Oppo et al., 2013).

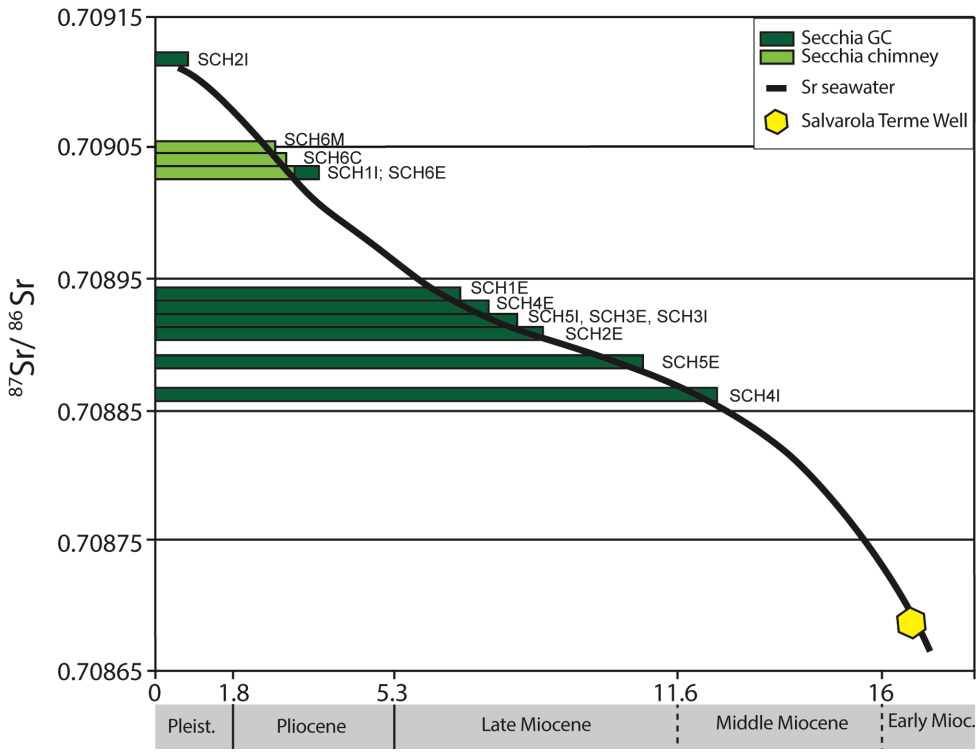

Fig. 9: *Strontium isotope data for the ACs considered in this study, the Salvarola Terme well and the seawater Sr curve from literature data (Hess et al., 1986; Elderfield, 1986; Paytan et al., 1993; Farrell et al., 1995). The length of the bars does not indicate the age of the relative sub-sample, but was chosen only to intersect the seawater Sr curve.*

Strontium isotope results for Secchia River carbonate samples cover a relatively large range from 0.70886 to 0.70912 (Fig. 9). The majority of the GCs sub-samples values are between 0.70886 and 0.70894 similar to the marine Sr isotope composition of Middle-Late Miocene seawater. These isotope compositions, hence, reflect considerable contributions from connate water. There are two exceptions among GCs subsamples: SCH1I, with a $^{87/86}Sr$ of 0.70903, has a minor contribution from connate water to Pleistocene seawater, and SCH2I, with $^{87/86}Sr$ of 0.70912, is in the range of Pleistocene seawater. Chimney sample values are between 0.70903 and 0.70905 characteristic for Pliocene seawater implying, also in this case, a minor contribution from connate water.

5.5 Sulfur isotope

The relative change in the sulfur isotope composition during microbial sulfate reduction has been used to track sulfate reduction. During the start and progress of the process ^{32}S is preferentially reduced to sulfide resulting in an enrichment of ^{34}S in the residual dissolved sulfate (Rees, 1973; Turchyn et al., 2016 and references therein). The sulfur isotope of the connate water of the Salvarola Terme well is $\delta^{34}S$ =22.7‰ close to the modern seawater value of 21‰ (e.g. Wu et al., 2014). However, anaerobic sulfate-reducing bacteria populations have been found in all seeping sites and indicate that anaerobic microbial degradation on hydrocarbons is presently active (Heller et al., 2011; Oppo et al., 2013, Kokoschka et al., 2015). Furthermore, the connate water is in a closed system without contribution of surficial water and shows very low content of sulfate (89 ppm). The unfractionated signature of sulfur in solution is, hence, unexpected and awaits further explanation.

5.6 Fluid mixing models and formation temperatures

An estimation of the contributions of seawater and connate water to the fluids from which the carbonates precipitated can be derived from Sr isotopes (e.g., Faure, 1998). Strontium is a conservative element in seawater and can, therefore, be used to define the mixing contributions, as the mixing occurs between two components with different isotopic signatures. The resulting Sr isotope compositions in precipitating carbonate minerals will reflect the contributions of Sr from each end-member:

(I) $$(^{87/86}Sr)_{carbonate} = (^{87/86}Sr)_{seawater}\, f_{Sr} + (^{87/86}Sr)_{connate}\, (1-f_{Sr})$$

where $(^{87/86}Sr)_{seawater}$ = 0.70915 (Paytan et al., 1993) and $(^{87/86}Sr)_{connate}$ = 0.708664 from Salvarola Terme well, and $f_{Sr} = Sr_{seawater}/(Sr_{seawater} + Sr_{connate})$ (mg seawater Sr/mg total Sr).

Table 4: *Mixing models based on Faure 1998 for strontium isotopes and oxygen isotopes in pore fluids during carbonate formation and formation temperature based on Vasconcelos et al., 2005.*

	Strontium Mixing Model			Oxygen Mixing Model		Temperature of formation		
	$^{87/86}Sr$	f_{Sr}	$f_{seawater}$	$\delta^{18}O$	$\delta^{18}O_M$	$\delta^{18}O$ (SMOW)	$\alpha_{dolomite\text{-}water}$	T (°C)
SCH1E	0.70894	0.56	0.86	5.49	2.45	36.57	34.12	10
SCH1I	0.70903	0.75	0.93	5.36	2.21	36.43	34.23	9
SCH2E	0.70891	0.50	0.83	5.34	2.55	36.42	33.87	11
SCH2I	0.70912	0.95	0.99	5.50	2.04	36.58	34.54	9
SCH3E	0.70892	0.53	0.84	5.18	2.50	36.25	33.75	12
SCH3I	0.70892	0.52	0.83	5.12	2.52	36.18	33.66	12
SCH4E	0.70893	0.54	0.85	5.06	2.49	36.12	33.63	12
SCH4I	0.70886	0.41	0.77	5.15	2.74	36.22	33.48	13
SCH5E	0.70889	0.47	0.80	5.73	2.62	36.82	34.20	9
SCH5I	0.70892	0.52	0.84	5.66	2.52	36.75	34.23	9
SCH6E	0.70903	0.75	0.93	5.12	2.21	36.19	33.98	10
SCH6M	0.70905	0.79	0.95	5.20	2.17	36.27	34.10	10
SCH6C	0.70904	0.78	0.94	5.18	2.18	36.26	34.07	10

**Seawater values: $^{87/86}Sr_{seawater}$ =0.70915 (Paytan et al., 1993); $[Sr]_{seawater}$ =8.08 mg/l (Emelyanov and Shimkus, 2012); $\delta^{18}O_{seawater}$ = 2‰ (SMOW) calculated signature of Adriatic Sea water coming from 100 m depth, analogues to the depositional conditions on the shelf for the Secchia River succession, based on a salinity of 38.3‰ and a water temperature that varies between 12°C and 13° (Lipizer et al., 2014).*

*** $(^{87/86}Sr)_{connate}$ = 0.708664; $[Sr]_{connate}$ =37.94 mg/l and $\delta^{18}O_{connate}$ = 5.16‰ (SMOW) are all referred to the Salvarola Terme well measured in this work.*

The fractions of Sr from seawater and connate water are converted to the respective mass fractions of both end-members ($f_{seawater}$, $f_{connate}$ = 1- $f_{seawater}$) using $[Sr]_{seawater}$ =8.08 mg/l (Emelyanov and Shimkus, 2012) and $[Sr]_{connate}$ =37.94 mg/l (this work). Deduced seawater fractions range between 0.77 and 0.99 (Tab. 4). In particular, the chimney (SCH6), SCH2I and SCH1I - the most radiogenic samples in Sr - imply that the fluid mixture consisted of 93% to 99% of seawater and only 1% to 7% of connate waters. The remaining GC subsamples only contained seawater fractions between 77% and 86% meaning that the contribution from connate water was higher, although seawater contributions still dominated. The mixing fractions deduced from Sr concentrations and isotope compositions permit to estimate $\delta^{18}O_M$, the oxygen signature of the water in which the carbonates formed:

(II) $\delta^{18}O_M = \delta^{18}O_{seawater}\, f_{seawater} + \delta^{18}O_{connate}\, f_{connate}$

The $\delta^{18}O_{seawater}$ = 2‰ (SMOW) used here is the calculated signature of Adriatic Sea water coming from 100 m depth, analogues to the depositional conditions on the shelf for the Secchia River succession, based on a salinity of 38.3‰ and a water temperature that varies between 12°C and 13° (Lipizer et al., 2014). $\delta^{18}O_{connate}$ = 5.16‰ (SMOW) corresponds to the value determined for the Salvarola Terme well. Calculated $\delta^{18}O_M$ vary between 2.04‰ (SMOW) in SCH2I with the largest seawater fraction ($f_{seawater}$ = 0.99) and 2.74‰ (SMOW) in the least seawater influenced sample (SCH4I, $f_{seawater}$ = 0.77, Tab. 4). The temperature of formation for each subsample can be calculated inserting $\delta^{18}O_M$ into the corresponding equation of Vasconcelos et al. (2005). The temperature varies between 9°C and 13°C whereby the chimney subsamples are homogenous at 10° C and GCs are more variable (Tab. 4). The values obtained fit well with the mean temperature of the Pleistocene interval considered, when the seawater temperature was possibly between 2°C and 4°C lower than today in the range of 8°C to 11°C (de Garidel-Thoron et al., 2005; de Boer et al., 2012). The higher temperatures of 12°C-13°C refer to subsamples where the connate water component is significant.

5.7 Formation process

The chimneys form due to a focused fluid flow through a narrow discontinuity across fine-grained sediments or via diffusion in coarser more permeable sediments (Choi et al., 2011). In the case of focused flux, the fluid progressively displaces the sediment particles and creates an open central vent that in our sample has been filled up until closure (Fig. 10). The process that promoted chimney formation, according to $\delta^{13}C$ signatures, could be mainly Anaerobic Oxidation of Methane coupled with Sulfate Reduction. The process of AOM is described in equation (1) (Peckmann et al., 2001; Magalhães et al., 2012 and references therein) and tends to occur at the interval between sediments containing dissolved sulfate and those containing methane, the Sulfate-Methane Transition Zone (SMTZ) (Magalhães et al., 2012 and references therein).

(1) $CH_4 + SO_4^{2-} \longrightarrow HCO_3^- + HS^- + H_2O$

Considering the negative values in $\delta^{13}C$ of the chimney sample SCH6, AOM-SR is the process that most likely promoted its formation (Magalhães et al., 2012; Loyd et al., 2012; 2016 and references therein). In any case the original source of methane in this study has a $\delta^{13}C$ of -46‰ and is classified as thermogenic (Oppo et al. 2013). This can result in a priori less negative signature in the authigenic carbonates, also influenced by coeval secondary methanogenesis and heavy carbon CO_2 generation (Oppo et al., in press). The dolomite phase suggests that the carbonates formed within the sediment pile near the SMTZ where the interstitial water is depleted in the sulfate component

(Greinert et al., 2001; Peckmann et al., 2001; Magalhães et al., 2012 and references therein; Oppo et al., 2015).

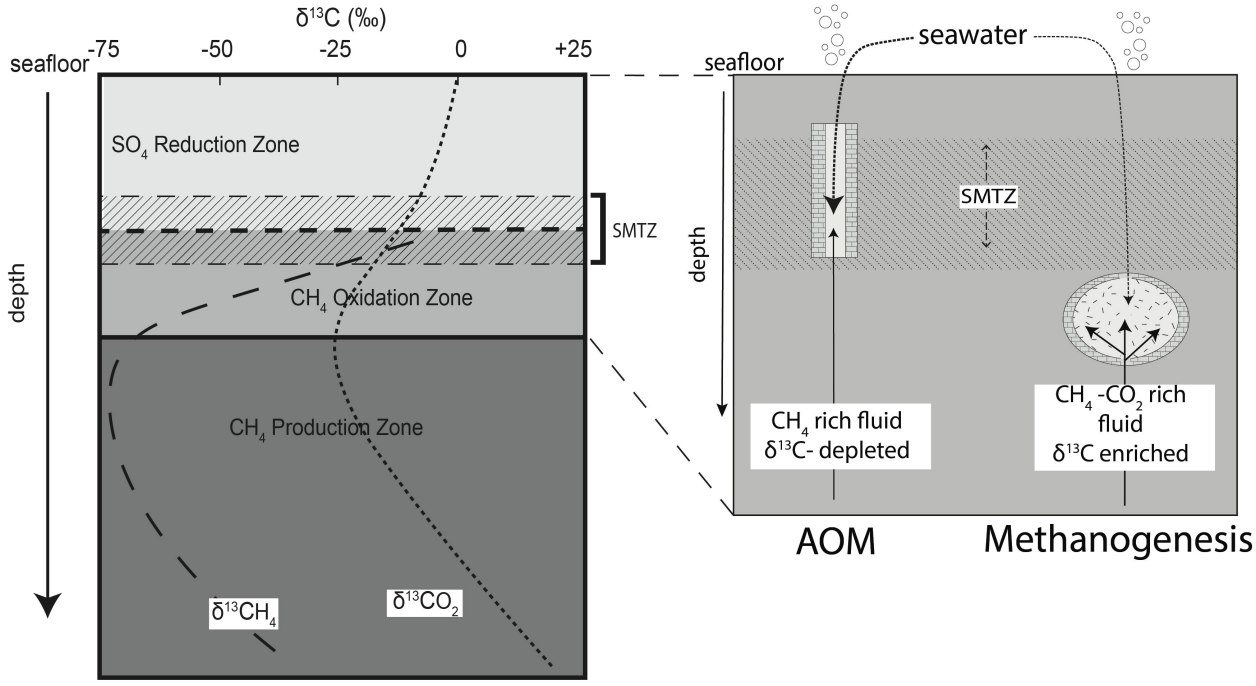

Fig. 10: *Formation process model, not to scale. On the left the variation of $\delta^{13}CH_4$ and $\delta^{13}CO_2$ within the sedimentary column is shown (after Whiticar, 1999; Oehlert and Swart, 2014 and references therein). On the right, the focus is around the SMTZ. The chimney likely formed due to a focused fluids flow through a narrow discontinuity opened through the sediments in the SMTZ. The higher permeability pathways could be exploited for more rapid gas diffusion originating the GCs likely below the SMTZ. The fluid flow was strong enough to allow the record of all the fluid components defined in this system, gas and connate water.*

The globular concretions followed a diffusion process for their formation: the higher permeability pathways exploited for gas diffusion can be provided by bedding planes, small faults and fractures. The fluid flow was strong enough to fill-up and enlarge the spaces between the sedimentary layers and discontinuities, whereby different shapes could reflect the width of fluid plumbing system linked to the permeability of sediments. The precipitation of the carbonate started in contact with the sediments creating a sort of shell-layer, of different thickness, that progressively bound the interior sediments (Fig. 10). The GC sub-samples, with the exception of SCH1B, exhibit positive carbon isotope values consistent with a carbonate formation associated to methanogenesis (Raiswell and Fisher, 2000; Loyd et al., 2012 and references therein). During this process ^{12}C is a preferentially incorporated in the CH_4 dissolved in the water and the result is residual pore water with elevated $\delta^{13}C$.

(2) $2HCO^{-}_{3} + 4H_2 \longrightarrow CH_4 + CO_3^{2-} + 3H_2O$

According to the reaction (2), methanogenesis supports conditions that promote carbonate

precipitation by reducing TCO_2 and maintaining constant alkalinity. The production of methanogenic CO_2 and carboxylic acids can, however, keep pore water under saturated with respect to carbonates due also to the lowering in pH (Canfield and Raiswell,1991; Meister, 2013). However, considering the influence of connate water found in the system, the condition prone to carbonate precipitation are assured by the bicarbonate ions concentration (199 ppm) which is higher than the normal marine content. In this case, the methanogenesis would be active below the Sufate-Methane Interface (SMI). In fact the fluid migrating from the deeper part of the studied system includes hydrocarbons that are degraded by bacterial activity into secondary methane. Bacterial degradation has been ascertained in modern fluid emissions (Heller et al., 2011; Oppo et al., 2013). The carbonates formed within the sediment pile where the interstitial water is depleted in sulfate and GCs were forming deeper with respect to chimneys or where ^{13}C enriched deep fluids could rise faster due to stronger fluxes (Fig. 10).

6. Conclusions

Cold seep systems in different marine geological settings are studied to gain information on hydrocarbon fields, hydrates, formation temperatures and gas escaping through the seafloor. Isotopic signatures of authigenic carbonates are useful to infer fluid flux variability and/or different fluid supply. However, the geochemical and isotopic record of seep carbonates is rarely studied in conjunction with feeding fluids, as they cannot be recovered. Geochemical and isotopic analyses on the Secchia River carbonates provide new insights into the fluid migration along the Northern Apennine foothills, initiated in the Plio-Pleistocene and still active today. The present day seepages allow a detailed study of the deep fluids migrating up to the surface, also providing useful information on the fossil system where carbonate formed. The Secchia carbonates, composed of dolomite, are part of a vast emission system represented by dolomitic pipes identified at other neighbouring sites, namely the Enza chimney field (Viola et al., 2015) and the Stirone River site (Cau et al., 2015). Petrographic observations support the role of fluids in the genesis of the carbonates. The occurrence of clotted and peloidal microfabric, which formation usually is induced by bacterial activities, is observed in authigenic carbonates samples. The dolomite fraction increases in the internal part of the samples reflecting the progressive isolation from SO_4-rich pore water.

Stable carbon isotopes in cements document the occurrence of two different gas components strictly linked to the evolution of the gas field in the subsurface and resulting in two different signatures. The positive $\delta^{13}C$ in most GCs points to the contribution from ^{13}C-enriched fluids due to secondary methanogenesis, which is still active in the study area. The negative $\delta^{13}C$ values in the sampled

chimney and a globular concretion are indicative of Anaerobic Oxidation of Methane and Sulfate Reduction during the carbonate precipitation. The $\delta^{18}O$ values in the authigenic carbonates depend on the $\delta^{18}O$ composition of the pore water from which the dolomitic carbonates precipitated and record variable contribution from seawater and connate water. The analysis of strontium isotopes attests that most GCs are clearly imprinted by connate waters coming from the Miocene reservoirs (typically 14 to 23%). Marine bottom water (93-99 %), however, dominates during the precipitation of chimney and the most radiogenic GCs subsample. These results indicate that different isotope signatures in seep carbonates result from variable relative contribution of gas and water components in spite the fact that carbonates precipitated under stable basin conditions with fluid supply from a well-defined hydrocarbon field. The seep carbonate characteristics mainly indicate variations in biogeochemical processes, which are rarely recognisable in ancient and present-day marine environments. The different morphologies of the seep carbonates are linked to different plumbing systems. The chimney likely formed due to AOM on a focused fluids flow through a narrow discontinuity crossing the sulphate-methane transition zone. The globular concretions preserve the deep fluid signature thanks to a more rapid fluid diffusion, through higher permeability pathways, resulting in gas pockets below the sulphate-methane interface.

References

Abrams, A. M., 2005. Significance of hydrocarbon seepage relative to petroleum generation and entrapment. Mar. Petrol. Geol. 22, 457-477.

Algeo, J. T., and Maynard, J. B., 2004. Trace-element behavior and redox facies in core shales of Upper Pennsylvanian Kansas-type cyclothems. Chem. Geol. 206, 289-318.

Aloisi, G., Pierre, C., Rouchy, J.-M., Foucher, J.-P., Woodside, J., 2000. Methane-related authigenic carbonates of eastern Mediterranean Sea mud volcanoes and their possible relation to gas hydrate destabilisation. Earth Planet. Sci. Lett. 184, 321–338.

Andrews, J.E., Stamatakis, M.G., Marca-Bell, A., Stewart, C., Millar, I.L., 2016. Exhumed hydrocarbon-seep authigenic carbonates from Zakynthos Island (Greece): Concretions not archaeological remains. Mar. Petrol. Geol., 76, 16-25.

Boetius, A., Ravenschlag, K., Schubert, C.J., Rickert, D., Widdel, F., Gieseke, A., Amann, R., Jùrgensen, B.B., Witte, U., Pfannkuche, O., 2000. A marine microbial consortium apparently mediating anaerobic oxidation of methane. Nature, 407, 623–626.

Bontognali, T.R.R., McKenzie, J.A., Warthmann, R.J., Vasconcelos, C., 2014. Microbially influenced formation of Mg-calcite and Ca-dolomite in the presence of exopolymeric substances produced by sulfate-reducing bacteria. Terra Nova, 26, 72-77.

Budd, D.A., 1997. Cenozoic dolomites of carbonate islands: their attributes and origin. Earth-Sci. Rev. 42, 1-47.

Canfield, D. E., Raiswell R. J., 1991. Pyrite formation and fossil preservation. In Taphonomy: Releasing the Information Locked in the Fossil Record (eds. P. A. Allison and D. G. Briggs). Plenum, New York, 337–37.

Capozzi, R., Picotti, V., 2010. Spontaneous fluid emissions in the Northern Apennines: geochemistry, structures and

implications for the petroleum system. Geol. Soc. London, Spec. Publ. 348, 115–135.

Capozzi, R., Guido, F.L., Oppo, D., Gabbianelli, G., 2012. Methane-Derived Authigenic Carbonates (MDAC) in northern-central Adriatic Sea: relationships between reservoir and methane seepages. Mar. Geol. 332-334, 174-188.

Choi, J.-H., Seol, Y., Boswell, R., Juanes, R., 2011. X-ray computed-tomography imaging of gas migration in water-saturated sediments: from capillary invasion to conduit opening. Geophys. Res. Lett. 38, LI7310.

Clari, P., Cavagna, S., Martire, L., Hunziker, J., 2004. A miocene mud volcano and its plumbing system: a chaotic complex revised (Monferrato, NW Italy). J. Sed. Res. 74, 662-676.

Cau, S., Franchi, F., Roveri, M., Taviani, M., 2015. The Pliocene-age Stirone River hydrocarbon chemoherm complex (Northern Apennines, Italy). Mar. Petrol. Geol. 66, Part 3, 582–595.

De Boer, B., Van de Wal, R.S.W., Lourens, L.J., Bintanja, R., 2012. Transient nature of the Earth's climate and the implications for the interpretation of benthic $\delta^{18}O$ records. Palaeogeogr. Palaeoclimatol. Palaeoecol. 335-336, 4–11.

de Garidel-Thoron, T., Rosenthal, Y., Bassinot, F., Beaufort, L., 2005. Stable sea surface temperatures in the western Pacific warm pool over the past 1.75 million years. Nature, 433, 294–298

de Kaenel, E., Siesser, W.G., Murat, A., 1999. Pleistocene calcareous nannofossil biostratigraphy and the western mediterranean sapropels, sites 974 to 977 and 979. In: Comas, M.C., Zhan, R., and Klaus, A., eds., Proceedings of the Ocean Drilling Program, Scientific Relults, 161,159-183.

De la Pierre, F., Martire, L., Natalicchio, M., Clari, P., Petrea, C., 2010. Authigenic carbonates in upper miocene sediments of the tertiary piedmont basin (NW Italy): Vestiges of an ancient gas hydrate stability zone? Bull. Geol. Soc. Am. 122, 994–1010.

de Souza, G.F., Reynolds, B.C., Kiczka, M., Bourdon, B., 2010. Evidence for mass-dependent isotopic fractionation of strontium in a glaciated granitic watershed. Geochim. Cosmochim. Acta 74, 2596-2614.

Deniel, C., Pin, C., 2001. Single-stage method for the simultaneous isolation of lead and strontium from silicate samples for isotopic measurements. Anal. Chim. Acta 426, 95-103.

Díaz-del-Río, V., Somoza, L., Martínez-Frias, J., Mata, M.P., Delgado, a., Hernandez-Molina, F.J., Lunar, R., Martín-Rubí, J. a., Maestro, a., Fernández-Puga, M.C., León, R., Llave, E., Medialdea, T., Vázquez, J.T., 2003. Vast fields of hydrocarbon-derived carbonate chimneys related to the accretionary wedge/olistostrome of the Gulf of Cádiz. Mar. Geol. 195, 177–200.

Douglas, S., 2005. Mineralogical footprints of microbial life. Am. J. Sci. 305, 503-525.

Elderfield, H., 1986. Strontium isotope stratigraphy. Palaeogeogr., Palaeoclimatol., Palaeoecol. 57, 71–90.

Emelyanov, E., M., Shimkus, K., M., 2012. Geochemistry and Sedimentology of the Mediterranean Sea. Springer Science & Business Media.

Farrell, J.W., Clemens, S.C., Gromet, L.P., 1995. Improved chronostratigraphic reference curve of late Neogene seawater 87Sr/86Sr. Geology, 23, 403–406.

Faure, G., 1986. Principles of isotope geology. (2nd edition) Wuley, New York.

Faure, G., 1998. Principles and application of Geochemistry. (2nd edition). Prentice Hall, New Jersey.

Formolo, M.J., Lyonsa T.W., Zhangb, C., Kelleya, C., Sassenc, R., Horitad, J., Coled, D.R., 2004. Quantifying carbon sources in the formation of authigenic carbonates at gas hydrate sites in the Gulf of Mexico. Chem. Geol. 205, 253-264

Franzini, M., Leoni, L., Saitta, M., 1972. A simple method to evaluate the matrix effects in X-Ray fluorescence analysis. X-Ray Spectrom. 1, 151-154.

Franzini, M., Leoni, L., Saitta, M., 1975. Revisione di una metodologia analitica per fluorescenza-X, basata sulla correzione completa degli effetti di matrice. Rend. Soc. Ital. Mineral. Petrol. 31, 365-378.

Ge, L., Jiang, S.Y., Swennen, R., Yang, T., Yang, J.H., Wu, N.Y., Liu, J., Chen, D.H., 2010. Chemical environment of

cold seep carbonate formation on the northern continental slope of South China Sea: Evidence from trace and rare earth element geochemistry. Mar. Geol., 277 (1–4), 21-30.

Goldsmith, J.R., Graf, D.L., 1958. Relation between lattice constants and composition of the Ca-Mg carbonates. Am. Mineral. 43, 84–101.

Greinert, J., Bohrmann, G., Suess, E., 2001. Gas hydrate-associated carbonates and methane-venting at Hydrate Ridge: classifica- tion, distribution, and origin of authigenic lithologies. In: Natural gas hydrates: occurrence, distribution, and detection. Geophys. Monogr. 124, 99–113.

Gunderson, K.L., Pazzaglia, F.J., Picotti, V., Anastasio, D. a., Kodama, K.P., Rittenour, T., Frankel, K.F., Ponza, A., Berti, C., Negri, A., Sabbatini, A., 2014. Unraveling tectonic and climatic controls on synorogenic growth strata (Northern Apennines, Italy). Bull. Geol. Soc. Am. 126, 532–552.

Heller, C., Blumenberg, M., Kokoschka, S., Wrede, C., Hoppert, M., Taviani, M., Reitner, J., 2011. Geomicrobiology of Fluid Venting Structures at the Salse di Nirano Mud Volcano Area in the Northern Apennines (Italy), in: Advances in Stromatolite Geobiology SE - 14, Lecture Notes in Earth Sciences. Springer Berlin Heidelberg, pp. 209–220.

Hess, J., Bender, M.L., Schilling, J.G., 1986. Evolution of the ratio of strontium-87 to strontium-86 in seawater from Cretaceous to Present. Science, 231, 979–984.

Kokoschka, S., Dreier, A., Romoth, K., Taviani, M., Schäfer, N., Reitner, J., Hoppert, M., 2015. Isolation of Anaerobic Bacteria from Terrestrial Mud Volcanoes (Salse di Nirano, Northern Apennines, Italy). Geomicrobiol. J. 32, 355–364.

Lein, A. Yu, 2004. Authigenic carbonate formation in the ocean. Lithol. Miner. Resour. 39, 1-30. Translated from Litologiya i Poleznye Iskopaemye 1, 3-35.

Leoni, L., Saitta, M., 1976. X-ray fluorescence analysis of 29 trace elements in rock and mineral standards. Rend. Soc. Ital. Mineral. Petrol. 32, 497-510.

Leoni, L., Menichini, M., Saitta, M., 1982. Determination of S, Cl, and F in silicate rocks by X-Ray fluorescence analyses. X-Ray Spectrom. 11, 156-158.

Liang, H., Chen, X., Wang, C., Zhao, D., Weissert, H., 2016. Methane-derived authigenic carbonates of mid-Cretaceous age in southern Tibet: Types of carbonate concretions, carbon sources, and formation processes. J. Asian Earth Sci., 115, 153-169.

Lipizer, M., Partescano, E., Rabitti, A., Giorgetti, A., Crise, A., 2014. Qualified temperature, salinity and dissolved oxygen climatologies in a changing Adriatic Sea. Ocean. Sci. 10, 771–797.

Loyd, S.J., Berelson, W.B., Lyons, T.W., Hammond, D.E., Corsetti, F.A., 2012. Constraining pathways of microbial mediation for carbonate concretions of the Miocene Monterey Formation using carbonate-associated sulfate: Geochim. Cosmochim. Acta, 78, 77–98.

Loyd, S.J., Sample, J., Tripati, R.E., Defliese, W.F., Brooks, K., Hovland, M., Torres, M., Marlow, J., Hancock, L.G., Martin, R., Lyons, T. , Tripati, A.E., 2016. Methane seep carbonates yield clumped isotope signatures out of equilibrium with formation temperatures. Nature Commun., 7, 122-174.

Lumsden, D., 1979. Discrepancy between thin-section and X-ray estimates of dolomite in limestone. J. Sediment. Res. 49, 429–436.

Magalhães, V.H., Pinheiro, L.M., Ivanov, M.K., Kozlova, E., Blinova, V., Kolganova, J., Vasconcelos, C., McKenzie, J.A., Bernasconi, S.M., Kopf, A.J., Díaz-del-Río, V., González, F.J., Somoza, L., 2012. Formation processes of methane-derived authigenic carbonates from the Gulf of Cadiz. Sediment. Geol. 243-244, 155–168.

Marzec, P., Sechman, H., Kasperska, M., Cichostępski, K., Guzy, P., Pietsch, K. and Porębski, S. J. 2016. Interpretation of a gas chimney in the Polish Carpathian Foredeep based on integrated seismic and geochemical data. Basin Res. 1-18.

Mazzini, A., Svensen, H.H., Planke, S., Forsberg, C.F., Tjelta, T.I., 2016. Pockmarks and methanogenic carbonates

above the giant Troll gas field in the Norwegian North Sea. Mar. Geol., 373, 26-38.

Meister, P., 2013. Two opposing effects of sulfate reduction on calcite and dolomite precipitation in marine, hypersaline and alkaline environments. Geology 41, 499-502.

Naehr, T.H., Rodriguez, N.M., Bohrmann, G., Paull, C.K., Botz, R., 2000. Methane-derived authigenic carbonates associated with gas hydrate decomposition and fluid venting above the Blake Ridge Diapir. In: Paull, C.K., Matsumoto, R., Wallace, P.J., Dillon, W.P. (Eds.), Proceedings of the Ocean Drilling Program, Sci. Res. ODP, Coll. Stat., TX, 285–300.

Naehr,, T.H., Eichhubl, P., Orphan, V.J., Hovland, M., Paull, C.K., Ussler III, W., Lorenson, T.D., Greene H.G., 2007. Authigenic carbonate formation at hydrocarbon seeps in continental margin sediments: A comparative study. Deep-Sea Res., II, 54,1268–1291.

Neumeuster, S., Algeo, J. T., Betchel, A., Gawlick, H. J., Gratzer, R., Sachsenhofer, R. F., 2016. Redox conditions and depositional environment of the lower jurassic Bächental bituminous marls (Tyrol, Austria). Aust. J. of Earth Sci., 109/2.

Nyman, S.L., Nelson, C.S., Campbell, K.A., 2010. Miocene tubular concretions in East Coast Basin, New Zealand: analogue for the subsurface plumbing of cold seeps. Mar. Geol. 272, 319-336.

Oppo, D., Capozzi, R., Picotti, V., 2013. A new model of the petroleum system in the Northern Apennines, Italy. Mar. Petrol. Geol. 48, 57–76.

Oppo, D., Capozzi, R., Picotti, V., Ponza, A., 2015. A genetic model of hydrocarbon-derived carbonate chimneys in shelfal fine-grained sediments: The Enza River field, Northern Apennines (Italy). Mar. Petrol. Geol. 66, Part 3, 555–565.

Oppo, D., Viola, I., Capozzi, R., in press. Fluid sources and stable isotope signatures in Authigenic Carbonates: examples from the Northern Apennines, Italy. Mar. Petrol.Geol. Submitted

Paytan, A., Kastner, M., Martin, E.E., MacDougall, J.D., Herbert, T., 1993. Marine barite as a monitor of seawater strontium isotope composition. Nature 366, 445–449.

Peckmann, J., Reimer, A., Luth, U., Hansen, B.T., Heinicke, C., Hoefs, J., Reitner, J., 200. Methane-derived carbonates and authigenic pyrite from the northwestern Black Sea. Mar. Geol, 177, 129–150.

Peckmann, J., Thiel, V., 2004. Carbon cycling at ancient methane–seeps. Chem. Geol. 205, 443–467.

Pierre, C., Rouchy, J.-M., 2004. Isotopic compositions of diagenetic dolomites in the Tortonian marls of the western Mediterranean margins: evidence of past gas hydrate formation and dissociation. Chem. Geol. 205, 469–484.

Pierre, C., Bayon, G., Blanc-Valleron, M. M., Mascle, J., Dupré, S., 2014. Authigenic carbonates related to active seepage of methane-rich hot brines at the Cheops mud volcano, Menes caldera (Nile deep-sea fan, eastern Mediterranean Sea). Geol. Mar. Lett. 34, Issue 2, 253–267.

Pinheiro, L.M., Ivanov, M.K., Sautkin, A., Akhmanov, G., Magalhaes, V.H., Volkonskaya, A., Cunha, M.R., 2003. Mud volcanism in the Gulf of Cadiz: results from the TTR-10 cruise. Mar. Geol. 195, 131-151.

Raiswell, R., Fisher, Q. J., 2000. Mudrock-hosted carbonate concretions: a review of growth mechanisms and their influence on chemical and isotopic composition. J. Geol. Soc., London 157, 239–251.

Rees, C. E., 1973. A steady-state model for sulphur isotope fractionation in bacterial reduction processes. Geochim. Cosmochim. Acta 37, 1141–1162.

Reitner, J., Blumenberg, M., Walliser, E.O., Schäfer, N., Duda, J.P., 2015. Methane-derived carbonate conduits from the late Aptian of Salinac (Marne Bleues, Vocontian Basin, France): Petrology and biosignatures. Mar. Petrol. Geol., 66 (3), 641-652.

Roberts, H.H., Feng, D., Joye, S.B., 2010. Cold-seep carbonates of the middle and lower continental slope, northern Gulf of Mexico. Deep-Sea Res. 57, pt. II, 2040-2054.

Rosenbaum, J., Sheppard, S.M.., 1986. An isotopic study of siderites, dolomites and ankerites at high temperatures. Geochim. Cosmochim. Acta 50, 1147–1150.

Roy, S., Hovland, M., Braathen, A., 2016. Evidence of fluid seepage in Grønfjorden, Spitsbergen: Implications from an integrated acoustic study of seafloor morphology, marine sediments and tectonics. Mar. Geol., 380, 67-78.

Sabatino, N., Neri, R., Bellanca, A., Jenkyns, H. C., Masetti, D., Scopelliti, G., 2011. Petrography and high-resolution geochemical records of Lower Jurassic manganese-rich deposits from Monte Mangart, Julian Alps. Palaeogeogr., Palaeoclimatol., Palaeoecol. 299, 97-109.

Saitoh, M., Ueno, Y., Isozaki, Y., Shibuya, T., Yao, J., Ji, Z., Shozugawa, K., Matsuo M., Yoshida, N., 2015. Authigenic carbonate precipitation at the end-Guadalupian (Middle Permian) in China: Implications for the carbon cycle in ancient anoxic oceans. Prog. Earth Planet. Sci. 2, 41.

Sample, J.C., Reid, M.R., 1998. Contrasting hydrogeologic regimes along strike-slip and thrust faults in the Oregon convergent margin: evidence from the chemistry of syntectonic carbonate cements and veins. Geol. Soc. Am. Bull. 110, pt. 1, 48–59.

Talukder, A. R., 2012. Review of submarine cold seep plumbing systems: leakage to seepage and venting. Terra Nova, 24, 255–272.

Taviani, M., 2001. Fluid venting and associated processes, in: Vai, G., Martini, I.P. (Eds.), Anatomy of an Orogen: The Apennines and Adjacent Mediterranean Basins SE - 20. Springer Netherlands, 351–366.

Thirlwall, M.F., 1991. Long-term reproducibility of multicollector Sr and Nd isotope ratio analysis. Chem. Geol., 94, 85-104.

Tong, H., Feng, D., Cheng, H., Yang, S., Wang, H., Angela, G.M., Edwards, R.L., Chen, Z., Chen, D., 2013. Authigenic carbonates from seeps on the northern continental slope of the South China Sea: New insights into fluid sources and geochronology. Mar. Petrol. Geol. 43, 260-271.

Turchyn, A.V., Antler, G., Byrne, D., Miller, M. Hodell, D. A., 2016. Microbial sulfur metabolism evidenced from pore fluid isotope geochemistry at Site U1385. Glob. and Plan. Chang. 141, 82-90.

Van Landeghem, K.J.J., Niemann, H., Steinle, L.I., O'Reilly, S.S., Huws, D.G., Croker, P.F., 2015. Geological settings and seafloor morphodynamic evolution linked to methane seepage. Geo-Mar. Lett., 35, 289.

Vasconcelos, C., McKenzie, J.A., Warthmann, R., Bernasconi, S.M., 2005. Calibration of the delta O-18 paleothermometer for dolomite precipitated in microbial cultures and natural environments. Geology 33, 317-320.

Viola, I., Oppo, D., Franchi, F., Capozzi, R., Dinelli, E., Liverani, B., Taviani, M., 2015. Mineralogy, geochemistry and petrography of methane-derived authigenic carbonates from Enza River, Northern Apennines (Italy). Mar. Petrol. Geol. 66, 566–581.

Wang, S., Magalhães, V.H., Pinheiro, L.M., Liu, J., Yan, W., 2015. Tracing the composition, fluid source and formation conditions of the methane-derived authigenic carbonates in the Gulf of Cadiz with rare earth elements and stable isotopes. Mar. Petrol. Geol., 68 (A), 192-205.

Whiticar, M.J., 1999. Carbon and hydrogen isotope systematics of bacterial formation and oxidation of methane. Chem. Geol. 161, 291–314.

Wu, N., Farquhar, J., Strauss, H., 2014, $\delta^{34}S$ and $\Delta^{33}S$ records of Paleozoic seawater sulfate based on the analysis of carbonate associated sulfate. Earth Planet. Sci. Lett., 399, 44-51.

Zattin, M., Picotti, V., Zuffa, G., 2002. Fission-track reconstruction of the front of the Northern Apennine thrust wedge and overlying Ligurian unit. Am. J. Sci. 302, 346–379.

PAPER 3

Fluid sources and stable isotope signatures in Authigenic Carbonates from the Northern Apennines, Italy

Davide Oppo, Irene Viola, Rossella Capozzi

Submitted to Marine and Petroleum Geology on November 15, 2016

Fluid sources and stable isotope signatures in Authigenic Carbonates from the Northern Apennines, Italy

Davide Oppo[1] *, Irene Viola [2], Rossella Capozzi [2]

1 - Department of Geology and Petroleum Geology, University of Aberdeen, King's College, Aberdeen AB24 3UF, Scotland, UK

2 - Department of Biological, Geological and Environmental Sciences, University of Bologna, Via Zamboni 67, 40127 Bologna, Italy.

*Corresponding author: davide.oppo@abdn.ac.uk

Abstract

Authigenic carbonates are frequently associated with methane cold-seep systems, which extensively occur in various geologic settings worldwide. Of interest is the relation between the fluids involved in their formation and the isotopic signals recorded in the carbonate cements. Along the Northern Apennines foothills (Italy), hydrocarbons and connate waters still seeping nowadays are believed to be the primary sources for the formation of fossil authigenic carbonate found in Plio-Pleistocene marine sediments. Four selected outcrops of dolomitic authigenic carbonates were analysed to compare signature of seeping fluids with fractionation of stable carbon and oxygen isotopes recorded in the carbonate.

Along the foothills, deep methane-rich fluids spontaneously rise to the surface through mud volcanoes or are exploited in wells drilled nearby to the fossil Plio-Pleistocene authigenic carbonates. The plumbing system providing fluids to present-day cold seeps was structurally achieved in Late Miocene and Plio-Pleistocene. $\delta^{13}C$ values of methane, which vary from -51.9 to -43.0‰ VPDB, indicate that gas composition from the deep hydrocarbon reservoirs is relatively uniform along the foothills. On the contrary, $\delta^{13}C$ in fossil authigenic carbonates strongly varies among different areas and also within the same outcrop.

The different carbon sources that fed the investigated carbonates were identified and include: thermogenic methane from the deep Miocene reservoirs, ^{13}C-enriched CO_2 derived from secondary methanogenesis and microbial methane from Pliocene successions buried in the Po Plain. The $\delta^{13}C$

variability documented among samples from a single outcrop testifies that the authigenic carbonates might represent a record of varying biogeochemical processes in the hydrocarbon reservoirs. The sources of stable oxygen isotopes in authigenic carbonates are often ascribed to marine water. Oxygen isotopic fractionation in the dolomite cements of considered samples indicates that marine pore water couldn't be the sole source of oxygen. $\delta^{18}O$ values of present-day connate waters provide a preliminary evidence that deep waters had a role in the carbonates precipitation. The concomitant occurrence of active cold seepages and fossil record of ancient plumbing systems suggests that generation and migration of hydrocarbons are long-lasting and very effective processes along the Northern Apennines foothills.

Keywords

Cold seep; Authigenic Carbonates; Oxygen and Carbon stable isotopes; Petroleum system; Methane migration; Connate water.

1 Introduction

Seafloor fluid seepages represent widespread and highly dynamic environments. Their physical and chemical characteristics are described and correlated with fluid sources, fluid flow intensities, tectonic setting, and properties of the hosting sediment (e.g. Judd et al., 2002; Judd and Hovland, 2007; Nyman and Nelson, 2011; Magalhães et al., 2012; Hensen et al., 2015). The various processes of formation, migration and alteration of hydrocarbons represent key factors to define the natural fluid seepage settings. The role of microbial consortia promoting the Anaerobic Oxidation of Methane (AOM), and coupled Sulphate Reduction (SR), was stressed to represent the major diagenetic processes occurring at cold seeps (e.g., Peckmann et al., 1999; Boetius et al., 2000). The formation of Methane-Derived Authigenic Carbonate (MDAC) represents the main by-product of the AOM-SR process in marine environment (e.g. Peckmann et al., 2001; Reitner et al., 2005), and could preserve the geochemical imprint of the fluids involved in their formation. The correlation between authigenic carbonates (AC) and hydrocarbon source in present-day cold seeps is often facilitated by associated gas leakage from the seafloor, which can be sampled and analysed. Otherwise, in fossil systems this correlation can be more challenging due to scarce knowledge of the associated petroleum system. Mineralogy, oxygen and carbon stable isotopes, and biomarkers (e.g., Peckmann and Thiel, 2004; Magalhães et al., 2012; Pierre et al., 2014; Reitner et al., 2015) are commonly used to describe processes and fluids involved during carbonate precipitation. Carbon stable isotopes are useful to identify carbon sources, whereas oxygen isotopes provide information

on the ambient water and temperature involved during carbonate formation. However, the isotopic composition might be influenced by mixing of hydrocarbon and waters from different sources, and by recrystallization processes, all of these masking the original signal and hindering a correct interpretation. The main objective of this work is to assess a possible direct correlation between the fluids that were present in fossil authigenic carbonate fields and those occurring in the present-day active fluid seepage sites along the Northern Apennine foothills (Italy). This research would contribute to shed light on the Northern Apennines seepage history, with the aim to better interpreting modern and fossil occurrences worldwide, both offshore and onshore, and to identify the processes resulting in different isotopic signature and geochemistry of authigenic carbonates. In particular, we evaluate the geological and geochemical constraints that could have influenced the oxygen and carbon isotopic compositions during the precipitation of fossil authigenic carbonates in four representative outcrops: Stirone River, Secchia River, Enza River and Nirano mud volcano field (NMVF) (Fig. 1). Present-day seeps and deep wells along the foothills are used to define the geochemical characteristics of the fluids contained in the reservoirs that are part of the Northern Apennines petroleum system.

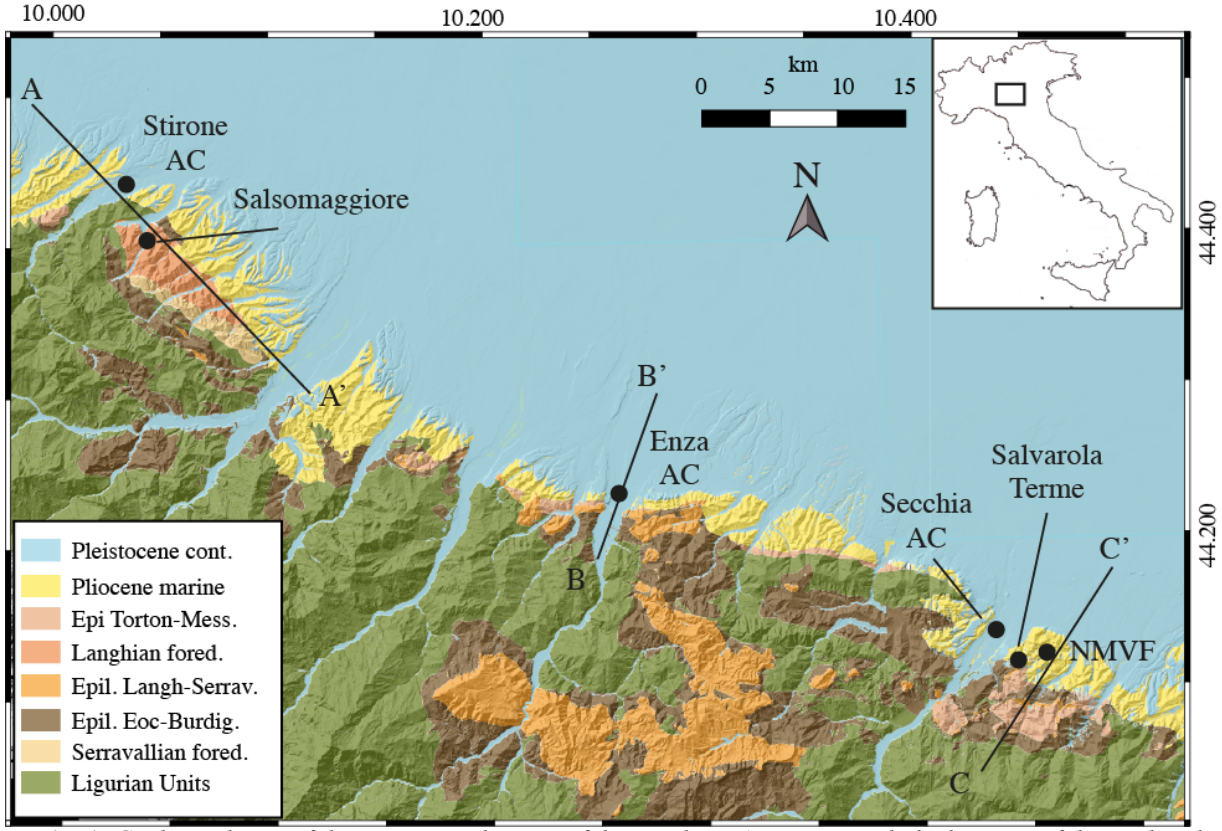

Fig. 1*: Geological map of the investigated sector of the Northern Apennines with the location of the analysed authigenic carbonate outcrops. Salsomaggiore and Salvarola Terme wells location is shown. The traces of cross sections of figures 2, 4 and 5 are indicated.*

2 Geological setting

The Northern Apennines formed in consequence of complex interactions between Adria and European plates. The Oligo-Miocene collision between Adria and the Corsica-Sardinia block rearranged the Jurassic-Eocene units belonging to the Ligurian deformed oceanic wedge, which progressively thrust over the foredeep successions of Miocene age, forming the Ligurian Nappe (Zattin et al., 2002). In the Po Plain side of the Northern Apennines, the Ligurian Nappe shows a wedge-shaped closure along the foothills with a gravitational reworking at its tip. The underlying foredeep deposits have been progressively incorporated into the orogenic belt, and the fold-and-thrust belt formed during Miocene and Pliocene provided the structural traps for hydrocarbon accumulation in the subsurface of Northern Apennines and Po Plain (e.g. Oppo et al., 2013 and references therein). Folds and thrusts in the foredeep succession formed during and after the tectonic and gravitational emplacement of the Ligurian Nappe, which acted as seal for the fluid reservoirs. The Epiligurian Units filled numerous satellite basins occurring above the Ligurian Nappe. Late orogenic extensional tectonics, crosscutting the sedimentary cover down to the Miocene units, is responsible for the formation of high-angle normal faults (Picotti and Pazzaglia, 2008; Picotti et al., 2009), which provide the main fluid migration pathways for numerous present-day spontaneous seepages (Picotti et al., 2009; Capozzi and Picotti, 2010; Oppo et al., 2013). The mountain range is characterized by Plio-Pleistocene uplift and exhumation (Balestrieri et al., 2003; Bartolini, 2003), with a consequent transition from exclusively marine to continental environments (e.g. Ghielmi et al., 2009; Gunderson et al., 2014).

2.1 Salsomaggiore and the Stirone authigenic carbonate field

The Salsomaggiore anticline is the westernmost structure considered in this study. It is formed by a Burdigalian-Serravallian succession of turbiditic sandstones and marls. It was deformed since Langhian through Tortonian as an intrabasinal structure, verging northeast, which was ultimately exposed and eroded at the thrust-top (Fig. 2). After a subsidence pulse during Messinian, the structure was covered and sealed by an olistostrome detached from the Ligurian nappe. A large wave-length folding and erosion phase in Plio-Pleistocene led to refolding of the upper thrust sheet with a northwest vergence.

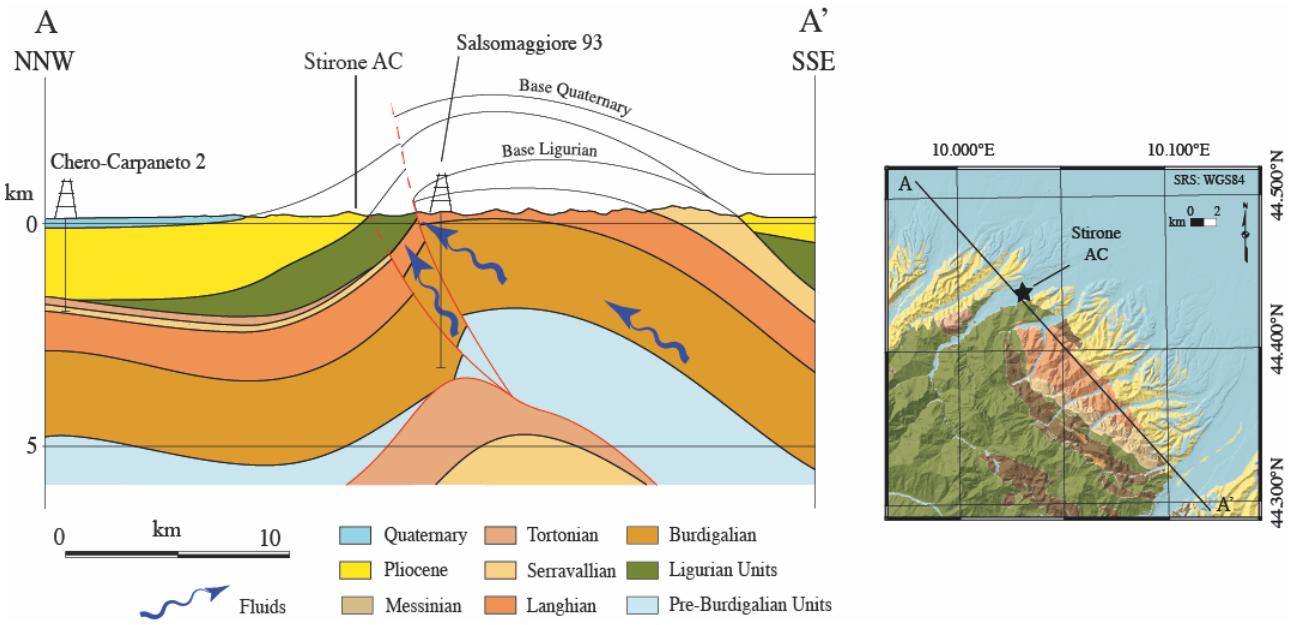

***Fig. 2**: Strike cross-section of Salsomaggiore anticline and Stirone authigenic carbonate field along the Northern Apennines foothills (Vertical exaggeration 2:1). In this area, Burdigalian to Serravallian reservoir outcrops after Plio-Pleistocene northwestward reactivation of a lateral ramp and erosion of sealing units. The fluids migrated up-dip along the sedimentary layers into the anticline culmination.*

Synsedimentary deformation and tectono-thermal evolution governed the migration of fluids in the anticline flanks since Serravallian, and caused various episodes of hydrocarbon venting on the seafloor, marked by several seep-related carbonate concretions and chemoherms (e.g., Ricci Lucchi and Vai, 1994; Terzi et al., 1994; Taviani, 2001; Conti et al., 2007; Cau et al., 2015). Authigenic carbonates occurring in the Pliocene hemipelagic succession that overlies the northwestern flank of Salsomaggiore structure outcrop along the Stirone River. The authigenic carbonates investigated in this study are located in a ca. 50 meters-long outcrop formed of hemipelagic clays and silty clays pertaining to the Argille Azzurre Fm., and deposited at the transition between Zanclean and Piacenzian (Cau et al., 2015). The authigenic carbonates form pipe-like conduits and slabs (Fig.3a). Moving up-section, various brecciated micritic limestones, Lucinid mudstones and chemosymbiotic organisms occur interspersed within organic-rich (sapropel) horizons (e.g., Cau et al., 2015), deposited during Piacenzian and controlled by precession cycles (e.g., Capozzi et al., 2006).

2.2 Enza River authigenic carbonate field

Authigenic carbonates outcropping along the Enza riverbanks (Blumenberg et al., 2015; Oppo et al., 2015; Viola et al., 2015) (Fig. 3b) develop at the Northern Apennines foothills in a well-preserved Early Pleistocene succession that marks the change from shallow marine to coastal sedimentary environment (Gunderson et al., 2014). Southwards of the authigenic carbonate outcrop, the Quattro Castella ramp anticline locally delineates the present-day mountain front, which was generated by the formation of a detachment within the Ligurian Nappe during Plio-Pleistocene (Gunderson et al.,

2014) (Fig. 4). A further E-W trending fold located in more external position was also actively growing in the Po Plain subsurface (Fig. 4; Oppo et al., 2015).

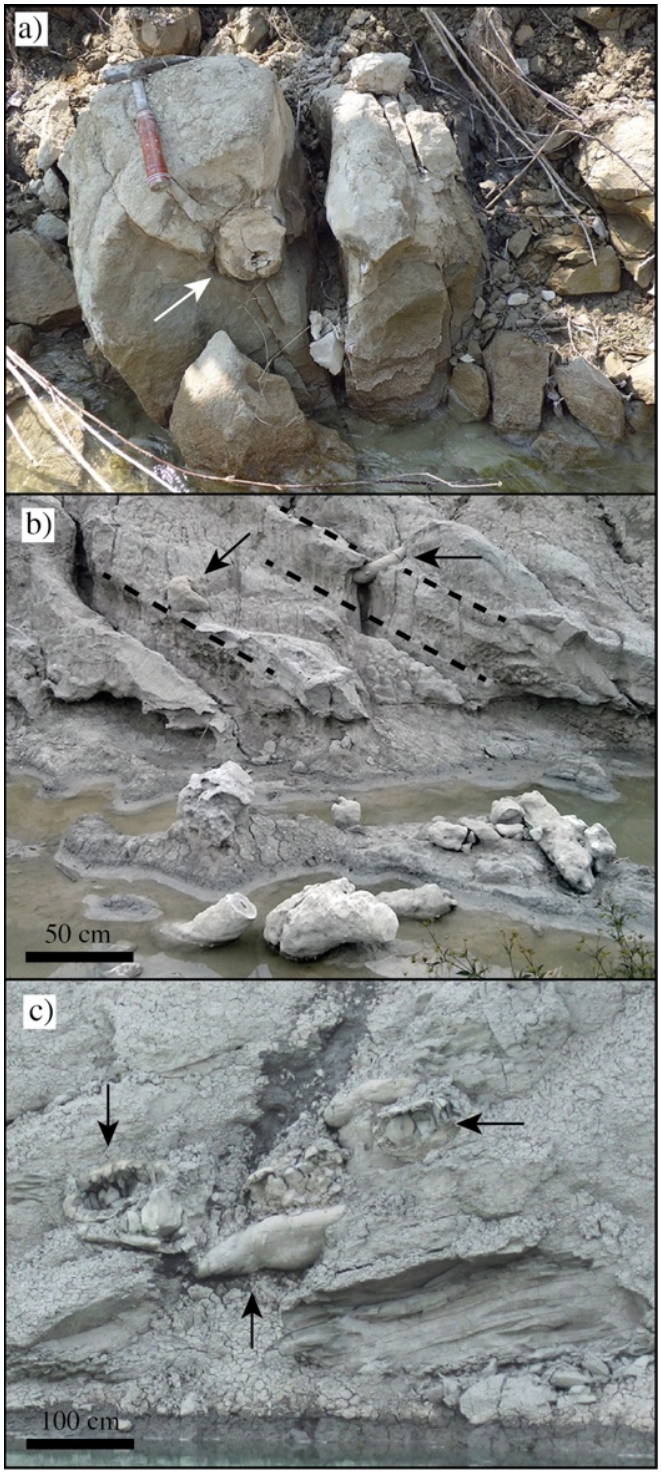

Fig. 3*: Authigenic carbonate outcrops in the studied areas. a) Stirone chimney ca. 1m wide with the conduit filled by cemented sediments (white arrow); b) Chimneys and irregular carbonate concretions outcropping along the Enza riverbanks. Arrows indicate chimneys perpendicular to the stratification of the hosting sediment (strata marked by dashed lines). Note the chimney emerging from the water in foreground; c) Bulbous, slab-like authigenic carbonate concretions in Secchia riverbanks. Arrows point to main concretions. The concretions are roughly aligned to sediment stratification, which is exposed in the lower-right corner of the image.*

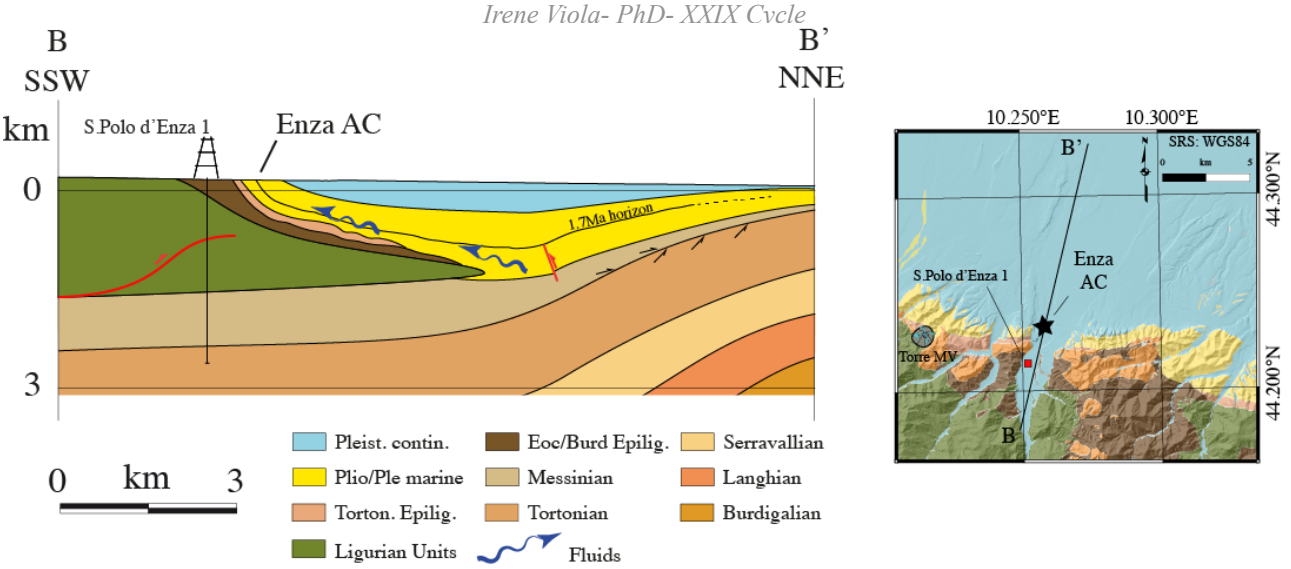

Fig. 4: *Cross-section in the Enza authigenic carbonate field along dip of Northern Apennines foothills. Deformation of the named Ghiardo Plateau fold can be observed on NNE; the erosional truncation of Tortonian units and following onlap of Messinian sediments are evidenced. Southwards to Enza authigenic carbonate field, a thrust detachment plane, related with the deformation of the Quattro Castella anticline, is located within the Ligurian Units. The source rocks in marine Pliocene sediments generated biogenic methane, which progressively migrated up-dip along the deformed sediments on the Ligurian Nappe forelimb. The horizon marking the base of the Enza River section (1.7 Ma) is shown.*

The authigenic carbonate field is located on the Quattro Castella anticline forelimb, which deforms a fine-grained succession belonging to the Lower Pleistocene Argille Azzurre Fm. and that represents part of the marine intervals before the transition to continental deposits (Gunderson et al., 2014). The authigenic carbonates occur as slabs and pipe-like bodies (chimneys, similar to those described in Magalhães et al., 2012) within a 35 meters-thick section formed of continuous inner shelf silty clays, with intercalations of cm-thick sandy layers progressively more frequent towards the top of the section. This latter, dated at 1.4 Ma, is marked by a significant angular unconformity and by a layer containing chimney fragments and reworked coarse siliciclastics. This layer is pervaded by dark grey micritic carbonate concretions and colonized by a corallinaceous assemblage (Oppo et al., 2015). Southwards to Enza field, a weakly-cemented body ca. 10 meters high (Enza Hills in Sec. 3.1) occurs within sand layers. These latter sediments pertain to the upper Argille Azzurre Fm., deposited after the pelitic succession hosting authigenic carbonates along the Enza riverbanks (Gunderson et al., 2014). This body was likely formed close to the seafloor due to its richness in benthic fauna and bioturbation.

2.3 The Secchia River authigenic carbonate field and Nirano mud volcanoes area

The stripe of Northern Apennines foothills comprised between Secchia River and Nirano shows several features that testify present-day fluid emission, such as the Nirano Mud Volcano Field (NMVF) and saline waters (exploited in spa activities at Salvarola) mixed with hydrocarbons (Fig.

1). In this area, thrusts deforming the Miocene foredeep units create structural traps for the fluids: Their growth proceeded during Late Miocene and Pliocene, with minor deformation also in Quaternary (Oppo et al., 2013) (Fig. 5). Later high-angle normal faults along the foothills are likely providing the main pathways for fluids migration and present-day fluids emission at surface (e.g. Oppo et al., 2013).

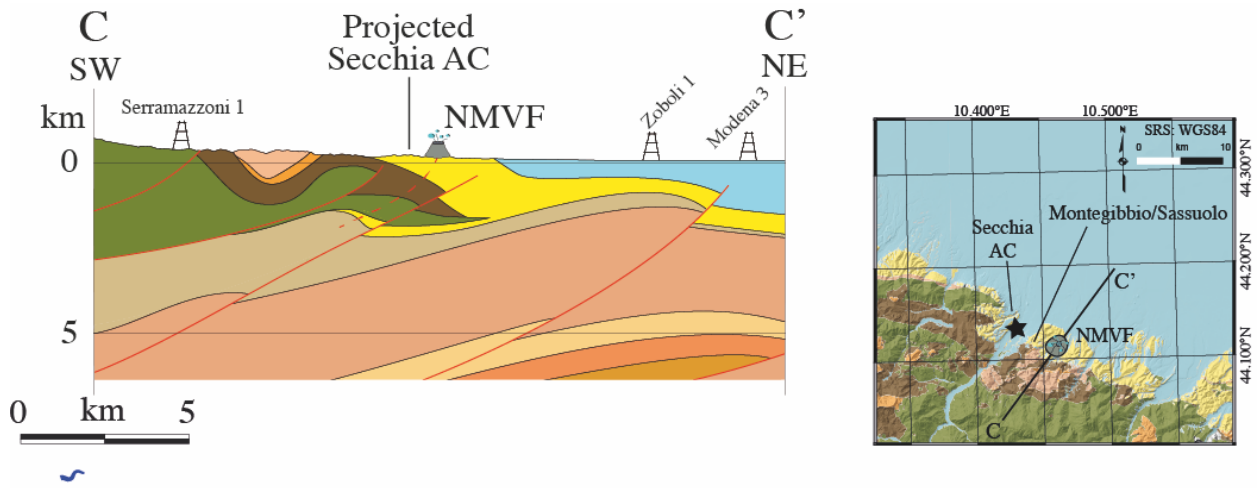

Fig. 5*: Cross-section through Nirano Mud Volcano Field along dip of the Northern Apennines foothills. Present-day fluid emissions are associated with ramp anticlines along the foothills. Normal faults likely allow upwards migration of saline water and thermogenic hydrocarbons, connecting Miocene reservoirs to the surface.*

Various authigenic carbonate concretions outcrop along Secchia riverbanks (Fig. 3c) within the Lower Pleistocene (1.7 Ma) succession of Argille Azzurre Fm. Carbonates mostly form meter-size bulbous and slab-like concretions, with a minor occurrence of smaller chimneys. Slab-like concretions are interlayered within the succession, whereas bulbous concretions and chimneys crosscut the stratification. Small normal faults, dipping northeast, are documented along the riverbanks close to the concretions. North-eastwards of Secchia River, NMVF develops over an area of ca. 75,000 m^2 into Plio-Pleistocene Argille Azzurre Fm., and at the bottom of a caldera-like structure that is likely resulting from a collapse within the pelitic succession following paroxysmal events of fluid expulsion. The ramp-anticline forming the fluid trap in Miocene foredeep sediments, and also deforming the Ligurian Nappe sealing units, is overlaid by outcropping Argille Azzurre Fm (Fig. 5) (Oppo et al., 2013). Mud cones and pools at NMVF are active with constant emission of saline waters and methane, together with small amounts of oil and condensates migrating from the Miocene reservoir (Oppo et al. 2013). Along a small creek to the west of NMVF, a few carbonate chimney concretions were recovered within the Argille Azzurre Fm.

3 Materials and Methods

3.1 Analysed samples

Samples from four authigenic carbonate outcrops were considered in this study. A total number of 45 subsamples, representing various carbonate morphologies, were selected and analysed. A total number of 21 subsamples from Enza River field were analysed, belonging to two chimneys (En5 and En10) (Figs.6a and 6b), one tabular slab (Cr2) (Fig. 6c) and one concretion within the upper horizon colonized by the corallinaceous assemblage (Cr3) (Fig. 6d). En10 chimney shows an open central conduit, is 170 cm long and 20 cm in diameter. The top and the bottom of the chimney were analysed. The top was divided in external (E) and internal (I) portions (Fig. 6b), whereas only the internal area of the bottom has been analysed. En5 chimney is 63 cm long and 20 cm in diameter. (Fig 6a). It was divided in 8 sections from bottom (1) to top (8), to investigate possible geochemical variations along the chimney. Each section, excluding 1 and 8, was longitudinally separated in internal (I), middle (M) and external (E) parts (Fig. 6a). In this paper, selected subsamples from sections 1, 3, 4, 6 and 8 are presented. Cr3 sample is a concretion at the top of the Enza section; the dark-grey portion of sample (Cr3A) was analysed and compared with the light-grey adjacent areas (Cr3B) (Fig. 6d). Cr2 slab is located stratigraphically below the corallinaceous assemblage layer and shows a general grey colour (Cr2A) with a light-grey area (Cr2B) (Fig. 6c). One sample from the semi-consolidated carbonate concretions cementing the sandy intervals at Enza Hills was also analysed (ENCO 1) (Fig. 6i). Five samples were collected from globular slab-like concretions of Secchia river (SCH1 to SCH5) (Figs. 6e and 6f), with weak cementation and meter-size dimensions. Subsamples were collected for the external (E) and internal (I) areas of each concretion. One chimney (SCH6) with high degree of cementation was subsampled: a light-grey layer in the more external area (E), a darker interval forming the bulk of the concretion (M), and the yellowish-grey poorly consolidated infilling of the conduit (I) (Fig. 6g). Eastward to NMVF, a single chimney ca. 20 cm in diameter and 30 cm long was recovered. Two subsamples of internal (I) and one of external (E) areas were analysed (Fig. 6h). Two cylindrical concretions collected at Stirone River (STN1B and STN2) are ca. 50 cm in diameter and 1 m long, contain abundant detrital fraction cemented by authigenic carbonate. The concretions are identified as chimneys where the central conduit is filled with carbonate cement and sediment arranged in a rose-like morphology. Both chimneys were subsampled in the external (E), middle (M) and internal (I) areas (Fig. 6j). The authigenic carbonate formation can be related to deep fluids generated by the Northern Apennines petroleum system. This can be stated from the reconstruction of geologic evolution and tectono-thermal history of the reservoirs (Capozzi and Picotti, 2010; Oppo et al., 2013). Therefore, gas samples collected in the four sites were used to understand the gas isotopic signature recorded in

carbonates. Three fluid samples have been collected in deep wells drilled in the Salsomaggiore anticline (Salsomaggiore 7 and 93, and Salsominore 16). Two samples represent fluids emitted by NMVF, one of which is related to a paroxysmal event. Methane gas has been also collected from Salvarola Terme wells, which were drilled in the same sedimentary succession occurring at Secchia authigenic carbonate field. One gas sample has been recovered from a small seepage occurring in the Enza riverbed stratigraphically at the top of the carbonate occurrences.

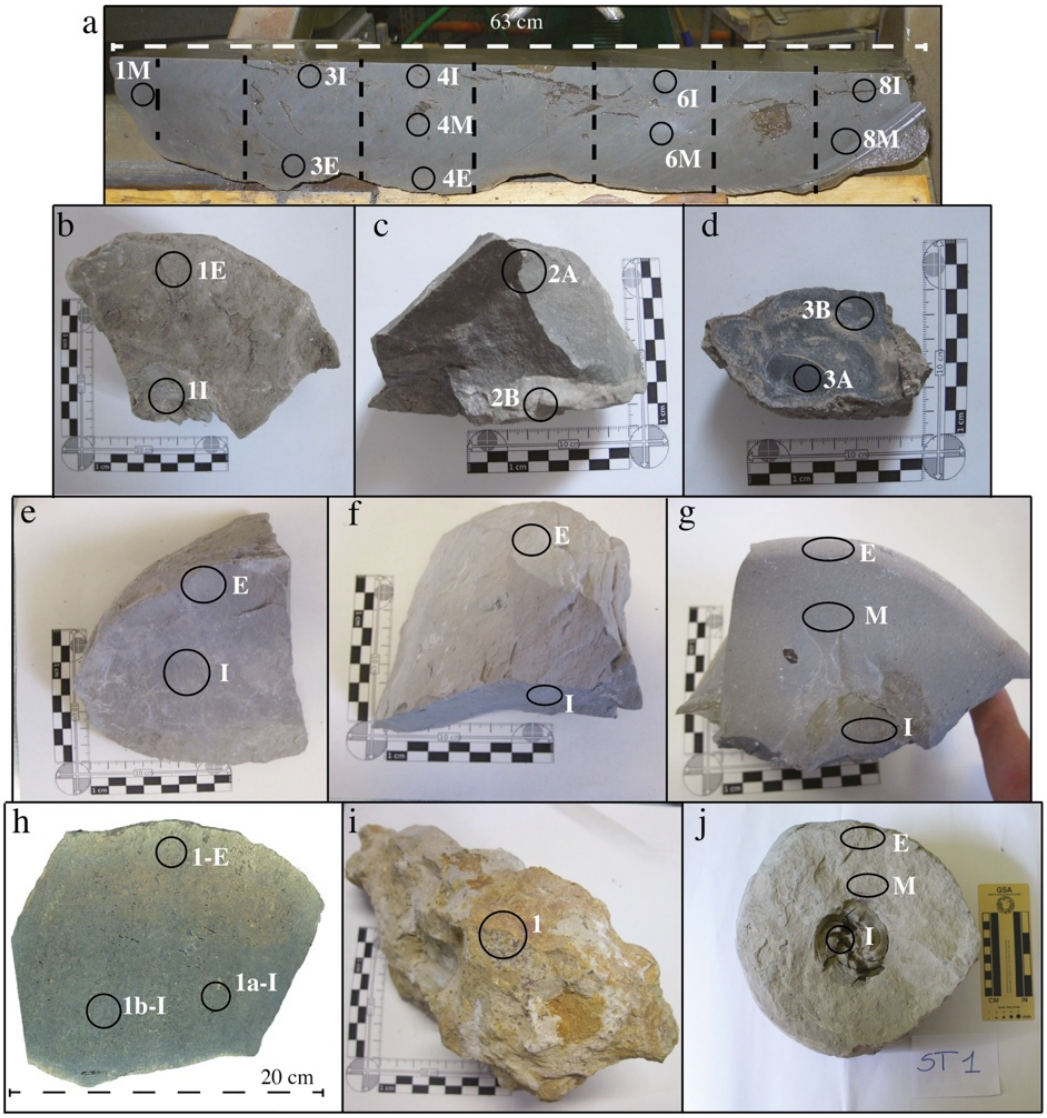

Fig. 6: *Carbonate samples representative of the concretions considered in this study. a) En5 chimney from Enza River, was divided in 8 sections bottom (1) to top (8); subsamples: external (E), middle (M) and internal (I); b) En10 chimney's top from Enza River, divided in external (1E) and internal (1I) portions; c) The Cr2 slab from Enza river divided in two subsamples according to colour variation: grey (2A) and light-grey (2B); d) Cr3 concretion from Enza River divided in two subsamples according to colour variation: dark-grey (3A) and light-grey matrix (3B); e-f) Two globular concretions at Secchia River, SCH3 (e) and SCH5 (f). Each sample was divided in external (E) and internal (I) areas; g) SCH6 chimney from Secchia River, three subsamples from external (E), internal(I) and middle(M) portions were analysed; h) Nirano chimney was divided in three subsamples: two internal (1a-I and 1b-I) and one external (1-E); i) Enza Hill sample; j) STN1 chimney from Stirone River. The three analysed subsamples belong to external (E), internal (I) and middle (M) portions.*

3.2 Methods

Subsamples of carbonate concretions were collected by micro-drilling, and homogenized in agate mortar for analysis of mineralogy. X-ray diffractometry (XRD) was performed using a Philips PW 1130 (Cu Ka radiation Ni filtered) in the Laboratory of BiGeA Department, University of Bologna. Powders were pressed into alumina holders in order to avoid preferential orientation of sheet-silicates. Estimates of the relative minerals abundance were determined using MacDiff software packages and carbonate mineral composition according to Goldsmith and Graf (1958) and Lumsden (1979). Carbon and oxygen isotopic analyses of carbonates were performed at CNR-Institute for Geosciences and Georesources (CNR-IGG) of Pisa (Enza carbonate samples), and at the Swiss Federal Institute of Technology in Zurich (ETHz) (Enza hills, Stirone and Secchia rivers, and Nirano samples). At CRN-IGG, powdered sub-samples (100 and 200 μg) were treated for 10 min at 90°C with 100% phosphoric acid on an automated carbonate device connected to a VG-PRISM mass spectrometer calibrated with NBS18, NBS19 and NBS20 standards. The results are reported in conventional δ‰ notation with reference to VPDB (Vienna Pee-Dee Belemnite). For samples with more than 20% of dolomite, $\delta^{18}O$ values were calculated with the Rosenbaum and Sheppard fractionation factor (Rosenbaum and Sheppard, 1986). Analytical reproducibility of the method, based on repeated analysis of standards, is better than ±0.1‰ for both carbon and oxygen (Rosenbaum, 1994; Rosenbaum and Sheppard, 1986). At ETHz, $\delta^{13}C$ and $\delta^{18}O$ values of carbonates were measured using Thermo Fisher DELTA Plus XP Gas Bench mass spectrometer. Between 90 and 140μg of powder were inserted in flasks then sealed and flushed by 99.99% helium gas. After the atmospheric air was swept out, 100% phosphoric acid was injected to react with the samples. Released CO_2 was purified and analysed. $\delta^{13}C$ and $\delta^{18}O$ values reported relative to the Vienna Pee-Dee Belemnite (VPDB) were corrected using IsolabB and MS1 standards, resulting in a precision of ±0.1‰. The gas from present-day seeping fluids and drilled wells was analysed to determine hydrocarbon composition and carbon isotopes of methane, ethane and CO_2 at ENI laboratories and at CNR- Institute for Geosciences and Georesources in Pisa, Italy.

4 Results

4.1 Hydrocarbon geochemistry

Analyses of gas from the sampled areas indicate that it is mainly composed of methane (up to 99.86%, Salvarola Terme), with only Nirano paroxysmal sample showing a lower concentration due to an increase in CO_2 content. Ethane was detected in all samples, and shows clear abundances dissimilarity in the four areas: Salsomaggiore and Salsominore wells content is 0.577 % to 1.392%,

Salvarola Terme 0.123% to 0.241%, Nirano 0.041% to 0.065%. The total content of higher hydrocarbon fractions is less than 2% (Tab. 1). Carbon dioxide occurs in measurable amount only in 4 samples and varies between 0.14% (Salsomaggiore 93) and 1.7% (Nirano Parox).

***Tab. 1**: Chemical and isotopic composition of sampled gases.*

	Type	CH_4	C_2H_6	ΣC_2+	CO_2	$\delta\ ^{13}C_1$	$\delta\ ^{13}C_2$	$\delta\ ^{13}C\ CO_2$
		%	%	%	%	‰ VPDB	‰ VPDB	‰ VPDB
Salsomaggiore 7	Well	96.94	1.392	1.920	-	-51.87	-27.56	7.98
Salsomaggiore 93	Well	96.90	1.220	1.450	0.14	-42.99	-25.70	-20.91
Salsominore 16	Well	97.44	0.577	0.630	0.33	-44.87	-21.10	-0.73
Nirano	MV	98.00	0.065	0.068	0.65	-46.87	bdl	19.90
Nirano Parox	MV	70.10	0.041	0.044	1.70	-48.44	-22.99	12.36
Salvarola Terme	Well	99.76	0.241	0.241	bdl	-47.60	-23.75	4.64
	Well	99.86	0.123	0.135	bdl	-47.50	-25.28	5.37
	Well	99.78	0.220	0.220	bdl	-46.89	-28.23	4.43

bdl: below detection level; - not determined; MV Mud Volcano

$\delta^{13}C$ of methane varies in the different sites and is comprised between -51.9‰ (Salsomaggiore 7) and -43.0‰ (Salsomaggiore 93). The gas sample collected along the Enza riverbed has significant lower $\delta^{13}C$ value (-72‰), which differentiates from all other areas. The carbon isotopic composition of CO_2 is generally enriched in ^{13}C, with the most positive $\delta^{13}C$ registered at Nirano (+19.9‰), and lowest value in Salsomaggiore 93 (-20.9‰).

4.2 Mineralogy and stable isotopes of authigenic carbonates

Authigenic carbonates from the sampling sites show similar mineralogy and petrography (Table 2; Fig. 7). Total carbonate fraction in bulk samples varies between 42 wt% and 81 wt%. Exception is the sandy concretion from Enza Hills that shows lower carbonate amounts, up to 37 wt%, due to elevated content of siliciclastic fraction. Carbonates are mainly composed of dolomite (up to 81wt%, En10 2A) (Table 2). Calcite is absent in concretions from Stirone and Secchia rivers, whereas it occurs in variable amount in Enza and Nirano. Viola et al. (2015) observed the preferential occurrence of calcite in external areas of chimneys along the Enza River, as in En5 4E

and En5 3E samples from this study. The detrital fraction includes mainly quartz and feldspars, with minor amounts of clays, micas, gypsum and oxides. Worth to note is the strong enrichment in sulphur (32,000 ppm) of Cr3B (Enza River), which accordingly shows high content of pyrite and arsenopyrite (5wt%). The carbon isotopic compositions of carbonates display a high degree of variation among the different areas (Fig. 9). The Enza Hills sample has the lowest $\delta^{13}C$ value (-53.0‰). The Enza River concretions have negative $\delta^{13}C$ values, with a large scattering comprised between -40.1‰ (Cr3A-2) and -8.2‰ (En5 4C) (Tab. 2). Internal subsamples of Enza chimneys have generally more negative $\delta^{13}C$ than middle and external subsamples.

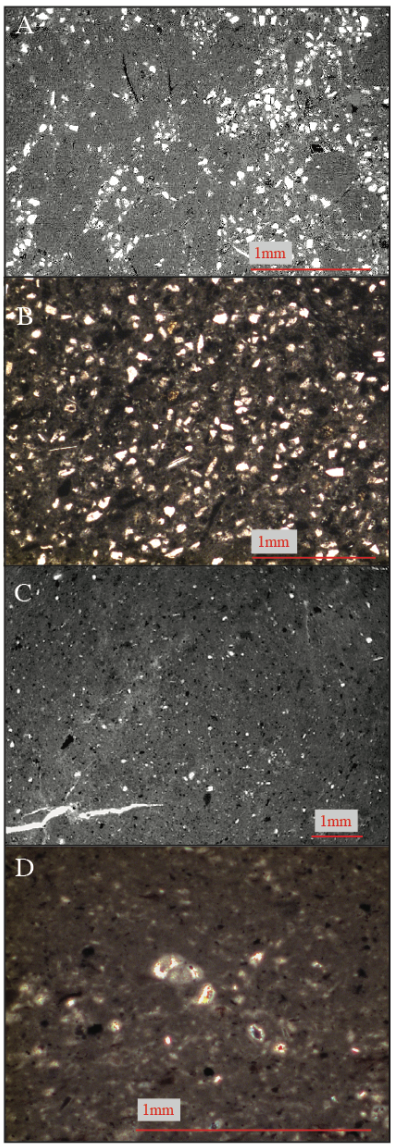

Fig. 7: *Photomicrographs of authigenic carbonates thin sections. A) Enza River: chimney concretion EN5 is formed by detrital grains, mainly quartz, within microcristalline dolomite cement and peloidal fabric (modified after Viola et al., 2015). B) Enza Hill concretion (image in crossed nicols): the sample shows elevated contents of siliciclastics sand-sized clasts and dense microcrystalline cement (sometimes clotted micrite). C) Stirone River: central part of chimney wall. Sparse siliciclastic grains cemented by micritic carbonate (modified after Cau et al., 2015). D) Secchia River: dense, clotted cement, sulphides (black spots), and sparse fine siliciclastic grains.*

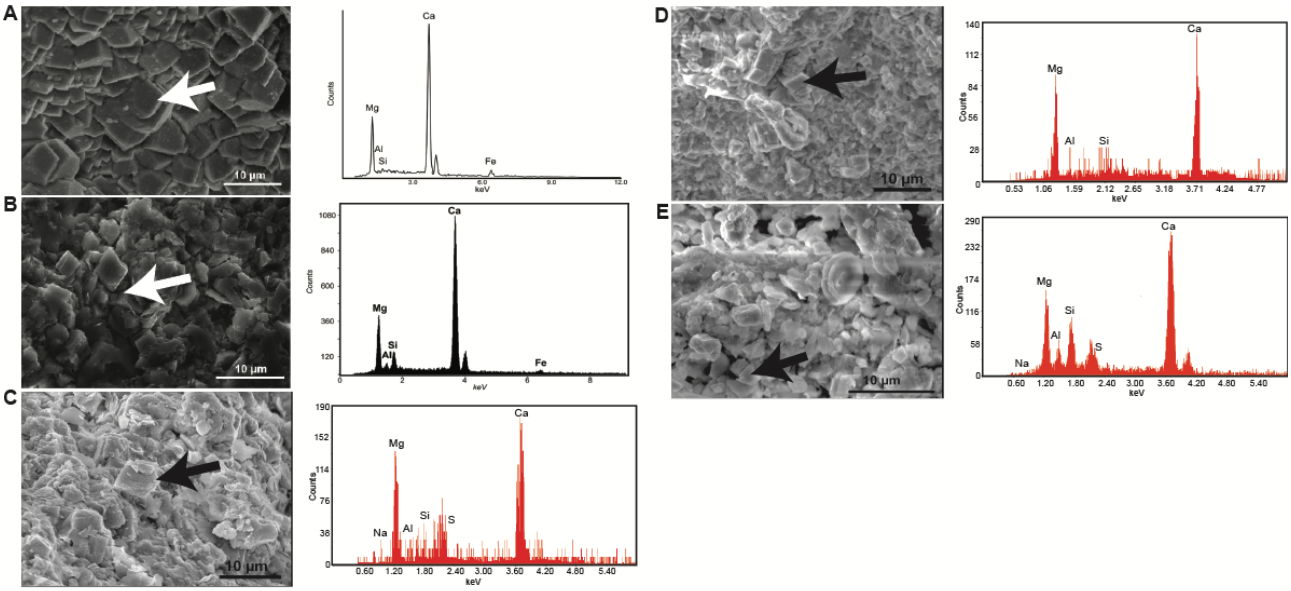

***Fig. 8**: Scanning Electron Microscope (SEM) photomicrographs and relative EDX spectrum of analysed carbonate cements. The spectrum was obtained at 15keV accelerating voltage. Arrows indicate areas and carbonate crystals selected for EDX analysis. A) Rhombohedral dolomite crystals forming microcrystalline cement in Enza River carbonates (images after Viola et al., 2015). B) Stirone River SEM photomicrograph of microcrystalline dolomite (image after Cau et al., 2015). C) Carbonate cement in Secchia River samples formed by dolomite crystals. D) Enza Hill dolomite cementing detrital rounded grains. E) Nirano SEM photomicrograph of dolomite with relative EDX spectrum. A calcitic coccolith is also visible.*

Stirone and Secchia chimneys have moderately negative $\delta^{13}C$. between -12.3‰ (SCH6 E) and -5.6‰ (STN1B M). In SCH6 chimney, $\delta^{13}C$ progressively increases from internal to external areas.

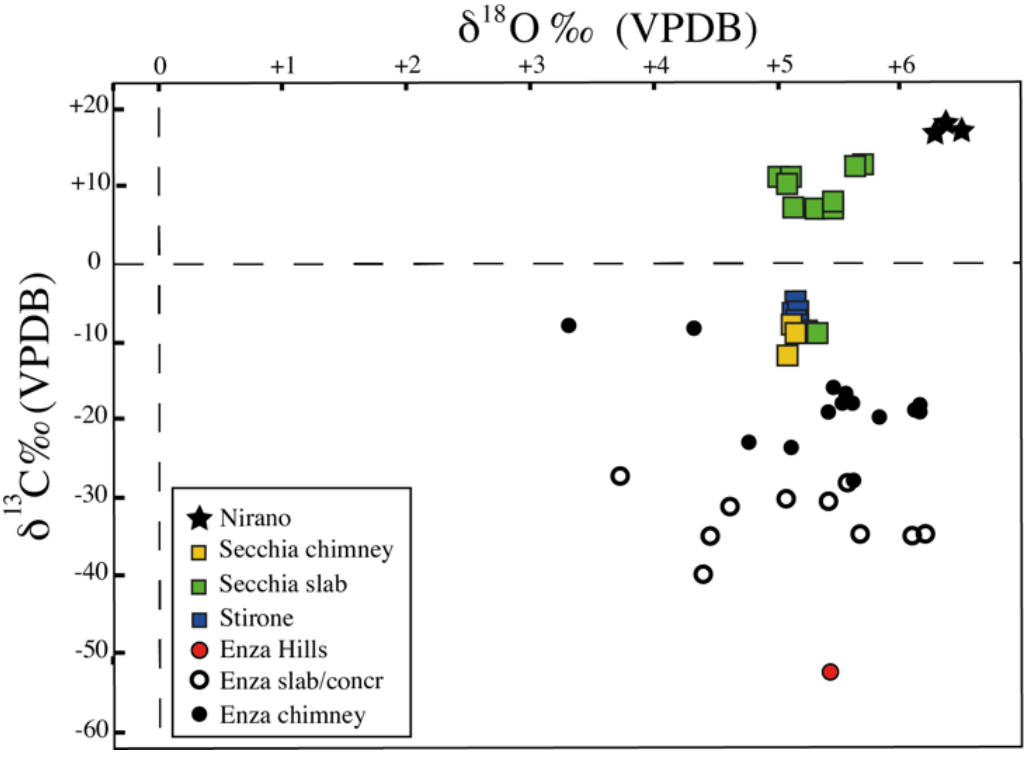

***Fig. 9**: $\delta^{13}C$ vs. $\delta^{18}O$ diagram for authigenic carbonate concretions considered in this study.*

Slab-like concretions of Secchia River have positive $\delta^{13}C$, from +6.4‰ (SCH2 E) to +11.9‰ (SCH5 M), and a general increase of $\delta^{13}C$ values is observed from the base (SCH1) to the top (SCH5) of the section. Carbonate from Nirano chimney has the highest $\delta^{13}C$ value (up to +17.7‰) among all the considered samples.

Differently from the carbon stable isotopes, the $\delta^{18}O$ values of in carbonates show a moderate variability. comprised between +3.4‰ (En5 4E) and +6.5 (NIR1a I) (Tab. 2). The Enza chimneys and the SCH6 chimney generally show higher $\delta^{18}O$ values in their inner parts.

***Tab. 2**: Mineralogy and stable isotopes in the analysed authigenic carbonates.*

		Type	Calcite	Dolomite	Others	$\delta^{13}C$	$\delta^{18}O$
			%wt	%wt	%wt	V-PDB	V-PDB
STIRONE	STN1B E	Chimney	0.0	54.9	48.1	-6.9	5.2
	STN1B I	Chimney	0.0	48.5	51.5	-6.5	5.2
	STN1B M	Chimney	0.0	51.2	48.8	-5.6	5.2
	STN2 E	Chimney	0.0	51.5	48.5	-8.0	5.2
	STN2 I	Chimney	0.0	53.3	46.7	-8.2	5.2
	STN2 M	Chimney	0.0	52.4	47.6	-9.1	5.3
ENZA	En10 1 I	Chimney	0.0	75.7	24.3	-28.3	5.7
	En10 1 E	Chimney	2.0	75.0	23.0	-23.4	4.8
	En10 2 I	Chimney	0.0	81.2	18.8	-24.1	5.2
	En5 8 I	Chimney	0.0	64.5	35.5	-20.1	5.9
	En5 8 M	Chimney	5.9	57.2	36.9	-19.5	5.5
	En5 6 I	Chimney	4.8	57.8	37.5	-19.3	6.2
	En5 6 M	Chimney	0.9	65.4	33.7	-19.0	6.1
	En5 4 I	Chimney	0.0	77.8	22.2	-18.4	5.6
	En5 4 M	Chimney	0.0	71.1	28.9	-18.4	5.6
	En5 4 E	Chimney	13.2	46.3	40.5	-8.2	3.4
	En5 3 I	Chimney	0.0	80.0	20.0	-18.6	6.2
	En5 3 E	Chimney	10.9	50.4	38.7	-8.6	4.4
	En5 1 M	Chimney	0.0	71.1	28.9	-17.1	5.6
	Cr2A	Slab	0.0	79.7	20.3	-28.5	5.6
	Cr2B	Slab	3.7	71.3	25.0	-27.7	3.8
	Cr3A-1	Concretion	0.0	64.9	35.1	-35.4	4.5
	Cr3A-2	Concretion	0.0	52.0	48.0	-40.1	4.4
	Cr3A -3	Concretion	0.0	42.0	58.0	-31.8	4.6
	Cr3B-1	Concretion	11.4	52.0	36.7	-35.1	5.7

	Cr3B-2	Concretion	-	-	-	-35.4	6.1
	Cr3B-4	Concretion	-	-	-	-30.9	5.4
ENZA HILLS	ENCO1	Concretion	1.0	36.0	63.0	-53.0	5.5
SECCHIA	SCH1 E	Slab	0.0	51.5	48.5	6.9	5.5
	SCH1 I	Slab	0.0	69.8	30.2	-9.4	5.4
	SCH2 E	Slab	0.0	51.9	48.1	6.4	5.3
	SCH2 I	Slab	0.0	51.3	48.7	7.5	5.5
	SCH3 E	Slab	0.0	46.8	53.0	6.5	5.2
	SCH3 I	Slab	0.0	55.7	44.0	9.7	5.1
	SCH4 E	Slab	0.0	59.1	40.9	10.6	5.1
	SCH4 I	Slab	0.0	47.5	52.5	10.7	5.1
	SCH5 E	Slab	0.0	50.1	49.9	11.9	5.7
	SCH5 I	Slab	0.0	57.1	42.9	11.8	5.7
	SCH6 E	Chimney	0.0	59.4	40.6	-12.3	5.1
	SCH6 M	Chimney	0.0	61.8	38.2	-9.3	5.2
	SCH6 I	Chimney	0.0	63.1	36.9	-8.3	5.2
NIRANO	NIR1-E	Chimney	4.0	41.0	55.0	17.7	6.4
	NIR1a-I	Chimney	4.0	41.0	55.0	16.7	6.5
	NIR1b-I	Chimney	4.0	41.0	55.0	16.6	6.3

5 Discussion

5.1 Methane generation and petroleum system

To better define origin and characteristics of concretions is crucial to reconstruct methane origin and its migration pathways towards the seafloor. In Salsomaggiore, NMVF and Salvarola Terme, the analysis of C_1 to C_3 gas fraction shows its thermogenic origin by oil cracking at temperatures exceeding 150°C (Oppo et al., 2013). The exact source rock responsible for generating of these thermogenic hydrocarbons is still unknown, but it is likely located in Upper Mesozoic successions involved in the Northern Apennine fold-and-thrust belt (Oppo et al., 2013). Carbon isotopic compositions of methane vs. ethane indicate that the gases are mixtures of thermogenic and biogenic methane contained in reservoirs into the deformed Miocene foredeep sequences (Fig. 10). Generation of primary biogenic methane could not account for significant contributions to the total gas budget in the Miocene reservoirs (Oppo et al, 2013). However, generation of secondary biogenic gas could be related to biodegradation of liquid hydrocarbons. Anaerobic microbial activity, responsible for altering the hydrocarbon geochemistry, was ascertained in connate waters

from both deep wells and mud volcanoes (Heller et al., 2011; Oppo et al., 2013, Kokoschka et al., 2015).

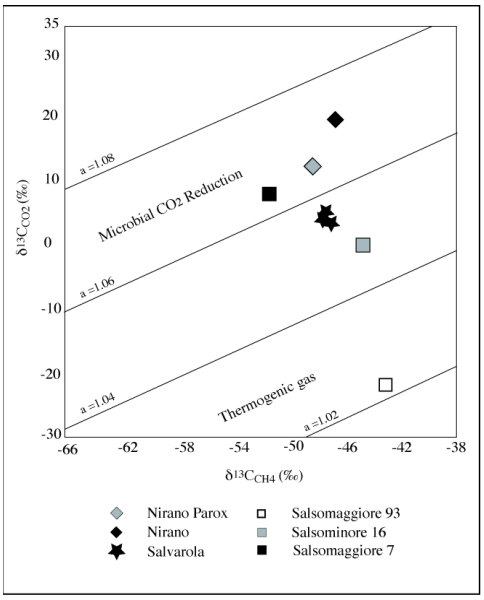

***Fig. 10**: Characterization of hydrocarbon gases by means of $\delta^{13}C$ in C_1 and C_2 fractions (Modified from Schoell, 1983). The diagram shows that mixing between biogenic and thermogenic components forms all considered gas samples. M, mixing of thermogenic and biogenic gas; T, thermogenic gas; TT, non-associated deep dry gases from humic (h) and marine (m) sources.*

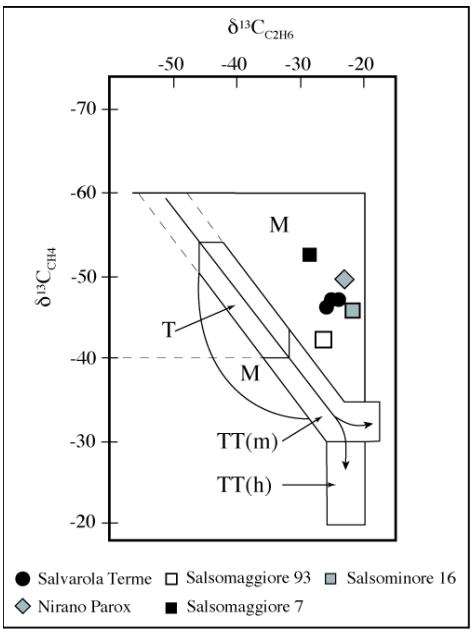

***Fig. 11**: Plot of $\delta^{13}C$ in CO_2 vs. $\delta^{13}C$ in CH_4. Lines and values represent constant isotope fractionation. The samples show different contributions of secondary biogenic methane to the total gas budget, except Salsomaggiore 93 where this process is thought to be inactive during sampling.*

This secondary methanogenesis follows the CO_2 reduction pathway and produces ^{3}C-rich CO_2 NMVF, Salvarola Terme and Salsomaggiore 7 (Tab. 1, Fig. 11). Differently, Salsomaggiore 93 and Salsominore 16 have negative $\delta^{13}C$ values in CO_2 that can be linked to a present-day very low

microbial degradation activity; however, the data suggest that a secondary biogenic methane component cannot be completely ruled out.

Biodegradation can be considered variable in time and space, even within a single area (Etiope et al. 2009). Therefore, $\delta^{13}C$ values likely indicate that generation of secondary biogenic methane was not relevant during the sampling, but could be active in other periods. This conclusion is supported by the calculated thermogenic methane end member ($\delta^{13}C$ -39.3‰ V-PDB), which indicates that the measured $\delta^{13}C$ values of methane are due to mixing with biogenic methane; this latter accounts for up to 41.5% of the total gas budget in the Northern-Apennines sites (Oppo et al., 2013).

The hydrocarbons contained in the Miocene reservoirs along the foothills migrate since Miocene (e.g. Barbieri and Cavalazzi, 2005; Conti et al., 2007; Capozzi and Picotti, 2010; Oppo et al., 2013) and still feed the present-day cold seeps. Diffusion of methane towards the seafloor within Plio-Pleistocene sediments at sites resulted in formation of authigenic carbonate fields.

On the other hand, methane presently seeping along the Enza riverbed has a clear biogenic signature ($\delta^{13}C$= -72‰ V-PDB), suggesting that thermogenic-generated hydrocarbons might be absent within the Pleistocene sediments of this section. This biogenic methane generated both from sapropel-bearing successions, such as the Piacenzian sapropel cluster observed in the Stirone River (Cau et al., 2015), and from the thick Pliocene turbidites buried under the Po plain (Mattavelli et al., 1993; Fantoni and Franciosi, 2010). This biogenic gas reached the Enza site migrating towards the forelimb of Quattro Castella Anticline along up-dip carrier beds (Oppo et al., 2015) (Fig. 4).

5.2 Isotopic signature of authigenic carbonates

Authigenic carbonates generally show substantial ^{13}C depletion, which indicates that the main dissolved inorganic carbon (DIC) source is methane oxidised during AOM. Possible contributions of other DIC sources, such as oxidation of organic matter and residual CO_2 from methanogenesis, could also occur (Formolo et al., 2004). Despite the relative homogeneity of $\delta^{13}C$ in gases of the Northern Apennines and the mineral similarity of all authigenic carbonates, $\delta^{13}C$ in these carbonates shows important variations among the different areas. This observation strongly suggests that carbon fractionation is linked to further DIC sources in addition to methane gas.

The definition of petroleum system and fluids migration pathways at Stirone, Secchia and NMVF rules out significant contributions of biogenic methane during the formation of authigenic carbonates in these sites. Therefore, thermogenic methane migrating from Miocene reservoirs can be identified as the gas source associated with these authigenic carbonates. A further DIC source can be related to the occurrence of ^{13}C-rich CO_2 during carbonate precipitation, which is consistent

with the important input of secondary methane production in the total gas budget still observed in Northern Apennines. Examples of $\delta^{13}C$ higher than +5‰ are reported in various fossil authigenic carbonates, indicating methane generation during carbonate precipitation (e.g., Peckmann and Thiel, 2004; Naehr et al., 2007; Gieskes et al., 2005; Loyd et al., 2016). This contribution can be observed in the positive $\delta^{13}C$ of NMVF chimney, which points towards the presence of ^{13}C-rich DIC in ambient fluids, as well occurs in the nearby Secchia River globular concretions. Moderately negative $\delta^{13}C$ in the Stirone River samples evidences that migrating thermogenic methane could represent the main source of DIC during carbonates precipitation; the likely occurring contribution from marine DIC and/or CO_2 from secondary biogenesis cannot be clearly recognized.

A different situation can be described for Enza River authigenic carbonates. Methane concentration in natural gas occurring into Pliocene foredeep successions of Northern Apennines reaches over 90%, and is characterized by average carbon and hydrogen isotopic compositions of $\delta^{13}C$= -75‰ V-PDB and δD= -171‰ V-SMOW (Oppo et al., 2013), indicating that it was generated via CO_2 reduction (Whiticar, 1999). The very low $\delta^{13}C$ values in Enza authigenic chimneys, if compared to those of the other areas, evidence the biogenic origin of methane responsible for their formation. Enza Hills has the lowest value, which might be linked to increased gas flux intensity and its diffusion within highly permeable sediments saturated by marine pore water near the seafloor. In this site, the main process leading to carbonate formation can be attributed to AOM (e.g. Oppo et al. 2015). The $\delta^{18}O$ value of a carbonate depends on both temperature and $\delta^{18}O$ value of pore water where the carbonate precipitates. Water forming methane hydrates is enriched by about 3‰ in ^{18}O relative to hydrate-unaffected pore water (e.g. Hesse and Harrison 1981; Ussler and Paull 1995; Greinert et al., 2001). As consequence, relatively high $\delta^{18}O$ value of authigenic carbonates in several occurrences have been ascribed to the dissolution of methane hydrates (e.g. Aloisi et al., 2000; Pierre and Rouchy, 2004; De la Pierre et al., 2010). However, this process cannot be considered active in the Plio-Pleistocene successions of the study area, as they were deposited at a depth that did never reach the gas hydrates stability zone, even during cold periods. $\delta^{18}O$ values of authigenic carbonates in this study (Tab. 2) are related to their dolomitic mineral phase; in fact, dolomite usually shows an increase of the heavy oxygen isotope of +2 - +4‰ with respect to initial water values (Budd, 1997). Oxygen stable isotopes can be useful to deduce information on palaeo temperature and water chemistry occurring during authigenic carbonate precipitation. A first attempt to estimate mineral precipitation temperature is assuming equilibrium crystallization for authigenic dolomite and marine bottom waters (Naehr et al., 2007).

Plio-Pleistocene bottom water temperature of the enclosed sea at the uplifting Apennine border is unknown. To overcome this problem, present-day bottom water sampled at 100m water depths in central Adriatic Sea can be used as analogue for the palaeo marine environment object of this study. The Adriatic Sea water analysed for this work has $\delta^{18}O$ 0.99‰ V-SMOW, associated to 13-14°C temperature measured by Lipizer et al. (2014) for bottom water during winter. The calculated temperatures listed in Tab. 3 are determined using the fractionation factor of Vasconcelos et al., (2005), and the resulted very low temperatures clearly attest isotopic disequilibrium. Connate waters $\delta^{18}O$ varies in the different sites (Tab. 3) and depends on diagenetic history of reservoirs and on migration processes (Capozzi and Picotti, 2010). They can be considered as the sole source of oxygen in the system to obtain a further estimation of palaeo temperature and to evaluate their possible contribution during carbonates precipitation (Tab. 3). To assess this relation, the $\delta^{18}O$ fractionation factor for dolomite precipitated under the seafloor was calculated, using the equations reported in Vaconcelos et al. (2005) and Zheng (1999), which are applicable for different temperature ranges. The connate waters in the area of NMVF and Salvarola belong to the same Late Miocene reservoir and the analysis carried out shows that their $\delta^{18}O$ varies from 4.62‰ and 5.16‰ (V-SMOW). The obtained higher paleo temperatures could provide a preliminary indication that the final oxygen signature in the carbonates derives from the mixing with connate waters migrating from depth, and thus characterised by higher temperature. The very positive $\delta^{18}O$ end-member of the connate waters is documented at Salsomaggiore. This signature (+9.5 and +13.45‰ V-SMOW) depends on the diagenetic process, as the original marine pore water was gradually mixed with water derived by progressive clay dehydration during recrystallization of smectite to illite during burial (Oppo et al., 2013). The calculated paleo temperatures for carbonate precipitation are very high, from 46° to 69°C, and are unrealistic as the carbonates could not be precipitated at depths of ca. 2km below the surface. Therefore, a contribution of deep waters on the observed $\delta^{18}O$ values in the chimneys of Stirone River can be inferred. The results of further detailed investigations on this last aspect using strontium and clumped isotope signatures will be presented in the dedicated Viola et al. (i*n prep*) paper.

Tab. 3*: Calculated pore water temperatures occurring during authigenic carbonates precipitation.*

Pleistocene							
Carbonate			**Adriatic Sea 0.99‰**		**Connate water**		
Area	Sample	$\delta^{18}O$ (V-PDB)	$\alpha_{\text{dolomite-water (1)}}$	T (°C)	$\delta^{18}O$ (V-SMOW)	$\alpha_{\text{dolomite-water (1)}}$	T (°C)

Enza River	En10 1 I	5.65	35.75	4	0.65‰	36.09	9
	En10 1 E	4.81	34.88	7	Po Plain Pleistocene	35.22	12
	En10 2 I	5.16	35.23	6		35.58	10
	En5 8 I	5.86	35.96	3		36.30	8
	En5 8 M	5.47	35.56	4		35.90	9
	En5 6 I	6.20	36.31	1		36.65	7
	En5 6 M	6.13	36.24	1		36.58	7
	En5 4 I	5.56	35.65	4		35.99	9
	En5 4 M	5.62	35.72	3		36.06	9
	En5 4 E	3.35	33.38	13		33.72	17
	En5 3 I	6.21	36.32	1		36.66	7
	En5 3 E	4.37	34.43	9		34.77	13
	En5 1 M	5.59	35.68	4		36.02	9
	Cr2A	5.63	35.72	3		36.06	9
	Cr2B	3.77	33.81	11		34.15	16
	Cr3A-1	4.49	34.55	8		34.89	13
	Cr3A-2	4.44	34.50	9		34.84	13
	Cr3A -3	4.65	34.71	8		35.05	12
	Cr3B-1	5.69	35.78	3		36.13	9
	Cr3B-2	6.13	36.24	1		36.58	7
	Cr3B-4	5.44	35.53	4		35.87	7
Enza Hill	ENCO1	5.47	35.56	4	0.65‰	35.90	3
Secchia River	SCH1E	5.49	35.59	4	5.16‰	31.41	22
	SCH1I	5.36	35.45	5	Salvarola terme	31.28	23
	SCH2E	5.34	35.44	5		31.26	23
	SCH2I	5.50	35.60	4		31.42	22
	SCH3E	5.18	35.27	5		31.09	24
	SCH3I	5.12	35.20	6		31.03	24
	SCH4E	5.06	35.14	6		30.97	24
	SCH4I	5.15	35.24	6		31.06	24
	SCH5E	5.73	35.84	3		31.66	21
	SCH5I	5.66	35.77	3		31.59	21
	SCH6E	5.12	35.21	6		31.03	24
	SCH6M	5.20	35.29	5		31.11	24

	SCH6I	5.18	35.28	5		31.10	24
Nirano MVF	NIR1-E	6.41	36.53	4	4.62‰	32.90	15
	NIR1a-I	6.54	36.66	4	Nirano MVF	33.03	15
	NIR1b-I	6.32	36.44	5		32.81	16

Pliocene

Carbonate			**Adriatic Sea 0.99‰**		**Connate water**		
Area	Sample	$\delta^{18}O$ (V-PDB) ‰	α dolomite-water (1)	T (°C)	$\delta^{18}O$ (V-SMOW)	α dolomite-water (2)	T (°C)
Stirone River	STN1BI	5.17	35.25	6	9.5‰ Salsomaggiore (well 93)	26.77	46
	STN1BE	5.20	35.28	5		26.74	47
	STN1BM	5.18	35.26	6		26.75	46
	STN2I	5.19	35.27	6		26.76	46
	STN2E	5.19	35.27	6		26.76	46
	STN2M	5.27	35.36	5		26.85	46
Stirone River	STN1BI				13.45‰ Salsominore	22.83	68
	STN1BE					22.79	69
	STN1BM					22.81	68
	STN2I					22.81	68
	STN2E					22.82	68
	STN2M					22.90	68

(1) Vasconcelos et al., 2005; (2) Zheng ,1999

The Pleistocene age Enza site shows higher scatter of calculated temperatures respect to the other areas, which can be related to the location of depositional environment close to coast and influenced by important freshwater inputs and, thus, varying salinity. When considering the $\delta^{18}O$ measured in connate waters sampled in Plio-Pleistocene reservoirs (0.65‰), the resulting temperatures are higher and more realistic.

6 Conclusions

Geological and geochemical analyses showed that authigenic carbonates in Stirone, Secchia and NMVF outcrops were generated thanks to methane and CO_2 migrating from Northern Apennines Miocene reservoirs. The gas contained in these reservoirs is mainly a mix of biogenic and thermogenic methane, with minor condensates and oil. Thermogenic methane was generated both within the oil window and by thermal cracking of oils. The biogenic methane component was mostly formed by biodegradation of oils. Secondary biogenic methane concentrations up to 41.5% of the total gas budget indicate that microbial degradation is an important process in reservoirs of this region.

The methane $\delta^{13}C$ in the reservoirs slightly varies around the average value of -46‰ V-PDB; otherwise, $\delta^{13}C$ of authigenic carbonates shows significant variations indicating contribution of different DIC sources during their precipitation. Moderately negative $\delta^{13}C$ in Stirone samples partly derives from AOM, while positive $\delta^{13}C$ in NMVF and Secchia carbonates points towards the contribution of ^{13}C-rich CO_2, linked to the generation of secondary biogenic methane. Wide variations of $\delta^{13}C$ in Secchia concretions also testify that authigenic carbonates provide a fossil record of changes in the biogeochemical processes active within the reservoirs.

A different situation can be described for authigenic carbonates formation in the Enza River area during the Pleistocene. The genesis of these concretions is linked to anaerobic oxidation of primary microbial methane that originated within the Pliocene sediments and migrated up-dip southwards from the sedimentary successions buried in the Po Plain. The observed decrease of $\delta^{13}C$ in progressively younger samples is possibly due to increased gas diffusion and flux to the seafloor, within more permeable sediments containing marine pore water. Intense gas migration led to increased efficiency of AOM process and fluids escape in the water column, and in turn to a more negative $\delta^{13}C$ record in authigenic carbonates.

Estimates of $\delta^{18}O$ in dolomite cements stress the presence of a temperature disequilibrium, which would indicate that marine bottom waters cannot be the sole oxygen source. Results from further studies on strontium and clumped isotope signature to better assess the mixing with connate waters migrating from the deep reservoirs will be presented in Viola et al. (*in prep.*).

The dataset presented in this work confirms that a direct correlation between authigenic carbonates and DIC sources might be difficult. The joint analysis of present-day seepages and fossil seepage-related carbonates can be considered a step forwards the better identification and definition of fluid sources influencing authigenic carbonate precipitation. Information on history of fluid migration in the Northern Apennines testifies that tertiary migration of hydrocarbon is a long-lasting

phenomenon in this region, in the scale of million years, which was first represented by submarine gas leakage and then by subaerial mud volcanism.

Acknowledgements

Funding was provided by the Italian PRIN 2009 Project (MIUR research grants to R. Capozzi). The authors wish to thank Joachim Reitner (Department of Geobiology, Centre for Geosciences, Georg-August-University of Göttingen, Germany), Stefano Bernasconi (Department of Earth Sciences, Geologisches Institut, ETH Zurich, CH) and Mario Mussi (CNR-Institute for Geosciences and Georesources, CNR-IGG, Pisa) for contributing in the stable isotopes analyses on MDACs.

References

Aloisi, G., Pierre, C., Rouchy, J.-M., Foucher, J.-P., Woodside, J., 2000. Methane-related authigenic carbonates of eastern Mediterranean Sea mud volcanoes and their possible relation to gas hydrate destabilisation. Earth Planet. Sci. Lett. 184, 321–338.

Balestrieri, M.L., Bernet, M., Brandon, M.T., Picotti, V., Reiners, P., Zattin, M., 2003. Pliocene and Pleistocene exhumation and uplift of two key areas of the Northern Apennines. Quat. Int. 101–102, 67–73.

Barbieri, R., Cavalazzi, B., 2005. Microbial fabrics from Neogene cold seep carbonates, Northern Apennine, Italy. Palaeogeogr. Palaeoclimatol. Palaeoecol. 227,143-155.

Bartolini, C., 2003. When did the Northern Apennine become a mountain chain? Quat. Int. 101–102, 75–80.

Blumenberg, M., Walliser, E.-O., Taviani, M., Seifert, R., Reitner, J., 2015. Authigenic carbonate formation and its impact on the biomarker inventory at hydrocarbon seeps – A case study from the Holocene Black Sea and the Plio-Pleistocene Northern Apennines (Italy). Mar. Pet. Geol. 66, 532–541.

Boetius, A., Ravenschlag, K., Schubert, C.J., Rickert, D., Widdel, F., Gieseke, A., Amann, R., Jùrgensen, B.B., Witte, U., Pfannkuche, O., 2000. A marine microbial consortium apparently mediating anaerobic oxidation of methane 407, 623–626.

Capozzi, R., Dinelli, E., Negri, A., Picotti, V., 2006. Productivity-generated annual laminae in mid-Pliocene sapropels deposited during precessionally forced periods of warmer Mediterranean climate. Palaeogeogr. Palaeoclimatol. Palaeoecol. 235, 208–222.

Capozzi, R., Picotti, V., 2010. Spontaneous fluid emissions in the Northern Apennines: geochemistry, structures and implications for the petroleum system. Geol. Soc. London, Spec. Publ. 348, 115–135.

Cau, S., Franchi, F., Roveri, M., Taviani, M., 2015. The Pliocene-age Stirone River hydrocarbon chemoherm complex (Northern Apennines, Italy). Mar. Pet. Geol. 66, Part 3, 582–595.

Conti, S., Artoni, A., Piola, G., 2007. Seep-carbonates in a thrust-related anticline at the leading edge of an orogenic wedge: The case of the middle–late Miocene Salsomaggiore Ridge (Northern Apennines, Italy). Sediment. Geol. 199, 233–251.

Dela Pierre, F., Martire, L., Natalicchio, M., Clari, P., Petrea, C., 2010. Authigenic carbonates in upper miocene sediments of the tertiary piedmont basin (NW Italy): Vestiges of an ancient gas hydrate stability zone? Bull. Geol. Soc. Am. 122, 994–1010.

Díaz-del-Río, V., Somoza, L., Martínez-Frias, J., Mata, M.P., Delgado, a., Hernandez-Molina, F.J., Lunar, R., Martín-Rubí, J. a., Maestro, a., Fernández-Puga, M.C., León, R., Llave, E., Medialdea, T., Vázquez, J.T., 2003. Vast

fields of hydrocarbon-derived carbonate chimneys related to the accretionary wedge/olistostrome of the Gulf of Cádiz. Mar. Geol. 195, 177–200.

Etiope, G., Feyzullayev, A., Baciu, C.L., 2009. Terrestrial methane seeps and mud volcanoes: A global perspective of gas origin. Mar. Pet. Geol. 26, 333–344.

Fantoni, R., Franciosi, R., 2010. Tectono-sedimentary setting of the Po Plain and Adriatic foreland. Rend. Lincei 21, 197–209.

Formolo, M.J., Lyonsa T.W., Zhangb, C., Kelleya, C., Sassenc, R., Horitad, J., Coled, D.R., 2004. Quantifying carbon sources in the formation of authigenic carbonates at gas hydrate sites in the Gulf of Mexico. Chemical Geology 205, 253-264

Ghielmi, M., Minervini, M., Nini, C., Rogledi, S., Rossi, M., Vignolo, A., 2009. Sedimentary and Tectonic Evolution in the Eastern Po Plain and Northern Adriatic Sea Area from Messinian to Middle Pleistocene (Italy), in: Convegno Natura E Geodinamica Della Litosfera Nell'alto Adriatico. pp. 2–5.

Gieskes, J., Mahn, C., Day, S., Martin, J.B., Greinert, J., Rathburn, T., McAdoo, B., 2005. A study of the chemistry of pore fluids and authigenic carbonates in methane seep environments: Kodiak Trench, Hydrate Ridge, Monterey Bay, and Eel River Basin. Chem. Geol. 220, 329–345.

Goldsmith, J.R., Graf, D.L., 1958. Relation between lattice constants and composition of the Ca-Mg carbonates. Am. Mineral. 43, 84–101.

Greinert, J., Bohrmann, G., Suess, E., 2001. Gas hydrate-associated carbonates and methane-venting at Hydrate Ridge: classification, distribution and origin of authigenic lithologies. Geophys. Monogr. Am. Geophys. Union 124, 99–114.Gunderson, K.L., Pazzaglia, F.J., Picotti, V., Anastasio, D. a., Kodama, K.P., Rittenour, T., Frankel, K.F., Ponza, A., Berti, C., Negri, A., Sabbatini, A., 2014. Unraveling tectonic and climatic controls on synorogenic growth strata (Northern Apennines, Italy). Bull. Geol. Soc. Am. 126, 532–552.

Heller, C., Blumenberg, M., Kokoschka, S., Wrede, C., Hoppert, M., Taviani, M., Reitner, J., 2011. Geomicrobiology of Fluid Venting Structures at the Salse di Nirano Mud Volcano Area in the Northern Apennines (Italy), in: Advances in Stromatolite Geobiology SE - 14, Lecture Notes in Earth Sciences. Springer Berlin Heidelberg, pp. 209–220.

Hensen, C., Scholz, F., Nuzzo, M., Valadares, V., Gracia, E., Terrinha, P., Liebetrau, V., Kaul, N., Silva, S., Martinez-Loriente, S., Bartolome, R., Pinero, E., Magalhães, V.H., Schmidt, M., Weise, S.M., Cunha, M., Hilario, a., Perea, H., Rovelli, L., Lackschewitz, K., 2015. Strike-slip faults mediate the rise of crustal-derived fluids and mud volcanism in the deep sea. Geology 43, 1–4.

Hesse, R., Harrison, W.E., 1981. Gas hydrates (clathrates) causing pore-water freshening and oxygen isotope fractionation in deep-water sedimentary sections of terrigenous continental margins. Earth Planet. Sci. Lett. 55, 453–462.

Judd, A., Hovland, M., Dimitrov, L.I., Garcia Gil, S., Jukes, V., 2002. The geological methane budget at Continental Margins and its in uence on climate change. Geofluids 2, 109–126.

Judd, A.G., Hovland, M., 2007. Seabed Fluid Flow. Cambridge University Press, Cambridge.

Khélifi, N., Sarnthein, M., Frank, M., Andersen, N., Garbe-Schönberg, D., 2014. Late Pliocene variations of the Mediterranean outflow. Mar. Geol. 357, 182–194.

Kokoschka, S., Dreier, A., Romoth, K., Taviani, M., Schäfer, N., Reitner, J., Hoppert, M., 2015. Isolation of Anaerobic Bacteria from Terrestrial Mud Volcanoes (Salse di Nirano, Northern Apennines, Italy). Geomicrobiol. J. 32, 355–364.

Lipizer, M., Partescano, E., Rabitti, A., Giorgetti, A., Crise, A., 2014. Qualified temperature, salinity and dissolved oxygen climatologies in a changing Adriatic Sea. Oc. Sci. 10, 771–797.

Loyd, S.J., Sample, J., Tripati, R.E., Defliese, W.F., Brooks, K., Hovland, M., Torres, M., Marlow, J., Hancock, L.G., Martin, R., Lyons, T., Tripati, A.E., 2016. Methane seep carbonates yield clumped isotope signatures out of equilibrium with formation temperatures. Nat. Commun. 7:12274 doi: 10.1038/ncomms12274.

Lumsden, D., 1979. Discrepancy between thin-section and X-ray estimates of dolomite in limestone. J. Sediment. Res. 49, 429–436.

Magalhães, V.H., Pinheiro, L.M., Ivanov, M.K., Kozlova, E., Blinova, V., Kolganova, J., Vasconcelos, C., McKenzie, J.A., Bernasconi, S.M., Kopf, A.J., Díaz-del-Río, V., González, F.J., Somoza, L., 2012. Formation processes of methane-derived authigenic carbonates from the Gulf of Cadiz. Sediment. Geol. 243-244, 155–168.

Mattavelli, L., Pieri, M., Groppi, G., 1993. Petroleum exploration in Italy: a review. Mar. Pet. Geol. 10, 410–425.

Naehr, T.H., Eichhubl, P., Orphan, V.J., Hovland, M., Paull, C.K., Ussler III, W., Lorenson, T.D., Greene H.G., 2007. Authigenic carbonate formation at hydrocarbon seeps in continental margin sediments: A comparative study Deep-Sea Res., II, 54,1268–1291

Nyman, S.L., Nelson, C.S., 2011. The place of tubular concretions in hydrocarbon cold seep systems: Late Miocene Urenui Formation, Taranaki Basin, New Zealand. Am. Assoc. Pet. Geol. Bull. 95, 1495–1524.

Oppo, D., Capozzi, R., Picotti, V., 2013. A new model of the petroleum system in the Northern Apennines, Italy. Mar. Pet. Geol. 48, 57–76.

Oppo, D., Capozzi, R., Picotti, V., Ponza, A., 2015. A genetic model of hydrocarbon-derived carbonate chimneys in shelfal fine-grained sediments: The Enza River field, Northern Apennines (Italy). Mar. Pet. Geol. 66, Part 3, 555–565.

Peckmann, J., Thiel, V., Michaelis, W., Clari, P., Gaillard, C., Martire, L., Reitner, J., 1999. Cold seep deposits of Beauvoisin (Oxfordian; southeastern France) and Marmorito (Miocene; northern Italy): Microbially induced authigenic carbonates. Int. J. Earth Sci. 88, 60–75.

Peckmann, J., Reimer, a., Luth, U., Luth, C., Hansen, B.T., Heinicke, C., Hoefs, J., Reitner, J., 2001. Methane-derived carbonates and authigenic pyrite from the northwestern Black Sea. Mar. Geol. 177, 129–150.

Peckmann, J., Thiel, V., 2004. Carbon cycling at ancient methane–seeps. Chem. Geol. 205, 443–467.

Picotti, V., Pazzaglia, F.J., 2008. A new active tectonic model for the construction of the Northern Apennines mountain front near Bologna (Italy). J. Geophys. Res. Solid Earth 113, 1–24.

Picotti, V., Ponza, A., Pazzaglia, F.J., 2009. Topographic expression of active faults in the foothills of the Northern Apennines. Tectonophysics 474, 285–294.

Pierre, C., Blanc-Valleron, M.M., Caquineau, S., März, C., Ravelo, a. C., Takahashi, K., Alvarez Zarikian, C., 2014. Mineralogical, geochemical and isotopic characterization of authigenic carbonates from the methane-bearing sediments of the Bering Sea continental margin (IODP Expedition 323, Sites U1343-U1345). Deep. Res. Part II Top. Stud. Oceanogr. 1–12.

Pierre, C., Rouchy, J.-M., 2004. Isotopic compositions of diagenetic dolomites in the Tortonian marls of the western Mediterranean margins: evidence of past gas hydrate formation and dissociation. Chem. Geol. 205, 469–484.

Reitner, J., Blumenberg, M., Walliser, E.-O., Schäfer, N., Duda, J.-P., 2015. Methane-derived carbonate conduits from the late Aptian of Salinac (Marne Bleues, Vocontian Basin, France): Petrology and biosignatures. Mar. Pet. Geol. 1–12.

Reitner, J., Peckmann, J., Reimer, A., Schumann, G., Thiel, V., 2005. Methane-derived carbonate build-ups and associated microbial communities at cold seeps on the lower Crimean shelf (Black Sea). Facies 51, 66–79.

Ricci Lucchi, F., Vai, G.B., 1994. A stratigraphic and tectonofacies framework of the “calcari aLucina” in the Apennine Chain, Italy. Geo-Marine Lett. 14, 210–218.

Rosenbaum, J., Sheppard, S.M.., 1986. An isotopic study of siderites, dolomites and ankerites at high temperatures. Geochim. Cosmochim. Acta 50, 1147–1150.

Rosenbaum, J.M., 1994. Stable-Isotope Fractionation between Carbon-Dioxide and Calcite at 900-Degrees-C. Geochim. Cosmochim. Acta 58, 3747–3753.

Schoell, M., 1983. Genetic Characterization of Natural Gases. Am. Assoc. Pet. Geol. Bull. 67, 2225–2238.

Smith, J.P., Coffin, R.B., 2014. Methane Flux and Authigenic Carbonate in Shallow Sediments Overlying Methane Hydrate Bearing Strata in Alaminos Canyon, Gulf of Mexico. Energies 7, 6118–6141.

Taviani, M., 2001. Fluid venting and associated processes, in: Vai, G., Martini, I.P. (Eds.), Anatomy of an Orogen: The Apennines and Adjacent Mediterranean Basins SE - 20. Springer Netherlands, pp. 351–366.

Terzi, C., Lucchi, F., Vai, G., Aharon, P., 1994. Petrography and stable isotope aspects of cold-vent activity imprinted on Miocene-age "calcari aLucina" from Tuscan and Romagna Apennines, Italy. Geo-Marine Lett. 14, 177–184.

Ussler III, W., Paull, C.K., 1995. Effects of ion exclusion and isotopic fractionation on pore water geochemistry during gas hydrate formation and decomposition. Geo-Marine Lett. 15, 37–44.

Vasconcelos, C., McKenzie, J.A., Warthmann, R., Bernasconi, S.M., 2005. Calibration of the delta O-18 paleothermometer for dolomite precipitated in microbial cultures and natural environments. Geology 33, 317 - 320.

Viola, I., Capozzi, R., Bernasconi, S., Rickli, J., in preparation. Mineralogy, geochemistry and isotopic signatures of authigenic carbonates from new discovered Secchia River site, Northern Apennines (Italy).

Viola, I., Oppo, D., Franchi, F., Capozzi, R., Dinelli, E., Liverani, B., Taviani, M., 2015. Mineralogy, geochemistry and petrography of methane-derived authigenic carbonates from Enza River, Northern Apennines (Italy). Mar. Pet. Geol. 66, 566–581..2015.03.011

Whiticar, M.J., 1999. Carbon and hydrogen isotope systematics of bacterial formation and oxidation of methane. Chem. Geol. 161, 291–314.

Zachos, J.C., Pagani, M., Sloan, L., Thomas, E., Billups, K., 2001. Trends, rhythms, and aberrations in global climate 65 Ma to present. Science (80-.). 292, 686–693.

Zattin, M., Picotti, V., Zuffa, G., 2002. Fission-track reconstruction of the front of the Northern Apennine thrust wedge and overlying Ligurian unit. Am. J. Sci. 302, 346–379.

Zheng, Y.-F., 1999. Oxygen isotope fractionation in carbonate and sulfate minerals. Geochemical Journal 33, 109-126.

6. General Conclusions

Geochemical analysis on carbonates, embedding sediments and connate waters in each site permitted to have a complete and high resolution database on ACs field and fluids migrating along the Northern Apennines foothills. All the wells and natural seepages considered, are linked to the Northern Apennines petroleum system and migrating fluids towards the surface in the foothills area. All the ACs fields considered occur in the sedimentary successions of the Argille Azzurre formation, that is formed by blue clay clays and silts deposited in marine environment during the Plio-Pleistocene period and successively uplifted and emerged. The composition of the detrital fraction in all the 73 subsamples of carbonates analysed in the different outcrops, reflects the ones from the Argille Azzurre Formation. In the carbonate samples analysed in this thesis, has been noticed an increase in dolomite in the internal areas, meaning that it could be caused by the progressive isolation from the SO_4-rich pore water, which, instead, favours the increased calcite precipitation in the external area. The siliciclastic content increases moving from the internal to external subsamples, due to the sediment displacement operated by the fluid flow along the central emission vent. The high concentration of S and the presence of sulphide minerals indicate that sulphate reduction process was active during the precipitation. Petrographic observations point out the occurrence of clotted and peloidal microfabric, which commonly represents bacterially induced precipitates and are frequently observed in authigenic carbonates. The gas that fed the carbonate system is still present in the deep reservoirs and is a mix of biogenic and thermogenic methane, with minor condensates and oil. Thermogenic methane was generated both within the oil window and by thermal cracking of oils. The biogenic methane component was mostly formed by biodegradation of oil. Secondary biogenic methane concentrations up to 41.5% of the total gas budget indicate that microbial degradation is an important process in reservoirs of this region. The methane $\delta^{13}C$ in the reservoirs slightly varies around the average value of -46‰ V-PDB. Analysis of stable carbon isotope ratios in ACs indicates different processes of formation and carbon sources among the fields. $\delta^{13}C$ signatures in Enza River field indicate anaerobic oxidation of methane and sulphate reduction exploiting primary microbial methane that originated within the Pliocene sediments and migrated up-dip southwards from the sedimentary successions buried in the Po Plain. The lowering of $\delta^{13}C$ in progressively younger samples in this field is possibly due to increased gas diffusion and flux to the seafloor, within more permeable sediments containing marine pore water. Intense gas migration led to increased efficiency of AOM process and fluids escape in the water column, and in turn to a more negative $\delta^{13}C$ record in authigenic carbonates. Moderately negative $\delta^{13}C$ in Stirone

samples and in Secchia field chimney indicate a partial derivation from AOM of thermogenic methane, while positive $\delta^{13}C$ in NMVF and Secchia carbonates points towards the contribution of ^{13}C-rich CO_2, linked to the generation of secondary biogenic methane. On Secchia river ACs $\delta^{18}O$ and $^{87/86}Sr$ were compared to the seawater and deep water to understand which were the fluids that promoted the carbonate precipitation and quantify their real mixing. The $\delta^{18}O$ values in the authigenic carbonates depends on different parameters, in particular temperature and $\delta^{18}O$ signatures in the pore water from which the dolomitic carbonates precipitated. Strontium isotope analysis indicates that many globular concretions record imprint of connate waters coming from the Miocene reservoirs (typically 14 to 23%) compared to the seawater fraction. The chimney sub-samples and the most radiogenic GCs subsample, on the other hand, precipitated from a mixture dominated by marine bottom water (93-99 %). In the other sites subsamples, only $\delta^{18}O$ in dolomite cements have been measured. Results obtained stress a temperature disequilibrium during formation, which would indicate that marine water cannot be the sole oxygen source. The dataset presented in this work confirms that defining a direct correlation between authigenic carbonates and fluid sources might be difficult, but it is clear that authigenic carbonates provide a fossil record of changes in the biogeochemical processes active within the reservoirs and of changes in flux intensity during deep fluid leakage. The joint analysis of present-day seepages and fossil seepage-related carbonates can be considered a step forwards for better defining fluid sources by means of isotopic markers in authigenic carbonates. In fact, this is the first time that was possible a high-resolution comparison between fluids and related carbonates former precipitation. Those fluids, including hydrocarbons, in the Northern Apennines underwent to tertiary migration in the last million years, with earlier expression as submarine gas leakages and presently as subaerial mud volcanism. This dataset, together with the geological, sedimentary and stratigraphic characterisations, is the first step to build a powerful integrated methodology that would allow to add information for interpreting fluid interactions during authigenic carbonates precipitation, in fossils and modern site as well, where information on fluid sources are not available.

References

Aharon, P. and B. Fu, (2000). *Microbial sulfate reduction rates and sulfur and oxygen isotope fractionations at oil and gas seeps in deepwater Gulf of Mexico*. Geochim. Cosmochim. Acta 64(2), 233–246.

Antler, G., Turchyn, A. V., Rennie, V., Herut, B., and Sivan, O., (2013). *Coupled sulfur and oxygen isotope insight into bacterial sulfate reduction in the natural environment.* Geochim. Cosmochim. Acta 118, 98-117.

Armstrong-Altrin, J.S., Lee, Y., Verma, S.P. Worden, R.H., (2009). *Carbon, oxygen and strontium isotope geochemistry of carbonate rocks of the upper Miocene Kudankulam Formation, southern India: implications for paleoenvironment and diagenesis*. Chemie der Erde, Geochemistry, 69, 45-60.

Balestrieri, M.L., Bigazzi, G., Pandeli, E., Bigazzi, G., Carosi, R., Montomoli, C., (2011). *Age and temperature constraints on metamorphism and exhumation of the syn-orogenic metamorphic complexes of Northern Apennines, Italy.* Tectonoph. 509, 254–27.

Bertello, F., Fantoni, R., Franciosi, F., (2008). *Exploration Country Focus: Italy.* Search and Discover Articles #10165 (2008), posted 16 October 2008. Web address: Http://www.searchanddiscovery.net/documents/2008/08158bertello/index.htm

Bettelli, G., and Vannucchi, P., (2003). *Structural style of the offscraped Ligurian oceanic sequences of the Northern Apennines: new hypothesis concerning the development of melange block-in- matrix fabric*. J. Struct. Geol., 25(3), 371–388.

Blumenberg, M., Walliser, E.-O., Taviani, M., Seifert, R., Reitner, J., (2015). *Authigenic carbonate formation and its impact on the biomarker inventory at hydrocarbon seeps – A case study from the Holocene Black Sea and the Plio-Pleistocene Northern Apennines (Italy)*. Mar. Pet. Geol. 66, 532–541.

Boccaletti, M., Bonini, M., Corti, G., Gasperini, P., Martelli, L., Piccardi, L., Tanini, C., Vannucci, G., (2004). *Carta Sismotettonica della Regione Emilia-Romagna in scala 1:250.000*. Regione Emilia-Romagna-Servizio Geologico, Sismico e dei Suoli – C.N.R.-I.G.G., sezione di Firenze. S.EL.CA., Firenze.

Boetius, A., Ravenschlag, K., Schubert, C.J., Rickert, D., Widdel, F., Gieseke, A., Amann, R., Jùrgensen, B.B., Witte, U., Pfannkuche, O., (2000). *A marine microbial consortium apparently mediating anaerobic oxidation of methane.* Nature 407, 623–626.

Bonini, M., (2007). *Interrelations of mud volcanism, fluid venting, and thrust- anticline folding: examples from the external northern Apennines (Emilia- Romagna, Italy)*. J. Geophy. Res. 112, 1-21.

Bontognali, T.R., Vasconcelos, C., Warthmann, R.J., Bernasconi, S.M., Dupraz, C., Strohmenger, C.J., McKenzie, J.A., (2010*). Dolomite formation within microbial mats in the coastal sabkha of Abu Dhabi (United Arab Emirates)*. Sedimentology, 57, 824–844.

Borowski, W.S., Rodriguez, N.M., Paull, C.K., Ussler, W., (2013). *Are S-enriched authigenic sulfide minerals a proxy for elevated methane flux and gas hydrates in the geologic record?* Mar. Pet. Geol. 43, 381-395.

Bottinga, Y., (1969). *Carbon isotope fractionation between graphite, diamond and carbon dioxide.* Earth Planet Sci. Lett. 5, 301–307.

Brüchert V. (2004) *Physiological and ecological aspects of sulfur isotope fractionation during bacterial sulfate reduction.* In Sulfur Biogeochemistry – Past and Present, 379 (eds. J. P. Amend, K. J. Edwards and T. W. Lyons): Geological Society of America Special Paper. Geological Society of America, Boulder CO, USA, 1–16.

Budd, D.A., 1997. *Cenozoic dolomites of carbonate islands: their attributes and origin.* Earth Sci. Rev. 42, 1-47.

Burke, W.H., Denison, R.E., Hetherington, E.A., Koepnick, R.B., Nelson, H.F., Otto, J.B., (1982). *Variation of seawater 87Sr/86Sr throught Phanerozoic time.* Geology 10, 516–519.

Campbell, K.A, Farmer, J.D, Des Marais, D., (2002). *Ancient hydrocarbon seeps from the Mesozioc convergent margin of California: carbonate geochemistry, fluids and palaeoenvironments*. Geofluids 2, 63–94.

Canfield, D. E. (2001). *Isotope fractionation by natural populations of sulfate-reducing bacteria.* Geochim. Cosmochim. Acta 65, 1117–1124.

Canfield, D. E., Olesen, C. A., Cox, R.P. (2006). *Temperature and its control of isotope fractionation by a sulfate-reducing bacterium*. Geochim. Cosmochim. Acta 70, 548–561.

Capozzi, R., Picotti, V. (2002). *Fluid migration and origin of a mud volcano in the northern Apennines (Italy): the role of deeply rooted normal faults*. Terra Nova, 14: 363–370.

Capozzi, R., Dinelli, E., Negri, A., Picotti, V., (2006). *Productivity-generated annual laminae in mid-Pliocene sapropels deposited during precessionally forced periods of warmer Mediterranean climate.* Palaeogeogr. Palaeoclimatol. Palaeoecol. 235, 208–222.

Capozzi, R., Picotti, V., (2010). *Spontaneous fluid emissions in the Northern Apennines: geochemistry, structures and implications for the petroleum system.* Geol. Soc. London, Spec. Publ. 348, 115–135.

Cau, S., Franchi, F., Roveri, M., Taviani, M., (2015). *The Pliocene-age Stirone River hydrocarbon chemoherm complex (Northern Apennines, Italy)*. Mar. Pet. Geol. 66 (3), 582–595.

Cerling, T.E., (1984). *The stable isotopic composition of modern soil carbonate and its relationship to climate*. Earth Planet Sci. Lett., 7, 229–240.

Chacko, T., Cole, D.R., Horita, J., (2001). *Equilibrium oxygen, hydrogen and carbon fractionation factors applicable to geologic systems.* Rev. Miner. Geochem. 43, 1–81.

Clari, P., Cavagna, S., Martire, L., Hunziker, J., (2004). *A miocene mud volcano and its plumbing system: a chaotic complex revised (Monferrato, NW Italy)*. J. Sed. Res. 74, 662-676.

Conti, S., Artoni, A., Piola, G., (2007). *Seep-carbonates in a thrust-related anticline at the leading edge of an orogenic wedge: The case of the middle–late Miocene Salsomaggiore Ridge (Northern Apennines, Italy)*. Sediment. Geol. 199, 233–251.

de Souza, G.F., Reynolds, B.C., Kiczka, M., Bourdon, B., (2010). *Evidence for mass-dependent isotopic fractionation of strontium in a glaciated granitic watershed.* Geochim. Cosmochim. Acta 74, 2596-2614

Demirbas, A. (2010). *Methane Gas Hydrate.* London Dordrecht Heidelberg New York, Springer.

Deniel, C., Pin, C., (2001). *Single-stage method for the simultaneous isolation of lead and strontium from silicate samples for isotopic measurements*. Anal. Chim. Acta 426, 95-103.

Dara, O.M., Kuz'mina, T.G. & Lein, A.Y. (2009). *Mineral associations of the Lost Village and Lost City hydrothethermal fields in the North Atlantic*. Oceanology, 49, 688.

Elter P., Giglia G., Tongiorgi M., Trevisan L., (1975). *Tensional and compressional areas in the recent (Tortonian to present) evolution of the Northern Apennines*. Bollettino di Geofisica Teorica e Applicata 42, 3-18.

Faccenna C., Becker T.W., Lucente F.P., Jolivet L., Rossetti F., (2001). *History of subduction and back-arc extension in the Central Mediterranean.* Geophy. J. Int.145, 809-820.

Farquhar, J., Johnston, D.T., Wing, B.A., Habicht, K.S., Canfield, D.E., Airieau, S., Thiemens, M.H. (2003). *Multiple sulphur isotope interpretations for biosynthetic pathways: implications for biological signatures in the sulphur isotope record.* Geobiology 1, 27–36.

Faure, G., (1986). *Principles of isotope geology*. (2nd edition) Wuley, New York.

Faure, G., (1998). *Principles and application of Geochemistry.* (2nd edition). Prentice Hall, New Jersey.

Ferrari, C., Vianello, G., (1985). *Le salse dell'Emilia-Romagna*. Regione Emilia-Romagna, Bologna (in Italian).

Formolo, M.J., Lyonsa T.W., Zhangb, C., Kelleya, C., Sassenc, R., Horitad, J., Coled, D.R., (2004). *Quantifying carbon sources in the formation of authigenic carbonates at gas hydrate sites in the Gulf of Mexico*. Chem. Geol. 205, 253-264

Foucher, J.-P., Westbrook, G.K., Boetius, A., Ceramicola, S., Dupré, S., Mascle, J., Mienert, J., Pfannkuche, O., Pierre, C., and Praeg, D. (2009). *Structure and drivers of cold seep ecosystems*. Oceanograph. 22(1), 92–109.

Franzini, M., Leoni, L., Saitta, M., (1972). *A simple method to evaluate the matrix effects in X-Ray fluorescence analysis.* X-Ray Spectrom. 1, 151-154.

Franzini, M., Leoni, L., Saitta, M., (1975). *Revisione di una metodologia analitica per fluorescenza-X, basata sulla correzione completa degli effetti di matrice.* Rend. Soc. Ital. Mineral. Petrol. 31, 365-378.

Gabitov, R. I., E. B. Watson, et al. (2012). *Oxygen isotope fractionation between calcite and fluid as a function of growth rate and temperature: An in situ study*. Chem. Geo. 306-307, 92-102

Goldsmith, J.R., Graf, D.L., (1958). *Relation between lattice constants and composition of the Ca-Mg carbonates*. Am. Mineral. 43, 84–101.

Gunderson, K.L., Pazzaglia, F.J., Picotti, V., Anastasio, D. a., Kodama, K.P., Rittenour, T., Frankel, K.F., Ponza, A., Berti, C., Negri, A., Sabbatini, A., (2014). *Unraveling tectonic and climatic controls on synorogenic growth strata (Northern Apennines, Italy)*. Bull. Geol. Soc. Am. 126, 532–552.

Habicht, K. S., Gade, M., Thamdrup, B., Berg, P., Canfield, D. E. (2002) *Calibration of sulphate levels in the Archean Ocean*. Science 298, 2372–2374.

Heller, C., Blumenberg, M., Kokoschka, S., Wrede, C., Hoppert, M., Taviani, M., Reitner, J., (2011). *Geomicrobiology of Fluid Venting Structures at the Salse di Nirano Mud Volcano Area in the Northern Apennines (Italy),* in: Advances in Stromatolite Geobiology SE - 14, Lecture Notes in Earth Sciences. Springer Berlin Heidelberg, pp. 209–220.

Hensen, C., Nuzzo M., Hornibrook E., Pinheiro L.M., Bock B., Magalhães V.H., and Brückmann W. (2007). *Sources of Mud Volcano Fluids in the Gulf of Cadiz - Indications for Hydrothermally Altered Fluids*. Geochim. et Cosmochim. Acta, 71(5) ,1232-48.

Hensen, C., Scholz, F., Nuzzo, M., Valadares, V., Gracia, E., Terrinha, P., Liebetrau, V., Kaul, N., Silva, S., Martinez-Loriente, S., Bartolome, R., Pinero, E., Magalhães, V.H., Schmidt, M., Weise, S.M., Cunha, M., Hilario, a., Perea, H., Rovelli, L., Lackschewitz, K., (2015). *Strike- slip faults mediate the rise of crustal-derived fluids and mud volcanism in the deep sea*. Geology 43, 1–4.

Hesterberg, R., Siegenthaler, U., (1991). *Production and stable isotopic composition of CO_2 in a soil near Bern, Switzerland*. Tellus 43, 197–205.

Hoefs, J. (2009). *Stable Isotope Geochemistry*, Springer.

Jorgensen, B.B., Weber, A., and Zopfi, J., (2001) *Sulfate Reduction and Anaerobic Methane Oxidation in Black Sea Sediments*, Deep-Sea Res., 1(48), 2097–2120.

Joseph, C., Torres, M. E., Martin, M.A., Haley, B.A., Pohlman, J.W., Riedel, M., Rose, K., (2012). *Using the 87Sr/86Sr of modern and paleoseep carbonates from northern Cascadia to link modern fluid flow to the past*. Chem. Geo, 334, 122-130.

Kasten, S., Jørgensen, B.B., (2000) *Sulfate reduction in marine sediments*. Marine Geochemistry, 263–281.

Kelley, D.S., Karson, J.A., Blackman, D.K., Fruh-Green, G.L., Butterfield, D.A., Lilley, M.D., Olson, E.J., Schrenk, M.O., Roe, K.K., Lebon, G.T., Rivizzigno, P., AT3–60 Shipboard Party, (2001). *An off-axis hydrothermal vent field near the Mid-Atlantic Ridge at 30°N*. Nature, 412, 145–149.

Kelley, D.S., Karson, J.A., Früh-Green, G.L., Yoerger, D.R., Shank, T.M., Butterfield, D.A., Hayes, J.M., Schrenk, M.O., Olson, E.J., Proskurowski, G., Jakuba, M., Bradley, A., Larson, B., Ludwig, K., Glickson, D., Buckman, K., Bradley, A.S., Brazelton, W.J., Roe, K., Elend, M.J., Delacour, A., Bernasconi, S.M., Lilley, M.D., Baross, J.A., Summons, R.E., Sylva, S.P. (2005). *A serpentinite-hosted ecosystem: the Lost City hydrothermal field*, Science, 307, 1428–1434.

Lapham, L. L., Chanton, J. P., Chapman, R., Martens, C.S., (2010). *Methane under-saturated fluids in deep-sea sediments: Implications for gas hydrate stability and rates of dissolution.* Earth Planet. Sci. Lett. 298(3-4), 275-285.

Lein, A.Yu., Vainshtein, M.B., Shakola, V.A., and Romankevich, E.A., (1986). *Rate of Biogeochemical Processes in Shallow- Water Sediments from the Bulgarian Shelf of the Black Sea*, Geokhimiya, 10, 1477–1486.

Lein, A.Yu., Pimenov, N.V., Guillou, C., et al. Ivanov, M. (2002). *Seasonal Dynamics of the Sulfate Reduction Rate on the North-Western Black Sea Shelf*. Estuar. Coast, Shel. Sci., 54, 337–354.

Lein, A. Yu, (2004). *Authigenic carbonate formation in the ocean*. Lithol. Miner. Resour. 39 (1), 1-30. Translated from Litologiya i Poleznye Iskopaemye 1, 2004: 3-35.

Lein, A.Y., Bogdanova, O.Y., Bogdanov, Y.A., Magazina, L.I., (2007) *Mineralogical and geochemical features of authigenic carbonates on seepings and hydrothermal fields (By the examples of the Black Sea reefs and the mounds of the lost city field)*. Oceanology, 47(4), 537-553.

Leoni, L., Saitta, M., (1976). *X-ray fluorescence analysis of 29 trace elements in rock and mineral standards*. Rend. Soc. Ital. Mineral. Petrol. 32, 497-510.

Leoni, L., Menichini, M., Saitta, M., (1982). *Determination of S, Cl, and F in silicate rocks by X-Ray fluorescence analyses*. X-Ray Spectrom. 11, 156-158.

Levin, L.A., Orphan, V.J., Rouse, G.W., Rathburn, A.E., Ussler, W., Cook, G.S., Goffredi, S.K., Perez, E.M., Waren, A., Grupe, B.M., Chadwick, G., Strickrott, B., (2012). *A hydrothermal seep on the Costa Rica margin: middle ground in a continuum of reducing ecosystems*. Proc. Biol. Sci. 279, 2580–2588.

Liang, H., Chen, X., Wang, C., Zhao, D., Weissert, H., (2016). *Methane-derived authigenic carbonates of mid-Cretaceous age in southern Tibet: Types of carbonate concretions, carbon sources, and formation processes*. J. Asian Earth Sci., 115, 153-169.

Lindquist, S.J. (1999). *Petroleum systems of the Po Basin Provence of Northern Italy and Northern Adriatic Sea: Porto Garibaldi (Biogenic), Meride/Riva di Solto (Thermal) and Marnoso Arenacea (Thermal)*. On-Line Report, USGS Open-File report 99-50.

Loyd, S.J., Sample, J., Tripati, R.E., Defliese, W.F., Brooks, K., Hovland, M., Torres, M., Marlow, J., Hancock, L.G., Martin, R., Lyons, T. , Tripati, A.E., (2016). *Methane seep carbonates yield clumped isotope signatures out of equilibrium with formation temperatures*. Nat. Commun., 7, 122-174.

Luff, R., Wallmann, K., Aloisi, G., (2004). *Numerical modeling of carbonate crust formation at cold vent sites: significance for fluid and methane budgets and chemosynthetic biological communities.* Earth Planet. Sci. Lett. 221, 337–35.

Lumsden, D., (1979). *Discrepancy between thin-section and X-ray estimates of dolomite in limestone*. J. Sediment. Res. 49, 429–436.

Luz, B., Barkan, E., Bender, M.L., Thiemens, M.H., Boering, K.A., (1999). *Triple-isotope composition of atmospheric oxygen as a tracer of biosphere productivity.* Nature, 400, 547–550.

Malinverno, A., Ryan, W.B.F., (1986). *Extension in the Tyrrhenian Sea and shortening in the Apennines as a result of arc migration driven by sinking of the lithosphere.* Tectonics 5, 227-243.

Magalhães, V. H. and L. M. Pinheiro (2009). *Episodes of gas hydrate dissociation and enhanced methane flux recorded by methane-derived authigenic carbonates in the Gulf of Cadiz.* Geochim. Cosmochim. Acta 73(13), A814-A814.

Magalhães, V.H., Pinheiro, L.M., Ivanov, M.K., Kozlova, E., Blinova, V., Kolganova, J., Vasconcelos, C., McKenzie, J.A., Bernasconi, S.M., Kopf, A.J., Díaz-del-Río, V., Gonza lez, F.J., Somoza, L., (2012). *Formation processes of methane-derived authigenic carbonates from the Gulf of Cadiz.* Sediment. Geol. 243e244, 155-168.

Marroni, M., Pandolfi, L., (1996). *The deformation history of an accreted ophiolite sequence: the internal Liguride units (Northern Appennines, Italy)*. Geodinam. Acta 9, 13-29.

Marroni, M., Meneghini, F., Pandolfi, L., (2004). *From accretion to exhumation in a fossil accretionary wedge: a case history from Gottero unit (Northern Apennines, Italy)*. Geodinam. Acta 17, 41-53.

Marroni, M., Meneghini, F., and Pandolfi, L., (2010). *Anatomy of the Ligure-Piemontese subduction system: evidence from Late Cretaceous–Middle Eocene convergent margin deposits in the Northern Apennines, Italy*. Internat. Geo. Rev., 52, 1160–1192.

Martinelli, G., Rabbi, E., (1998). *The Nirano mud volcanoes* (abs.). In: Curzi, P.V., Judd, A.G. (Eds.), Abstracts and Guide Book, Vth International Conference on Gas in Marine Sediments, Bologna, Italy, September 1998. Grafiche A & B, Bologna, pp. 202-206.

Martinelli, G., Judd, A., (2004). *Mud volcanoes of Italy*. Geolog. J. 39, 49-61.

Marzec, P., Sechman, H., Kasperska, M., Cichostępski, K., Guzy, P., Pietsch, K. and Porębski, S. J. (2016). *Interpretation of a gas chimney in the Polish Carpathian Foredeep based on integrated seismic and geochemical data*. Basin Res. 1-18.

Mattavelli, L., Ricchiuto, T., Grignani, D., Schoell, M., (1983). *Geochemistry and habitat of natural gases in Po basin, Northern Italy.* AAPG Bulletin 67, 2239-2254.

Mazzini, A., Svensen, H., Hovland, M., Planke. S. (2006). *Comparison and implications from strikingly different authigenic carbonates in a Nyegga complex pockmark, G11, Norwegian Sea*. Mar. Geol. 231, 89–102.

Mazzini, A., Svensen, H.H., Planke, S., Forsberg, C.F., Tjelta, T.I., (2016). *Pockmarks and methanogenic carbonates above the giant Troll gas field in the Norwegian North Sea.* Mar. Geol., 373, 26-38.

Mickler. P.J., Stern, L.A., Banner, J.L. (2006). *Large kinetic isotope effects in modern speleothems*, Geol. Soc. Am. Bull. 118 (1-2), 65-81.

Miller, M.F., (2002). *Isotopic fractionation and the quantification of ^{17}O anomalies in the oxygen three-isotope system: an appraisal and geochemical significance.* Geochim Cosmochim Acta 66, 1881–1889.

Minissale, A., Magro, G., Martinelli, G., Vaselli, O., Tassi, G., (2000). *Fluid geochemical transect in the Northern Apennines (central-northern Italy): fluid genesis and migration and tectonic implications.* Tectonophysics 319, 199-222.

Molli, G., (2008). *Northern Apennines Corsica orogenic system: An updated overview*, in Siegesmund, S., Fügenschuh, B., and Froitzheim, N., eds., Tectonic Aspects of the Alpine-Dinaride-Carpathian System: Geological Society of London Special Publication 298, 413– 442.

Molli, G., Malavieille, J., (2011). *Orogenic processes and the Corsica/Apennines geodynamic evolution: insights from Taiwan.* Internat. J. Earth Sci. (Geologische Rundschau) 100 (5), 1207-1224.

Monegatti, P., Raffi, S., Roveri, M., Taviani, M., (2001). *A one day trip in the outcrops of the Castell'Arquato Plio-Pleistocene Basin: from the Badlands of Monte Giogo to the Stirone River,* International conference "No Geology without Paleontology" Paleobiogeography & Paleoecology, Guida all'escursioni. 22 pp.

Niewöhner C., Hensen C., Kasten S., Zabel M. and Schulz H. D. (1998) *Deep sulfate reduction completely mediated by anaer- obic methane oxidation in sediments of the upwelling area off Namibia*. Geochim. Cosmochim. Acta 62, 455–464.

Nissenbaum, A., (1984). *Methane Derived Organic Matter and Carbonates*, Org. Geochem., 5(4), 187–192.

Nyman, S.L., Nelson, C.S., Campbell, K.A., (2010). *Miocene tubular concretions in East Coast Basin, New Zealand: analogue for the subsurface plumbing of cold seeps*. Mar. Geol. 272, 319-336.

Nyman, S.L., Nelson, C.S., (2011). *The place of tubular concretions in hydrocarbon cold seep systems: Late Miocene Urenui Formation, Taranaki Basin, New Zealand*. Am. Assoc. Pet. Geol. Bull. 95, 1495–1524.

Ohmoto, H., Goldhaber, M.B., (1997). *Sulfur and carbon isotopes*. In: Barnes, H.L. (Ed.), Geochemistry of hydrothermal ore deposits, 3rd ed. John Wiley and Sons, New York, 517–612.

Olu, K., Duperret, A., Sibuet, M., Foucher, J. P., Fiala-Médioni, A. (1996). *Structure and distribution of cold seep communities along the Peruvian active margin: relationship to geological and fluid patterns.* Mar. Ecol. Prog. Ser. 132, 109–125.

Ono, S., Wing, B.A., Johnston, D., Farquhar, J., Rumble, D., (2006). *Mass-dependent fractionation of quadruple sulphur isotope system as a new tracer of sulphur biogeochemical cycles.* Geochim. Cosmochim. Acta 70, 2238–2252.

Ono, S., Shanks, W.C., Rouxel, O.J., Rumble, D., (2007). *S-33 constraints on the seawater sulphate contribution in modern seafloor hydrothermal vent sulfides.* Geochim. Cosmochim. Acta 71, 1170– 1182.

Oppo, D., Capozzi, R., Picotti, V., (2013). *A new model of the petroleum system in the Northern Apennines, Italy*. Mar. Pet. Geol. 48, 57–76.

Oppo, D., Capozzi, R., Picotti, V., Ponza, A., (2015). *A genetic model of hydrocarbon-derived carbonate chimneys in shelfal fine-grained sediments: The Enza River field, Northern Apennines (Italy)*. Mar. Pet. Geol. 66 (3), 555–565.

Paytan, A., Kastner, M., Martin, E.E., MacDougall, J.D., Herbert, T., (1993). *Marine barite as a monitor of seawater strontium isotope composition.* Nature 366, 445–449.

Peckmann, J., Thiel, V., (2004). *Carbon cycling at ancient methane–seeps*. Chem. Geol. 205, 443– 467.

Picotti, V., Capozzi, R., Bertozzi, G., Mosca, F., Sitta, A., Tornaghi, M., (2007). *The Miocene petroleum system of the Northern Apennines in the central Po Plain (Italy)*. In: Lacombe, O., Lavé, J., Roure, F., Vergés, J. (Eds.), Thrust Belts and Foreland Basins, From Fold Kinematics to Hydrocarbon System. Springer Verlag, Berlin, 117-131.

Picotti, V., Pazzaglia, F.J., (2008). *A new active tectonic model for the construction of the Northern Apennines mountain front near Bologna (Italy).* J. Geophy. Res. 113,

Picotti, V., Ponza, A., Pazzaglia, F.J., (2009). *Topographic expression of active faults in the foothills of the Northern Apennines*. Tectonophysics, 474(1-2), 285-294.

Pierre, C., Blanc-Valleron, M.M., Caquineau, S., März, C., Ravelo, a. C., Takahashi, K., Alvarez-Zarikian, C., (2014). *Mineralogical, geochemical and isotopic characterization of authigenic carbonates from the methane-bearing sediments of the Bering Sea continental margin (IODP Expedition 323, Sites U1343-U1345)*. Deep. Res. Part II Top. Stud. Oceanogr. 1–12.

Price, G.D., Gröcke, D.R., (2002). *Strontium isotope stratigraphy and oxygen and carbon isotope variation during the middle Jurassic early Cretaceous of the Falkland plateau, south Atlantic*. Palaeogeogr. Palaeoclimatol. Palaeoecol. 183, 209–222.

Proskurowski, G, Lilley, M.D, Kelley, D.S, Olson, E.J, (2006). *Low temperature volatile production at the Lost City Hydrothermal Field, evidence from a hydrogen stable isotope geothermometer.* Chem. Geol. 229, 331–343.

Ravelo, A.C., Hillaire-Marcel, C. (2007). *The Use of Oxygen and Carbon Isotopes of Foraminifera in Paleoceanography* . Dev. Mar. Geol., 1, 735-764.

Reeburgh, W.S. and Alperin, M.J., (1988). *Studies on Anaerobic Methane Oxidation*, Mitt. Geol. Paleontol. Inst., Hamburg: Univ. Hamburg, 66, 367–375.

Reitner, J., Peckmann, J., Reimer, A., Schumann, G., Thiel, V., (2005). *Methane-derived carbonate build-ups and associated microbial communities at cold seeps on the lower Crimean shelf (Black Sea)*. Facies 51, 66–79.

Reitner, J., Blumenberg, M., Walliser, E.-O., Schäfer, N., Duda, J.-P., (2015). *Methane-derived carbonate conduits from the late Aptian of Salinac (Marne Bleues, Vocontian Basin, France): Petrology and biosignatures.* Mar. Petrol. Geol. 1–12.

Ricci Lucchi, F., and Ori, G. G., (1985) - *Field excursion D: syn-orogenic deposits of a migrating basin system in the NW Adriatic Foreland*. In: P.H. Allen, P. Homewood e G. Williams (Eds.) “Excursion Guidebook”. Foreland Basins Symposium. Fribourg, 137-176.

Ricci Lucchi, F., Vai, G.B., (1994). *A stratigraphic and tectonofacies framework of the "calcari a Lucina" in the Apennine Chain, Italy*. Geo-Marine Lett. 14, 210–218.

Roberts, H. H., Feng, D., Joyce, S.B., (2010). *Cold-seep carbonates of the middle and lower continental slope, northern Gulf of Mexico*. Deep Sea Res. Part II: Topical Studies in Oceanography 57(21-23), 2040-2054.

Roy, S., Hovland, M., Braathen, A., (2016). *Evidence of fluid seepage in Grønfjorden, Spitsbergen: Implications from an integrated acoustic study of seafloor morphology, marine sediments and tectonics*. Mar. Geol., 380, 67-78.

Saitoh, M., Ueno, Y., Isozaki, Y., Shibuya, T., Yao, J., Ji, Z., Shozugawa, K., Matsuo M., Yoshida, N., (2015). *Authigenic carbonate precipitation at the end-Guadalupian (Middle Permian) in China: Implications for the carbon cycle in ancient anoxic oceans*. Prog. Earth Planet. Sci. 2, 41.

Scholz, F., C. Hensen, A. Reitz, R. L. Romer, V. Liebetrau, A. Meixner, S. M. Weise, and M. Haeckel. (2009). *Isotopic Evidence (Sr-87/Sr-86, Delta Li-7) for Alteration of the Oceanic Crust at Deep-Rooted Mud Volcanoes in the Gulf of Cadiz, Ne Atlantic Ocean*. Geochim. et Cosmochim. Acta, 73(18), 5444-59.

Scicli, A., (1972). *L'attività estrattiva e le risorse minerarie della Regione Emilia- Romagna*. Artioli, Modena (in Italian).

Sibuet, M. and Olu, K., (1998). *Biogeography, Biodiversity and Fluid Dependence of Deep-Sea Cold Seep Communities at Active and Passive Margins*, Deep-Sea Res., 1(45), 517–567.

Sim, M. S., Ono, S., Donovan, K., Templer, S. P., Bosak, T. (2011) *Effect of electron donors on the fractionation of sulfur isotopes by a marine Desulfovibrio sp.*. Geochim. Cosmochim. Acta 75, 4244–4259.

Spadafora, A., Perri, E., Mckenzie, J.A., Vasconcelos, C., (2010). *Microbial biomineralization processes forming modern Ca, Mg carbonate stromatolites.* Sedimentology, 57, 27–40.

Spallanzani, L., (1795). *Viaggi alle Due Sicilie e in alcune parti dell'Appennino*, vol. 5. Pavia. (in Italian).

Stam, M. C., Mason, P. R. D., Laverman, A. M., Pallud, C. and Cappellen, P. V. (2011). *$^{34}S/^{32}S$ fractionation by sulfate-reducing microbial communities in estuarine sediments.* Geochim. Cosmochim. Acta 75, 3903–3914.

Stoppani, A., (1871*). Corso di Geologia*, vol. 1. Milano. (in Italian).

Strakhov, N.M., (1951). *Calc–Dolomitic Facies of Modern and Ancient Basins*, Trudy IGN Akad. Nauk SSSR, issue 124, Ser. geol., 45, 211–218.

Talukder, A. R., (2012). *Review of submarine cold seep plumbing systems: leakage to seepage and venting.* Terra Nova, 24, 255–272.

Taviani, M., (2001). *Fluid venting and associated processes*, in: Vai, G., Martini, I.P. (Eds.), Anatomy of an Orogen: The Apennines and Adjacent Mediterranean Basins SE - 20. Springer Netherlands, 351–366.

Terzi, C., Lucchi, F., Vai, G., Aharon, P., (1994). *Petrography and stable isotope aspects of cold-vent activity imprinted on Miocene-age "calcari aLucina" from Tuscan and Romagna Apennines, Italy.* Geo-Marine Lett. 14, 177–184.

Thirlwall, M.F., (1991). *Long-term reproducibility of multicollector Sr and Nd isotope ratio analysis*. Chem. Geol., 94, 85-104.

Tong, H., Feng, D., Cheng, H., Yang, S., Wang, H., Angela, G.M., Edwards, R.L., Chen, Z., Chen, D., (2013). *Authigenic carbonates from seeps on the northern continental slope of the South China Sea: New insights into fluid sources and geochronology*. Mar. Petrol. Geol. 43, 260-271.

Unterseh, S.L., (2013), May 6. *Early Recognition of Seabed and Sub-seabed Natural Hydrocarbon Seeps in Deep Offshore Angola*. Offshore Technology Conference.

Ussler, W., Paull, C.K., Fullagar, P.D. (2001). *Pore-water strontium isotopes from the Leg 171B drilling transect down the Blake Spur*. Texas A & M University, Ocean Drilling Program, College Station, TX, United States 171B.

Vai, G.B., Martini, I.P., (2001). *Anatomy of an orogene: the Apennines and adjacent Mediterranean basins.* Kluver Academic Publishers, 632.

Valentine, D.L. and Reeburgh, W.S. (2000). *New Perspectives on Anaerobic Methane Oxidation*, Environ. Microbiol., 2, 477–484.

Van Landeghem, K.J.J., Niemann, H., Steinle, L.I., O'Reilly, S.S., Huws, D.G., Croker, P.F., (2015). *Geological settings and seafloor morphodynamic evolution linked to methane seepage.* Geo-Mar. Lett., 35, 289.

Vanneste, H., Kastner, M., James, R.H., Connelly, D.P., Fisher, R.E., Kelly-Gerreyn,B.A., Heeschen, K., Haeckel, M., Mills, R.A. (2012). *Authigenic carbonates from the Darwin Mud Volcano, Gulf of Cadiz: A record of palaeo-seepage of hydrocarbon bearing fluids*. Chem. Geo., 24(39), 300-301.

Vannucchi, P., and Bettelli, G., (2002). *Mechanisms of subduction accretion as implied from the broken formations in the Apennines, Italy*. Geology, 30(9), 835–838.

Vannucchi, P., Remitti, F., and Bettelli, G., (2008). *Geological record of fluid flow and seismogenesis along an erosive subducting plate boundary*. Nature, 451, 699–703.

Vasconcelos, C., McKenzie, J.A., Warthmann, R., Bernasconi, S.M., (2005). *Calibration of the delta O-18 paleothermometer for dolomite precipitated in microbial cultures and natural environments.* Geology 33, 317-320.

Viola, I., Oppo, D., Franchi, F., Capozzi, R., Dinelli, E., Liverani, B., Taviani, M., (2015). *Mineralogy, geochemistry and petrography of methane-derived authigenic carbonates from Enza River, Northern Apennines (Italy)*. Mar. Pet. Geol. 66, 566–581.

Viola, I., Capozzi, R., Bernasconi, S.M., Rickli, J. *Mineralogy, geochemistry and isotopic signatures of authigenic carbonates from new discovered Secchia River site, Northern Apennines (Italy)*. Sedimentology, Submitted.

Wang, J. S., Jiang, G. Q., Xiao, S., Li, Q., Wei, Q., (2008). *Carbon isotope evidence for widespread methane seeps in the ca. 635 Ma Doushantuo cap carbonate in south China.* Geology 36(5), 347-350.

Wang, S., Yan, W., Magalhães, V.H., Chen, Z., Pinheiro, L.M., Gussone, N., (2012). *Calcium isotope fractionation and its controlling factors over authigenic carbonates in the cold seeps of the northern South China Sea.* Chin. Sci. Bull. 57(11), 1325-1332.

Wang, S., Magalhães, V.H., Pinheiro, L.M., Liu, J., Yan, W., (2015). *Tracing the composition, fluid source and formation conditions of the methane-derived authigenic carbonates in the Gulf of Cadiz with rare earth elements and stable isotopes*. Mar. Petrol. Geol., 68 (A), 192-205.

Whiticar, M. J. (1999). *Carbon and hydrogen isotope systematics of bacterial formation and oxidation of methane*. Chem. Geol. 161, 291–314.

Young, E.D., Galy, A., Nagahara, H. (2002). *Kinetic and equilibrium mass-dependent isotope fractionation laws in nature and their geochemical and cosmochemical significance.* Geochim. Cosmochim. Acta 66, 1095–1104.

Zattin, M., Picotti, V., Zuffa, G., (2002). *Fission-track reconstruction of the front of the Northern Apennine thrust wedge and overlying Ligurian unit*. Am. J. Sci. 302, 346–379.

Zhang, T. and B. M., Krooss (2001). *Experimental investigation on the carbon isotope fractionation of methane during gas migration by diffusion through sedimentary rocks at elevated temperature and pressure.* Geochim. Cosmochim. Acta 65(16), 2723–2742.